10.1161/CIRCULATIONAHA.118.035648

# SmgGDS Prevents Thoracic Aortic Aneurysm Formation and Rupture by Phenotypic Preservation of Aortic Smooth Muscle Cells

**Running Title:** *Nogi et al.; SmgGDS in TAA*

Masamichi Nogi, MD[1]; Kimio Satoh, MD, PhD[1]; Shinichiro Sunamura, MD[1]; Nobuhiro Kikuchi, MD, PhD[1]; Taijyu Satoh, MD, PhD[1]; Ryo Kurosawa, MD[1]; Junichi Omura, MD, PhD[1]; Md. Elias-Al-Mamun, PhD[1]; Mohammad Abdul Hai Siddique, PhD[1]; Kazuhiko Numano MD[1]; Shun Kudo, MD, PhD[1]; Satoshi Miyata, PhD[1]; Masatoshi Akiyama, MD, PhD[2]; Kiichiro Kumagai, MD, PhD[2]; Shunsuke Kawamoto, MD, PhD[2]; Yoshikatsu Saiki, MD, PhD[2]; Hiroaki Shimokawa, MD, PhD[1]

[1]Department of Cardiovascular Medicine, Tohoku University Graduate School of Medicine, Sendai, Japan; [2]Department of Cardiovascular Surgery, Tohoku University Graduate School of Medicine, Sendai, Japan

**Address for Correspondence:**
Hiroaki Shimokawa, MD, PhD
Professor and Chairman
Department of Cardiovascular Medicine
Tohoku University Graduate School of Medicine
1-1 Seiryo-machi, Aoba-ku
Sendai 980-8574, Japan
Tel: +81-22-717-7151
Fax: +81-22-717-7156
Email: shimo@cardio.med.tohoku.ac.jp

Downloaded from http://circ.ahajournals.org/ by guest on June 20, 2018

## Abstract

***Background*—**Thoracic aortic aneurysm (TAA) and dissection (TAD) are fatal diseases, which cause aortic rupture and sudden death. The small GTP-binding protein GDP dissociation stimulator (SmgGDS) is a crucial mediator of the pleiotropic effects of statins. Previous studies revealed that reduced force generation in AoSMCs causes TAA and TAD.
***Methods*—**To examine the role of SmgGDS in TAA formation, we employed an angiotensin II (AngII, 1,000 ng/min/kg, 4 weeks)-induced TAA model.
***Results*—**33% *Apoe*$^{-/-}$*SmgGDS*$^{+/-}$ mice died suddenly due to TAA rupture, whereas there was no TAA rupture in *Apoe*$^{-/-}$ control mice. In contrast, there was no significant difference in the ratio of abdominal aortic aneurysm rupture between the two genotypes. We performed ultrasound imaging every week to follow the serial changes in aortic diameters. The diameter of the ascending aorta progressively increased in *Apoe*$^{-/-}$*SmgGDS*$^{+/-}$ mice compared with *Apoe*$^{-/-}$ mice, whereas that of the abdominal aorta remained comparable between the two genotypes. Histological analysis of *Apoe*$^{-/-}$*SmgGDS*$^{+/-}$ mice showed dissections of major thoracic aorta in the early phase of AngII infusion (day 3~5) and more severe elastin degradation compared with *Apoe*$^{-/-}$ mice. Mechanistically, *Apoe*$^{-/-}$*SmgGDS*$^{+/-}$ mice showed significantly higher levels of oxidative stress, matrix metalloproteinases, and inflammatory cell migration in the ascending aorta compared with *Apoe*$^{-/-}$ mice. For mechanistic analyses, we primary cultured aortic smooth muscle cells (AoSMCs) from the 2 genotypes. After AngII (100 nM) treatment for 24 hours, *Apoe*$^{-/-}$*SmgGDS*$^{+/-}$ AoSMCs showed significantly increased MMP activity and oxidative stress levels compared with Apoe$^{-/-}$ AoSMCs. In addition, SmgGDS deficiency increased cytokines/chemokines and growth factors in AoSMCs. Moreover, expressions of *FBN1*, *ACTA2*, *MYH11*, *MLK* and *PRKG1*, which are force generation genes, were significantly reduced in *Apoe*$^{-/-}$*SmgGDS*$^{+/-}$ AoSMCs compared with Apoe$^{-/-}$ AoSMCs. Similar tendency was noted in AoSMCs from TAA patients compared with those from controls. Finally, local delivery of the SmgGDS gene construct reversed the dilation of the ascending aorta in *Apoe*$^{-/-}$*SmgGDS*$^{+/-}$ mice.
***Conclusions*—**These results suggest that SmgGDS is a novel therapeutic target for the prevention and treatment of TAA.


**Key Words:** thoracic aortic aneurysm; thoracic aortic dissection; SmgGDS

Downloaded from http://circ.ahajournals.org/ by guest on June 20, 2018

## Clinical Perspective

### What is new?

- Downregulation of SmgGDS in aortic smooth muscle cells (AoSMCs) contributes to the pathogenesis of thoracic aortic aneurysm (TAA) and dissection (TAD), which involves dysfunction of AoSMCs, and enhanced oxidative stress and matrix metalloproteinases (MMPs) activities.
- Using genetically modified mice, we demonstrated a pathogenic role of SmgGDS in the development of AngII-induced TAA and TAD.
- Local overexpression of SmgGDS around the thoracic aorta inhibited aortic dilatation and rupture in SmgGDS-deficient mice.

### What are the clinical implications?

- The present study adds to the current understanding of TAA pathology, showing that mechanical stretch induces SmgGDS and downstream force generation proteins, all of which are important for mechanical support in the aortic wall.
- Given the severe side effects of protease inhibitors in clinical trials, SmgGDS could be a promising and potentially safe drug target.
- Additionally, further studies are needed to use SmgGDS as a diagnostic biomarker for TAA.
- Genome screening for the SmgGDS gene and SmgGDS-associated genes could be beneficial for TAA patients.

Downloaded from http://circ.ahajournals.org/ by guest on June 20, 2018

## Introduction

Thoracic aortic aneurysm (TAA) and dissection (TAD) are fatal diseases, which cause aortic rupture and sudden death.[1] A major cause of TAA is genetic disorders, whereas risk factors for abdominal aortic aneurysm (AAA) are also involved, including male sex, smoking, and higher plasma low-density lipoprotein.[2] Many gene mutations have been identified to cause TAA and TAD, such as *FBN1*,[3] *ACTA2*,[4] *MYH11*,[5] *MYLK*,[6] *TGFB2*,[7] *TGFB3*,[8] *TGFBR1*,[9] *TGFBR2*,[10] *SMAD3*,[11] and *PRKG1*.[12] These genes encode proteins involved in contractile components and functional signaling pathways of aortic smooth muscle cells (AoSMCs).[13] It is suggested that impaired ability of AoSMCs to generate force through the elastin-contractile units in response to pulsatile hemodynamic stress may be the major promoting factor for TAA and TAD.[14] The disruption of the elastin-contractile unit leads to impaired mechanosensing of AoSMCs, resulting in dilatation and destabilization of the aortic wall. Other triggers for TAA and TAD, such as hypertension, aging, and atherosclerosis, also potentially cause changes in mechanosensing and signaling pathways and affect the elastin-contractile unit.[13] Marfan syndrome is a disorder, in which *FBN1* gene mutation causes progressive TAA and TAD.[3] Fbn1 is the major component of the extracellular matrix (ECM) and allows the formation of elastic fibers.[13] *FBN1* mutation causes loss of connections between AoSMCs, elastin fibers, and force generation.[13] Taken together, reduced force generation in AoSMCs causes TAA and TAD.[13]

An early event of TAA formation seems to be the phenotypic switching of AoSMCs.[15] AoSMCs with contractile phenotype are essential for stabilization of the aortic wall.[16] Multiple signaling pathways, such as transforming growth factor-β (TGF-β)-dependent, RhoA-dependent, and p38-dependent signaling, have been identified that maintain contractile AoSMC phenotype

Downloaded from http://circ.ahajournals.org/ by guest on June 20, 2018

through regulation of AoSMC-specific transcriptional machinery.[17] However, gene mutations in proteins involved in cell contraction and stabilization, such as *ACTA2*,[4] *MYLK*,[6] and *MYH11*,[5] induce switching of AoSMCs from a contractile to a synthetic inflammatory phenotype. AoSMCs with the synthetic phenotype secrete abundant matrix metalloproteinases (MMPs), inflammatory cytokines/chemokines, and growth factors,[16] resulting in the recruitment of inflammatory cells to the aortic wall. Additionally, the phenotypic switching of AoSMCs from the normal contractile phenotype to the synthetic and inflammatory one induces the production of reactive oxygen species (ROS) and proteoglycans.[16] Inflammatory cells accumulated in the aortic wall, especially those in the adventitia, create a vicious circle leading to the increased production of ROS.[18] All these changes promote the degradation of ECM and weakening of the aortic wall, resulting in TAA rupture.[15,19] The mechanisms through which dissection and rupture frequently occur in the ascending aorta have not been fully elucidated yet. However, it has been shown that the embryonic origins of AoSMCs in the ascending aorta are different from those of AoSMCs located in other parts of the aorta, which may explain the potential of AoSMCs to alter their phenotype and develop TAA and TAD.[20]

RhoA is one of the small GTPases, and contributes to the maintenance and morphological support of the aortic structure.[21] Moreover, Rho GTPase-accelerating proteins (GAPs) play a protective role against TAA formation by preventing the switch of AoSMCs from the contractile type to the synthetic and pro-inflammatory phenotype.[16] By keeping AoSMCs in their normal contractile cell phenotype, small GTPases that maintain RhoA in its active form, contribute to the stability of Rho-kinase, and activate downstream substrates, such as calponin (*CNN1*), α-smooth muscle actin (αSMA, *ACTA2*), myosin light chain kinase (*MYLK*), myosin-11 (*MYH11*),

Downloaded from http://circ.ahajournals.org/ by guest on June 20, 2018

and myosin phosphatase target subunit 1 (MYPT1, *PPP1R12A*).[22] As mentioned above, gene mutations of these force generation proteins cause hereditary TAA and TAD. In addition to the genetic background, environmental factors, such as vascular injury, hypoxia, oxidative stress, and angiotensin II (AngII), accelerate phenotype switching of AoSMCs from the normal contractile type to the synthetic inflammatory phenotype. In contrast, the active form of RhoA helps to keep AoSMCs as the normal contractile phenotype by increasing gene expression of contractile proteins and contractility.[23] Thus, small GTPases contribute to maintaining AoSMCs in their contractile phenotype and morphologically support and stabilize the aortic wall.

Small GTP-binding protein GDP dissociation stimulator (SmgGDS) is one of the guanine nucleotide exchange factors (GEF),[24] which interacts with RhoA,[25] kinesin-associated protein 3 (*KIFAP3*),[26] and GTPase HRas (*HRAS*).[27] Here, SmgGDS controls the small G proteins, including the Rho and Rap1 family members, as well as KRAS,[28] thereby promoting the GDP/GTP exchange reactions, while inhibiting the interactions with membranes. Importantly, SmgGDS regulates the link between human chromosome-associated polypeptide (HCAP) and KIF3A/B, a kinesin superfamily protein located in the nucleus, which plays a crucial role in the interaction of chromosomes with an ATPase motor protein.[26] Additionally, SmgGDS translocates Rac1 into the nucleus to degrade it.[29] Indeed, we have demonstrated that statins selectively inhibit Rac1,[30] promoting its degradation and preventing AngII-induced cardiac hypertrophy and fibrosis in a SmgGDS-dependent manner.[31-33] Thus, SmgGDS has multiple roles to regulate the activities of RhoA and epigenetic gene modifications. In the present study, to determine whether SmgGDS participates in the pathogenesis of TAA and TAD, we employed

Downloaded from http://circ.ahajournals.org/ by guest on June 20, 2018

a multidisciplinary translational approach. We report that the deletion of SmgGDS promotes the phenotypic switching of AoSMCs into the synthetic and inflammatory phenotype. Using SmgGDS-knockout mice, we demonstrated the protective role of SmgGDS against the development of AngII-induced TAA and TAD. Importantly, in AngII-induced TAA mouse model, local delivery of the SmgGDS gene construct reversed the dilatation of the ascending aorta in SmgGDS-knockout mice. Thus, our data demonstrate that SmgGDS is a novel and promising therapeutic target in TAA and TAD.

Downloaded from http://circ.ahajournals.org/ by guest on June 20, 2018

## Methods

Additional detailed methods are included in the online-only Data Supplement. The data that support the findings of this study are available from the corresponding author upon reasonable request.

American Heart Association
Circulation

### Human Aorta Samples

All protocols using human specimens were approved by the Institutional Review Board of Tohoku University, Sendai, Japan (No. 2017-1-094). Aortic tissues were obtained from patients with thoracic aortic aneurysm (TAA) or non-TAA such as coronary bypass. All patients provided written informed consent for the use of the aortic tissues for the present study.

### Isolation of Human AoSMCs

Human aortic smooth muscle cells (AoSMCs) were primary cultured from aortic tissues. AoSMCs were cultured in Dulbecco's modified eagle medium (DMEM) containing 10% fetal bovine serum (FBS) at 37°C in a humidified atmosphere of 5% $CO_2$ and 95% air. AoSMCs of passages 4 to 7 at 70% to 80% confluence were used for experiments.

**Animal Experiments**

All animal experiments were performed in accordance with the protocols approved by the Tohoku University Animal Care and Use Committee (No. 2015-Kodo-002) based on the ARRIVE guideline. In all animal experiments, we used littermates or saline treatment group as controls. We used an angiotensin II (AngII)-induced aneurysm model to assess the effect of SmgGDS deficiency on TAA development in *Apoe*$^{-/-}$ mice. We infused 6- to 8-week-old male *Apoe*$^{-/-}$*SmgGDS*$^{+/-}$ mice on a normal chow diet with 1000 ng/kg/min AngII (MP Biomedicals) or saline for 4 weeks. We dissolved AngII in sterile saline and infused with ALZET osmotic pumps (model 2004, DURECT). We anesthetized the mice with isoflurane (1.0%) and placed the pumps into the subcutaneous space through a small incision in the back of the neck that we closed by suturing. All incision sites healed rapidly without any infection. To determine the effect of SmgGDS deficiency on AngII-induced aneurysm formation, we quantified TAA and AAA incidence and aortic diameters. For *in vivo* ultrasound images, the aortic diameter was monitored in isoflurane (1.0%)-anesthetized mice by high-frequency ultrasound with a Vevo 2100 (Visualsonics, Toronto, Canada). Maximal internal diameters of aortic images were measured using Vevo 2100 software, version 1.6.0. We quantified aneurysm incidence based on a definition of aneurysm as an external width of the aorta that was increased by 50% or greater[1] compared with the same aortas before AngII infusion (http://cvrc.med.uky.edu/lab-protocols).

**Generation of Mice**

*SmgGDS*$^{+/-}$ mice were obtained from Dr. Takai in Kobe University and were backcrossed to C57BL/6J mice for 10 generations. *Apoe*$^{-/-}$ mice on a C57BL/6J background were obtained

Downloaded from http://circ.ahajournals.org/ by guest on June 20, 2018

from the Jackson Laboratory (Bar Harbor, Maine, USA). Double knockout (*Apoe*$^{-/-}$ *SmgGDS*$^{+/-}$) mice were generated by crossing *SmgGDS*$^{+/-}$ mice with *Apoe*$^{-/-}$ mice. The F1 generation was backcrossed with *Apoe*$^{-/-}$ mice to fix the *Apoe*$^{-/-}$ genotype, and littermates were crossed. All mice were genotyped by PCR on tail clip samples using primers specific for the SmgGDS gene (*RAP1GDS1*) (5′-CCGCTTGGGTGGAGAGGCTAT-3′ and 5′-ATCGAGGTTGAGCCTAGCAA-3′) and the *Apoe* gene (5′-GCCTAGCCGAGGGAGAGCCG-3′, 5′-TGTGACTTGGGAGCTCTGCAGC-3′ and 5′-GCCGCCCCGACTGCATCT-3′). All experiments were performed with generations F4-F6 using littermate *Apoe*$^{-/-}$*SmgGDS*$^{+/+}$ as controls. All experiments were performed with 8–10 weeks old male mice.

**Statistical Analyses**

All results are shown as mean ± SEM. Comparisons of means between 2 groups were performed by unpaired Student's *t*-test. Comparisons of means in some treatment groups against one control group were performed with the Dunnett's test for multiple comparisons. Comparisons of mean responses associated with the two main effects of the different treatments were performed by two-way analysis of variance (ANOVA) with interaction terms, followed by Tukey's HSD (honestly significant difference) for multiple comparisons. The survival rates of SmgGDS deficiency and control mice during AngII infusion were analyzed with the log-rank test. Statistical significance was evaluated with JMP 12 (SAS Institute Inc, Cary, America) or R version 3.3.2 (http://www.R-project.org/). The ratio of fully muscularized vessels was analyzed by the Poisson regression with the offset equals to the sum of total vessels with multcomp 1.4-6 package of R. All reported P values are 2-tailed, with a P value of less than 0.05 indicating statistical significance.

Downloaded from http://circ.ahajournals.org/ by guest on June 20, 2018

## Results

### Reduced Aortic SmgGDS Expression in Patients with TAA

To test the hypothesis that SmgGDS is related to the pathogenesis of TAA, we compared SmgGDS expression in the ascending aorta between patients with TAA and non-TAA controls undergoing bypass surgery (**Supplementary Fig. 1A**). Immunostaining showed that, in the aortic walls of the ascending aortas, SmgGDS was more weakly expressed in TAA patients than in controls (**Supplementary Fig. 1A**). To further confirm the phenotype of AoSMCs in TAA patients, we established cell libraries of primary cultured AoSMCs obtained from TAA patients (TAA-AoSMCs) undergoing aortic replacement surgery for artificial blood vessels and performed gene expression microarray analysis (**Supplementary Table 1**). The microarray analysis showed significant changes in 1262 genes, which were up-regulated or down-regulated in TAA-AoSMCs compared with control AoSMCs (**Supplementary Fig. 1B**). Genes with significant changes were submitted to Ingenuity Pathway Analysis (IPA) software to reveal gene sets representing specific biological processes or functions. Interestingly, heatmap analysis showed that the gene sets from TAA-AoSMCs showed downregulations of the pathways related to cellular assembly, connective tissue, and cardiovascular development compared with control AoSMCs (**Supplementary Fig. 1C**). For example, the IPA analysis showed significant alteration in signaling related to cell proliferation/apoptosis, senescence, and inflammation in TAA-AoSMCs (**Supplementary Table 2**). Real-time PCR (RT-PCR) showed that the expression of *SmgGDS* was lower in TAA-AoSMCs than in control AoSMCs (**Supplementary Fig. 1D**). Importantly, immunostaining showed that the expression of Fbn1, which is a large extracellular matrix glycoprotein functioning as a structural component, was reduced in the

Downloaded from http://circ.ahajournals.org/ by guest on June 20, 2018

aortic walls of the ascending aortas of TAA patients compared with those of the controls (**Supplementary Fig. 1E**). Fbn1 provides force bearing structural support in elastic tissue throughout the body, contributing to the stabilization of the aortic morphology.[13] Here, the expression of *Fbn1* was significantly lower in TAA-AoSMCs than in control AoSMCs (**Supplementary Fig. 1F**). Additionally, the expressions of *Acta2* and *Myh11*, mutations of which cause TAA and TAD, were reduced in TAA-AoSMCs compared with control AoSMCs (**Supplementary Fig. 1F**). These results suggest that SmgGDS in AoSMCs may be involved in the development of TAA and TAD.

**Deletion of SmgGDS Promotes the Development of AngII-induced TAA Formation**

To examine the role of SmgGDS in AngII-induced TAA formation (**Supplementary Fig. 1G**), we newly developed *Apoe*$^{-/-}$*SmgGDS*$^{+/-}$ mice (**Supplementary Table 3**). Since complete SmgGDS disruption (*SmgGDS*$^{-/-}$) in mice results in perinatal lethality,[34] we used *SmgGDS*$^{+/-}$ mice in the present study. *Apoe*$^{-/-}$*SmgGDS*$^{+/-}$ mice and controls (*Apoe*$^{-/-}$ mice) showed normal growth under physiological conditions. Systolic blood pressure was comparable between the two genotypes during the time course of AngII infusion (**Supplementary Fig. 2A**). The morphology of the ascending aortas in saline-infused *Apoe*$^{-/-}$*SmgGDS*$^{+/-}$ mice did not differ from that of *Apoe*$^{-/-}$ mice (**Supplementary Fig. 2B**). In contrast, a significant difference in the medial thickness and degradation of the ascending aorta was noted after the animals were subjected to AngII infusion for 4 weeks (**Supplementary Fig. 2B**). During AngII treatment, 33% of *Apoe*$^{-/-}$*SmgGDS*$^{+/-}$ mice died suddenly due to TAA rupture, whereas there was no TAA rupture in *Apoe*$^{-/-}$ mice (**Fig. 1A**). In contrast, there was no significant difference in the ratio of AAA rupture between the two genotypes (**Fig. 1B**). AngII treatment rapidly triggered TAA or

Downloaded from http://circ.ahajournals.org/ by guest on June 20, 2018

lethal TAD in 40% of *Apoe*$^{-/-}$*SmgGDS*$^{+/-}$ mice, whereas this treatment did not induce TAA or lethal TAD in *Apoe*$^{-/-}$ mice (**Fig. 1C**). In contrast, there was no significant difference in the development or rupture of AAA between the two genotypes (**Fig. 1D**). To analyze the aortic aneurysm formation, we performed ultrasound imaging every week to follow the changes in aortic diameter (**Supplementary Fig. 3**). Diameters of the ascending aorta were significantly larger and progressively increased in *Apoe*$^{-/-}$*SmgGDS*$^{+/-}$ mice compared with *Apoe*$^{-/-}$ mice (**Fig. 1E**). In contrast, the diameters of the abdominal aorta were comparable between the 2 genotypes (**Fig. 1F**). Histological analysis of Elastica-Masson (EM) staining showed that disruption and degradation of medial elastic lamina in the ascending aorta were more severe in *Apoe*$^{-/-}$*SmgGDS*$^{+/-}$ mice compared with *Apoe*$^{-/-}$ mice (**Fig. 1G, H**). In contrast, there was no significant difference in the disruption and degradation of medial elastic lamina in the abdominal aorta between the 2 genotypes (**Fig. 1H**). Consistent with the significant increase in the incidence of TAA formation and rupture in *Apoe*$^{-/-}$*SmgGDS*$^{+/-}$ mice, EM staining showed dramatic changes in the walls of the ascending aorta (**Supplementary Fig. 4**). The degradation of the ascending aortic walls was especially severe in the lamina beside the adventitia, resulting in the disconnection of the medial walls (arrow, **Supplementary Fig. 4**). These results indicate that SmgGDS plays important protective roles against the development of TAA and TAD (**Fig. 1I**).

**Deletion of SmgGDS Induces TAD at Day 3 after AngII Infusion**

*Apoe*$^{-/-}$*SmgGDS*$^{+/-}$ mice suddenly died due to TAA rupture in the early days after AngII infusion. To evaluate the initial changes in the ascending aorta before TAA rupture, we harvested aortas at day 3 (**Fig. 2A**). Interestingly, there was no change in the aorta of AngII-infused *Apoe*$^{-/-}$ mice,

Downloaded from http://circ.ahajournals.org/ by guest on June 20, 2018

whereas we found frequent aortic dissection in the ascending aorta harvested from *Apoe*$^{-/-}$ *SmgGDS*$^{+/-}$ mice (**Fig. 2A**). EM staining showed that there was no change in the aorta of *Apoe*$^{-/-}$ mice at day 3 (**Fig. 2B**). In contrast, the elastic lamina was partially disrupted and degraded in the ascending aorta of *Apoe*$^{-/-}$*SmgGDS*$^{+/-}$ mice (**Fig. 2C**), and an entry could be seen, in which red blood cells were present between the elastic laminas of the degraded aortic walls (**Fig. 2C**, arrow). Additionally, in the descending aorta (**Fig. 2D**), we found accumulation of red blood cells in the false lumen of the aortic wall, which was connected to the enlarged abdominal aorta (**Fig. 2E**). In the aorta of *Apoe*$^{-/-}$ mice, almost all cells within the medial layer showed immunoreactivity for ACTA2 (**Fig. 2B**), whereas most of the cells in the aortic wall showed low ACTA2 expression in the thoracic aorta of *Apoe*$^{-/-}$*SmgGDS*$^{+/-}$ mice, especially around the dissection site (**Fig. 2F, G**, arrows). In contrast, the degradation of AoSMCs in the abdominal aorta was not severe compared with that observed in the ascending aorta of *Apoe*$^{-/-}$*SmgGDS*$^{+/-}$ mice at 3 days after AngII infusion (**Fig. 2H**). These histological changes were confirmed by electron microscopic analysis, showing the degradation of elastic fibers in the ascending aortic walls of *Apoe*$^{-/-}$*SmgGDS*$^{+/-}$ mice after AngII treatment (**Supplementary Fig. 5**, red arrows). Recent studies have shown that CD45$^{+}$ leukocytes in the adventitia are crucial for the development of TAA.[35] Thus, to determine the migration and accumulation of CD45$^{+}$ leukocytes at 3 days after AngII infusion, we used immunofluorescence and confocal microscopy (**Fig. 3A**). At day 3 after AngII infusion, CD45$^{+}$ leukocytes were only present in the adventitia of the ascending aorta obtained from *Apoe*$^{-/-}$*SmgGDS*$^{+/-}$ mice (**Fig. 3A**). Moreover, we found that the ACTA2 expression in the ascending aorta was reduced in *Apoe*$^{-/-}$ *SmgGDS*$^{+/-}$ mice compared with *Apoe*$^{-/-}$ mice, especially in the outer medial area of *Apoe*$^{-/-}$

Downloaded from http://circ.ahajournals.org/ by guest on June 20, 2018

*SmgGDS*$^{+/-}$ aorta (**Fig. 3A** and **Supplementary Fig. 6**, yellow arrows). These results indicate that AoSMCs in the ascending aorta of *Apoe*$^{-/-}$*SmgGDS*$^{+/-}$ mice show phenotype switching at the early phase of AngII infusion.

**Deletion of SmgGDS Reduces Fbn1 Expression in AoSMCs**

Fbn1 is secreted from AoSMCs and polymerizes to form microfibrils. Thus, mutations at this level disrupt the aortic structure and cause deposition of microfibrils into the matrix.[13] In light of the crucial role of Fbn1 as a secretory protein that provides force bearing structural support in elastic tissues, we then examined the role of SmgGDS in Fbn1 expression in the ascending aorta of both types of mouse. Immunostaining showed that Fbn1 expression was reduced in the aortic walls of *Apoe*$^{-/-}$*SmgGDS*$^{+/-}$ mice compared with *Apoe*$^{-/-}$ mice (**Fig. 3B**). Consistently, RT-PCR showed that Fbn1 expression was significantly lower in the ascending aorta of *Apoe*$^{-/-}$ *SmgGDS*$^{+/-}$ mice compared with *Apoe*$^{-/-}$ mice (**Fig. 3C**). Thus, to further evaluate the role of SmgGDS in AoSMCs, we performed microarray analysis using *Apoe*$^{-/-}$ and *Apoe*$^{-/-}$*SmgGDS*$^{+/-}$ AoSMCs. Heat map analysis showed significant changes in gene expressions of cardiovascular system development and function in *Apoe*$^{-/-}$*SmgGDS*$^{+/-}$ AoSMCs (**Supplementary Fig. 7A**). Importantly, IPA analysis showed downregulations of TGF-β1 and ROCK pathways in *Apoe*$^{-/-}$ *SmgGDS*$^{+/-}$ AoSMCs compared with *Apoe*$^{-/-}$AoSMCs (**Supplementary Fig. 7B, C**). In the aortic wall, the expression of Fbn1 was increased in the smooth muscle layers of both types of mouse. Thus, to further examine the possible role of SmgGDS in the development of TAA *in vivo*, we performed mechanistic experiments using AoSMCs *in vitro*. To evaluate the role of SmgGDS in AoSMCs, we harvested AoSMCs from the ascending aorta of *Apoe*$^{-/-}$ and *Apoe*$^{-/-}$ *SmgGDS*$^{+/-}$ mice. As a result, immunostaining showed that Fbn1 expression was reduced in

Downloaded from http://circ.ahajournals.org/ by guest on June 20, 2018

*Apoe*$^{-/-}$*SmgGDS*$^{+/-}$ AoSMCs compared with *Apoe*$^{-/-}$ AoSMCs (**Fig. 3D**). Consistently, RT-PCR showed that Fbn1 expression was significantly lower in *Apoe*$^{-/-}$*SmgGDS*$^{+/-}$ AoSMCs compared with *Apoe*$^{-/-}$AoSMCs (**Fig. 3E**). Additionally, compared with *Apoe*$^{-/-}$ AoSMCs, RT-PCR with *Apoe*$^{-/-}$*SmgGDS*$^{+/-}$ AoSMCs showed significantly reduced expression of *Acta2*, *Mlk*, *Myh11*, and *Prkg1*, all of which are causative gene mutations of TAA and TAD, compared with *Apoe*$^{-/-}$ AoSMCs (**Fig. 3F**). Importantly, *Apoe*$^{-/-}$*SmgGDS*$^{+/-}$ AoSMCs showed significantly reduced protein levels of SmgGDS, as well as Acta2 and calponin, compared with *Apoe*$^{-/-}$ AoSMCs (**Fig. 3G**). Additionally, *Apoe*$^{-/-}$*SmgGDS*$^{+/-}$ AoSMCs showed increased migration compared with *Apoe*$^{-/-}$ AoSMCs (**Fig. 3H**). *Apoe*$^{-/-}$*SmgGDS*$^{+/-}$ AoSMCs also showed significantly reduced activities of RhoA and Rap1 compared with *Apoe*$^{-/-}$ AoSMCs (**Fig. 3I**). Finally, we assessed the RhoC activity in response to cyclic stretch and AngII. Interestingly, AngII treatment significantly increased RhoC activity in *Apoe*$^{-/-}$AoSMCs, which was significantly lower in *Apoe*$^{-/-}$*SmgGDS*$^{+/-}$AoSMCs (**Fig. 3J**). In contrast, cyclic stretch significantly recued RhoC activity in *Apoe*$^{-/-}$AoSMCs, which was again significantly lower in *Apoe*$^{-/-}$*SmgGDS*$^{+/-}$AoSMCs (**Fig 3J**). These results indicate that deletion of SmgGDS in AoSMCs reduces expression of cytoskeleton genes and induces the pro-migrative phenotype in AoSMCs (**Fig. 3K**).

Based on the phenotype switching resulting from SmgGDS deficiency, we then examined the factors involved in the induction of SmgGDS in AoSMCs. In patients with TAA or TAD, pulsatile hemodynamic stress is one of the major promoting factors.[14] Thus, we stimulated AoSMCs with cyclic stretch (1 Hz) for 0, 3, and 24 hours (**Fig. 3L and Supplementary Fig. 8A**). Interestingly, we found significant upregulation of SmgGDS after

Downloaded from http://circ.ahajournals.org/ by guest on June 20, 2018

cyclic stretch for 3 hours (**Fig. 3L and Supplementary Fig. 8A**). SmgGDS interacts with RhoA[25] as a GEF[24] and controls the Rho and Rap1 family members,[28] promoting the GDP/GTP exchange reactions. Thus, we next checked the downstream signaling of RhoA. Interestingly, we observed stretch-mediated upregulation of RhoA, ROCK1, and ROCK2 in AoSMCs in a time-dependent manner (**Fig. 3L and Supplementary Fig. 8A**). Here, we further used *Apoe*$^{-/-}$ and *Apoe*$^{-/-}$*SmgGDS*$^{+/-}$ AoSMCs to evaluate the response to cyclic stretch. Importantly, *Apoe*$^{-/-}$ *SmgGDS*$^{+/-}$ AoSMCs showed significantly lower protein levels of Acta2 and calponin compared with *Apoe*$^{-/-}$ AoSMCs before and after the cyclic stretch (**Supplementary Fig. 8B**). Additionally, cyclic stretch significantly increased protein levels of Acta2 and calponin only in *Apoe*$^{-/-}$ AoSMCs (**Supplementary Fig. 8B**). In contrast, protein levels of Myh11 was significantly increased by cyclic stretch in *Apoe*$^{-/-}$*SmgGDS*$^{+/-}$ AoSMCs but not in *Apoe*$^{-/-}$ AoSMCs (**Supplementary Fig. 8B**). Next, examined the response to cyclic stretch in *SmgGDS*$^{+/+}$ *(wild-type)* AoSMCs and *SmgGDS*$^{+/-}$ AoSMCs (C57BL6 wild-type background) to evaluate the response to cyclic stretch. At baseline, there was no difference in the RhoA activity between *SmgGDS*$^{+/+}$ and *SmgGDS*$^{+/-}$ AoSMCs (**Supplementary Fig. 8C**). However, cyclic stretch significantly reduced RhoA activity only in *SmgGDS*$^{+/-}$ AoSMCs in a time-dependent manner (**Supplementary Figure 8C**). In contrast, RhoC activity was significantly lower in *SmgGDS*$^{+/-}$ AoSMCs compared with *SmgGDS*$^{+/+}$ AoSMCs at baseline, which was further exaggerated by cyclic stretch in a time-dependent manner (**Supplementary Figure 8C**). Additionally, gene mutations for TAA include the downstream signaling of TGF-β members, such as *TGFB2*, *TGFB3*, *TGFBR1*, *TGFBR2*, and *SMAD3*.[7-11] Here, *Apoe*$^{-/-}$*SmgGDS*$^{+/-}$ AoSMCs showed significantly reduced phosphorylation of Smad2/3 and protein levels of TGF-β,

Downloaded from http://circ.ahajournals.org/ by guest on June 20, 2018

and compensatory upregulation of Smad4, compared with *Apoe*$^{-/-}$ AoSMCs (**Fig. 3M and Supplementary Fig. 8D**). These results indicate that mechanical stretch induces SmgGDS, which activates downstream signaling of RhoA/Rho-kinase and TGF-β/Smad2/3/4 in AoSMCs (**Supplementary Fig. 8E**).

**Vascular SmgGDS, But Not Bone Marrow-derived SmgGDS, Plays a Protective Role Against TAA Formation**

Inflammation is a prerequisite for the development of cardiovascular diseases.[36] Indeed, it has been reported that mitogen-activated protein kinase (ERK1/2),[37] c-Jun N-terminal kinase (JNK),[38] and TGF-β[39] promote the development of aortic aneurysms. Here, to further elucidate the role of SmgGDS, we examined the levels of inflammatory cytokines and expressions of these signaling molecules in the thoracic aorta of *Apoe*$^{-/-}$ and *Apoe*$^{-/-}$*SmgGDS*$^{+/-}$ mice. We found higher levels of interleukin (IL)-1β, IL-2, IL-5, IL-6, IL-10, and CXCL1 in *Apoe*$^{-/-}$*SmgGDS*$^{+/-}$ aortas than in *Apoe*$^{-/-}$ aortas (**Fig. 4A**). Moreover, Western blotting showed that phosphorylation of ERK1/2 and JNK, and protein levels of TGF-β were significantly increased in thoracic aortas of *Apoe*$^{-/-}$*SmgGDS*$^{+/-}$ mice compared with *Apoe*$^{-/-}$ mice (**Fig. 4B and Supplementary Fig. 9A**). As these molecules are activated by several cytokines and chemokines, these results are consistent with the higher levels of inflammatory cytokines in *Apoe*$^{-/-}$*SmgGDS*$^{+/-}$ mouse aorta. Next, we analyzed the serum levels of cytokines/chemokines and growth factors in *Apoe*$^{-/-}$ and *Apoe*$^{-/-}$*SmgGDS*$^{+/-}$ mice. Again, we found higher levels of cytokines and growth factors in *Apoe*$^{-/-}$*SmgGDS*$^{+/-}$ mice compared with *Apoe*$^{-/-}$ mice (**Supplementary Fig. 9B**), suggesting that SmgGDS deficiency promotes aortic inflammation. Based on these results, we hypothesized that SmgGDS deficiency in inflammatory cells may

Downloaded from http://circ.ahajournals.org/ by guest on June 20, 2018

play crucial roles toward the development of aortic inflammation and TAA formation. Indeed, it is widely known that bone marrow (BM)-derived cells are involved in the pathogenesis of aortic aneurysm.[40] Thus, we hypothesized that SmgGDS deficiency in BM cells could promote AngII-induced TAA in *Apoe*$^{-/-}$*SmgGDS*$^{+/-}$ mice. To test this hypothesis, green fluorescent protein (GFP)-positive BM cells were transplanted into irradiated *Apoe*$^{-/-}$ or *Apoe*$^{-/-}$*SmgGDS*$^{+/-}$ mice (**Fig. 4C**). After reconstitution of the BM, chimeric mice were exposed to AngII for 4 weeks. En face aortic staining showed that the number of GFP$^{+}$ cells adhered to the aortic endothelial layer in the ascending aorta was greater in *Apoe*$^{-/-}$*SmgGDS*$^{+/-}$ mice than in *Apoe*$^{-/-}$ mice (**Fig. 4D**). Moreover, the number of GFP$^{+}$ cells in the adventitia of the chimeric mice was greater in *Apoe*$^{-/-}$*SmgGDS*$^{+/-}$ mice than in *Apoe*$^{-/-}$ mice (**Figs. 4E, F**). In particular, degradation of AoSMCs occurred in the medial layers adjacent to adventitial layers (**Supplementary Fig. 10**). Importantly, ACTA2 expressing aortic walls in the ascending aorta were degraded and invaded by GFP$^{+}$ BM-derived cells (**Figs. 4F, Supplementary Fig. 10**, yellow arrow). To further elucidate the cell phenotypes in the adventitia, we performed immunostaining of CD45$^{+}$ leukocytes (**Fig. 4G**). The number of CD45$^{+}$ leukocytes in the aortic walls was significantly higher in *Apoe*$^{-/-}$*SmgGDS*$^{+/-}$ chimeric mice compared with *Apoe*$^{-/-}$ chimeric mice (**Supplementary Fig. 11**). Moreover, GFP$^{+}$ cells migrated into the aortic walls between the elastic lamina (**Fig. 4G**, white arrows), and the aortic wall was degraded and almost ruptured (**Fig. 4G**, yellow arrow), suggesting a crucial role of BM-derived cells in AngII-induced TAA formation. Interestingly, the expression of cyclophilin A (CyPA), which augments ROS production,[40] was especially elevated in the accumulated inflammatory cells located within the adventitia or atherosclerotic lesions (**Fig. 4H**, **Supplementary Fig. 12**). Consistently, the

Downloaded from http://circ.ahajournals.org/ by guest on June 20, 2018

secretions of cytokines/chemokines and growth factors were significantly increased in AoSMCs harvested from the thoracic aorta of *Apoe*$^{-/-}$*SmgGDS*$^{+/-}$ mice compared with *Apoe*$^{-/-}$ mice (**Supplementary Fig. 13A**). We prepared conditioned medium (CM) from *Apoe*$^{-/-}$ or *Apoe*$^{-/-}$ *SmgGDS*$^{+/-}$ AoSMCs (**Supplementary Fig. 13B**). Treatment of AoSMCs showed significantly higher proliferation with *Apoe*$^{-/-}$*SmgGDS*$^{+/-}$ CM than *Apoe*$^{-/-}$ CM (**Supplementary Fig. 13C**). Moreover, treatment of AoSMCs with *Apoe*$^{-/-}$*SmgGDS*$^{+/-}$ CM resulted in significantly higher ROS production, assessed by staining with 2,7-dichlorodihydrofluorescein (DCF) and dihydroethidium (DHE), compared with *Apoe*$^{-/-}$ CM (**Supplementary Fig. 13C**). Thus, contrarily to our original notion, these results indicate that enhanced aortic inflammation in *Apoe*$^{-/-}$*SmgGDS*$^{+/-}$ mice is due to phenotypic changes in AoSMCs and upregulated inflammation in the recipient aorta. These results indicate that SmgGDS deficiency in the aorta promotes inflammatory cell migration and aortic rupture in response to AngII (**Supplementary Fig. 13D**).

**Deletion of SmgGDS Increases ROS in the Ascending Aorta**

Considering the importance of SmgGDS in AoSMC phenotypic changes, we next focused on the intracellular metabolic roles of SmgGDS toward inducing a higher inflammatory status. Recent studies have shown an emerging role of SmgGDS in nuclear translocation and degradation of Rac1, which is one of the components of NADPH oxidases.[32,33] To examine the role of SmgGDS as a modulator of ROS and mitochondrial function in AoSMCs, we used *Apoe*$^{-/-}$ and *Apoe*$^{-/-}$*SmgGDS*$^{+/-}$ AoSMCs. CellROX staining showed significantly higher levels of ROS in *Apoe*$^{-/-}$*SmgGDS*$^{+/-}$ AoSMCs than in *Apoe*$^{-/-}$ AoSMCs in response to AngII (**Fig. 5A, B**). Analyses with DCF and DHE also showed significantly higher levels of ROS in *Apoe*$^{-/-}$ *SmgGDS*$^{+/-}$ AoSMCs than in *Apoe*$^{-/-}$ AoSMCs in response to AngII (**Fig. 5C, D**). Likewise,

Downloaded from http://circ.ahajournals.org/ by guest on June 20, 2018

MitoSOX analysis showed significantly higher levels of mitochondrial ROS in *Apoe*$^{-/-}$ *SmgGDS*$^{+/-}$ AoSMCs than in *Apoe*$^{-/-}$ AoSMCs in response to AngII (**Fig. 5E**). Recent studies have suggested a mechanistic link among NADPH oxidase activities, ROS production, and SmgGDS-mediated Rac1 degradation.[31,33] Thus, we next examined the expression of NOX isoforms and NADPH activities in *Apoe*$^{-/-}$ and *Apoe*$^{-/-}$*SmgGDS*$^{+/-}$ AoSMCs. Interestingly, *Apoe*$^{-/-}$*SmgGDS*$^{+/-}$ AoSMCs showed higher *Nox1* expression compared with *Apoe*$^{-/-}$ AoSMCs, whereas there were no significant changes in *Nox2* or *Nox4* after AngII treatment (**Fig. 5F**). Moreover, Rac1 expression was significantly increased in *Apoe*$^{-/-}$*SmgGDS*$^{+/-}$ AoSMCs compared with *Apoe*$^{-/-}$AoSMCs after AngII treatment (**Fig. 5G**). Additionally, expression of Nrf2, which plays protective roles against oxidative stress, was significantly reduced in *Apoe*$^{-/-}$*SmgGDS*$^{+/-}$ AoSMCs compared with *Apoe*$^{-/-}$AoSMCs after AngII treatment (**Fig. 5G**). Consistently, *Apoe*$^{-/-}$*SmgGDS*$^{+/-}$ AoSMCs showed higher NADPH oxidase activities compared with *Apoe*$^{-/-}$ AoSMCs after AngII treatment (**Fig. 5H**).

To examine the effect of SmgGDS deficiency on ROS generation *in vivo*, aortic sections were incubated with DHE, in the presence of superoxide forms oxy-ethidium. In saline-infused ascending aorta, ROS production (red fluorescence) was very low in both *Apoe*$^{-/-}$ and *Apoe*$^{-/-}$ *SmgGDS*$^{+/-}$ mice (**Fig. 5I**). After 7 days of AngII treatment, oxy-ethidium fluorescence was increased in *Apoe*$^{-/-}$ mice aortas (**Fig. 5I**). Moreover, in *Apoe*$^{-/-}$*SmgGDS*$^{+/-}$ mice, ROS production was significantly higher in response to AngII compared with *Apoe*$^{-/-}$ mice (**Fig. 5I, J**). These *in vivo* and *in vitro* data suggest that AngII-induced ROS production in AoSMCs is inhibited by SmgGDS. Consistently, Rac1 levels were significantly increased in *Apoe*$^{-/-}$ *SmgGDS*$^{+/-}$ aortas compared with *Apoe*$^{-/-}$ aortas (**Fig. 5K**). These results indicate that

Downloaded from http://circ.ahajournals.org/ by guest on June 20, 2018

SmgGDS plays protective roles against AngII-induced NADPH oxidase activation and ROS production in AoSMCs.

**SmgGDS Prevents MMP Activation and Perivascular Inflammation**

Development of aortic aneurysm and rupture depends on MMP activities in the aortic wall, which are promoted by extracellular CyPA-mediated ROS augmentation.[18,40,41] Secreted CyPA activates MMPs through the extracellular MMP protein inducer (EMMPRIN).[42,43] Based on the increased ROS in *Apoe*$^{-/-}$*SmgGDS*$^{+/-}$ aortas compared with *Apoe*$^{-/-}$ aortas, we considered that MMP activities would increase in the absence of SmgGDS. Indeed, RT-PCR showed significantly higher expression of *Mmp2* and *Mmp9* in *Apoe*$^{-/-}$*SmgGDS*$^{+/-}$ AoSMCs compared with *Apoe*$^{-/-}$ AoSMCs (**Fig. 6A**). Consistently, MMP activities, assessed by *in situ* zymography (DQ gelatin), which generates green fluorescence in the presence of active MMPs, were significantly increased in *Apoe*$^{-/-}$*SmgGDS*$^{+/-}$ AoSMCs compared with *Apoe*$^{-/-}$ AoSMCs after AngII treatment (**Figs. 6B, C**). Moreover, secretion of CyPA from AoSMCs was significantly higher in *Apoe*$^{-/-}$*SmgGDS*$^{+/-}$ AoSMCs than in *Apoe*$^{-/-}$ AoSMCs (**Fig. 6D**), suggesting an inhibitory role of SmgGDS in CyPA-mediated MMP activation. To examine the effect of SmgGDS deficiency on MMP activation *in vivo*, ascending aortic sections were incubated with DQ gelatin. MMP activity was negligible in the saline-treated aorta (**Fig. 6E**). Following AngII treatment, the media and adventitia of *Apoe*$^{-/-}$*SmgGDS*$^{+/-}$ mice showed higher MMP activity compared with *Apoe*$^{-/-}$ mice (**Figs. 6E, F**). Similarly, CyPA expression was higher in ascending *Apoe*$^{-/-}$*SmgGDS*$^{+/-}$ aorta compared with *Apoe*$^{-/-}$ aorta, especially in the TAA lesions with higher MMP activities (**Supplementary Fig. 14**). In organ culture, conditioned medium obtained from the aorta of AngII-treated *Apoe*$^{-/-}$*SmgGDS*$^{+/-}$ mice showed higher levels of

Downloaded from http://circ.ahajournals.org/ by guest on June 20, 2018

proMMP-9 and activated MMP-9 assessed by zymography compared with the *Apoe*$^{-/-}$ aorta (**Fig. 6G**). Additionally, Western blotting showed that secretion of MMP-12 from AngII-treated *Apoe*$^{-/-}$*SmgGDS*$^{+/-}$ aorta was significantly higher compared with the *Apoe*$^{-/-}$ aorta (**Fig. 6H**). Next, since the activation of MMPs promotes perivascular inflammation, we further examined the protective roles of SmgGDS against AngII-induced inflammatory cell migration. As expected, AngII exacerbated perivascular inflammation in the *Apoe*$^{-/-}$ aorta, whereas the *Apoe*$^{-/-}$ *SmgGDS*$^{+/-}$ aorta showed more accumulation of perivascular Mac-3$^{+}$ inflammatory cells (**Supplementary Fig. 15**). These *in vivo* and *in vitro* data indicate that SmgGDS plays protective roles against MMP activation and perivascular inflammation through inhibition of CyPA secretion (**Fig. 6I**).

**SmgGDS Inhibits CyPA-mediated MMP Activation in TAA-AoSMCs**

Based on the influence of SmgGDS on MMP activities and CyPA secretion *in vivo* and *in vitro*, we next examined the role of SmgGDS in human TAA lesions. SmgGDS expression was lower in the ascending aortic wall of TAA lesions, especially in the areas with active MMPs (**Fig. 7A**). Based on the inhibitory role of SmgGDS on MMPs, we considered that MMP activities would be reduced by SmgGDS in TAA-AoSMCs. Here, we used TAA-AoSMCs to evaluate SmgGDS-mediated MMP activities. Importantly, AngII-mediated secretion of CyPA from AoSMCs was significantly higher in TAA-AoSMCs compared with control AoSMCs (**Fig. 7B**). Consistently, plasma levels of CyPA were significantly increased in patients with TAA compared with controls (**Fig. 7C and Supplementary Table 4**). Moreover, plasma CyPA levels were significantly increased in patients with AAA compared with controls (**Fig. 7C**). In response to AngII, MMP activity was strongly increased in TAA-AoSMCs compared with control AoSMCs

Downloaded from http://circ.ahajournals.org/ by guest on June 20, 2018

(**Fig. 7D**). Consistently, AngII-mediated ROS production, assessed by DCF and DHE, was significantly increased in TAA-AoSMCs compared with control AoSMCs (**Fig. 7E**). Moreover, AngII-mediated mitochondrial ROS production, assessed by MitoSOX, was significantly increased in TAA-AoSMCs compared with control AoSMCs (**Fig. 7E**). Importantly, AngII treatment of AoSMCs for 3 days significantly reduced ACTA2 levels in TAA-AoSMCs, but not in control AoSMCs (**Fig. 7F**). In contrast, AngII treatment of AoSMCs for 3 days significantly reduced calponin levels in both TAA-AoSMCs and control AoSMCs (**Fig. 7F**). Moreover, AngII treatment of AoSMCs significantly reduced SmgGDS levels only in TAA-AoSMCs in a time-dependent manner (**Fig. 7G**). These results suggest the AngII-mediated downregulation of SmgGDS in TAA-AoSMCs, plays crucial roles in CyPA secretion, MMP activation, and ROS production in human TAA lesions. Thus, SmgGDS-mediated phenotypic control of TAA-AoSMCs may play a crucial role in the maintenance of the ascending aorta and inhibit aortic dilatation and TAA. Thus, we finally performed an *in vivo* study aiming at rescuing *Apoe*$^{-/-}$*SmgGDS*$^{+/-}$ mice from the development of TAA by local overexpression of SmgGDS in the ascending aorta (**Fig. 8A**). Local delivery of SmgGDS gene construct around the ascending aorta successfully enabled the overexpression of SmgGDS in the ascending aorta of *Apoe*$^{-/-}$*SmgGDS*$^{+/-}$ mice (**Fig. 8B**). Pathological analyses of the ascending aorta showed an enhanced expression of SmgGDS, especially in the adventitia (**Fig. 8C**), reduced ROS production (**Fig. 8D**), and MMP activities (**Fig. 8E**) in the ascending aortas of *Apoe*$^{-/-}$*SmgGDS*$^{+/-}$ mice after AngII treatment for 3 days. Importantly, AngII-mediated degradation of the ascending aorta was protected by local SmgGDS overexpression in *Apoe*$^{-/-}$*SmgGDS*$^{+/-}$ mice (**Fig. 8F**). Thus, local SmgGDS overexpression completely inhibited TAA rupture in *Apoe*$^{-/-}$

Downloaded from http://circ.ahajournals.org/ by guest on June 20, 2018

*SmgGDS*$^{+/-}$ mice (**Fig. 8G**). In contrast, local SmgGDS overexpression in the ascending aorta did not affect AAA formation in *Apoe*$^{-/-}$*SmgGDS*$^{+/-}$ mice (**Fig. 8H**). Finally, local SmgGDS overexpression completely inhibited ascending aortic dilatation in *Apoe*$^{-/-}$*SmgGDS*$^{+/-}$ mice (**Fig. 8I**), whereas there was no change in the abdominal aorta (**Fig. 8J**). These results indicate that local SmgGDS overexpression rescues *Apoe*$^{-/-}$*SmgGDS*$^{+/-}$ mice from TAA formation and rupture through downregulation of ROS production and MMP activation in AoSMCs.

Downloaded from http://circ.ahajournals.org/ by guest on June 20, 2018

## Discussion

The present study demonstrates for the first time that downregulation of SmgGDS in AoSMCs contributes to the pathogenesis of TAA, which involves dysfunction of AoSMCs, and enhanced ROS production and MMP activities. These conclusions are based on the following findings; SmgGDS deficiency (1) enhanced the development of AngII-induced TAA and TAD in mice, (2) increased migration of inflammatory cells, (3) reduced gene expression of force generation proteins, (4) increased ROS production and activated MMPs, (5) increased cytokines/chemokines and growth factors in AoSMCs, (6) promoted phenotypic switching from the contractile phenotype to the synthetic and inflammatory one in AoSMCs, and (7) local overexpression of SmgGDS around the thoracic aorta inhibited aortic dilatation and rupture in SmgGDS-deficient mice. Thus, the present study proposes SmgGDS as a novel target toward the development of innovative therapies for patients with TAA and TAD.

### SmgGDS as a Novel Pathogenic Protein in TAA

AoSMCs in the aorta need to adhere to the extracellular matrix to form contractile elements that link to microfibrils surrounding the elastin fibers.[13] Fbn1 is a cysteine-rich glycoprotein that

plays a major role in the function mechanism of microfibrils.[13] Genetic mutation of *FBN1* predisposes patients with Marfan syndrome to thoracic aortic disease.[44] In addition, genome-wide association studies (GWAS) have shown that common variants in *FBN1* predispose the general population to TAA and TAD.[45] In the present study, we showed a significant reduction of Fbn1 expression in the aortas and AoSMCs as a result of SmgGDS deletion in mice. Importantly, we found lower expression of *FBN1* and *SmgGDS* in AoSMCs from non-Marfan TAA patients, suggesting that Fbn1 may also play a crucial role in non-heritable TAA patients. The mechanistic link between SmgGDS inhibition and downregulation of Fbn1 in TAA patients still remains unclear. However, we consider that the risk factors for TAA, such as hypertension, aging, and smoking, enhance ROS production, thereby reducing SmgGDS in AoSMCs, resulting in destabilization of the aortic walls and promotion of TAA formation. In the present study, mechanical stretch induced SmgGDS expression, which stabilizes the active form of RhoA and increases expression of force generating proteins in AoSMCs. Thus, mechanical stretch-mediated SmgGDS induction may play a crucial role toward protecting the ascending aorta from continuous mechanical stretch, which in turn, prevents the ascending aorta from dilatation, dissection, and rupture, especially in patients with hypertension. Indeed, force generation genes, such as *Myh11*, *Mlk*, *Acta2*, and *Prkg1*, were significantly downregulated in *SmgGDS*$^{+/-}$ AoSMCs. Since mutations of these force generation genes cause hereditary TAA and TAD, SmgGDS-mediated activation of RhoA and downstream Rho-kinase should be substantially involved in the conservation of the contractile phenotype of AoSMCs.[23] Indeed, SmgGDS is one of the GEFs for RhoA, and therefore, regulates its activities.[25] In contrast, SmgGDS deficiency reduces RhoA activity, leading to the phenotypic switching of AoSMCs.

Downloaded from http://circ.ahajournals.org/ by guest on June 20, 2018

Since Fbn1 is one of the ECM that maintains the aortic wall, phenotypic switching of AoSMCs and altered gene interactions may downregulate the Fbn1 expression. Interestingly, AoSMCs exposed to AngII for a long period of time reduced their SmgGDS expression in a time-dependent manner. Additionally, SmgGDS translocate Rap1 to the plasma membrane,[46] which in turn inhibits GAPs, leading to inactivation of RhoA.[47] Thus, this switching phenomenon from the active form of RhoA to its inactive one, results in reduced expression of force generation genes and promotes the synthetic phenotype in AoSMCs (**Supplementary Fig. 16**). Further analyses will help us clearly understand the mechanisms driving the SmgGDS-mediated regulations of Fbn1 and force generation genes.

Downloaded from http://circ.ahajournals.org/ by guest on June 20, 2018

**SmgGDS Deficiency Induces ROS Production**

ROS levels in the aortas are significantly increased in mouse models of Marfan and Loeys-Dietz syndromes.[48,49] SmgGDS degrades Rac1, which is a key component of NADPH oxidases.[29] AngII stimulates $O_2^-$ generation by activating an NADH/NADPH oxidase and leads to vascular hypertrophy. In addition, Nox1-dependent ROS generation is regulated by Rac1.[50] In the present study, expressions of Rac1 and NADPH oxidase activities were increased in *SmgGDS*$^{+/-}$ AoSMCs after AngII treatment. In addition, secretion of CyPA from AoSMCs, which augments ROS production,[40] was significantly increased in *SmgGDS*$^{+/-}$ AoSMCs and aortic tissues. Indeed, deletion of SmgGDS augmented ROS production in AoSMCs and the aortic walls after AngII treatment. Increased ROS production promotes migration of inflammatory cells and ECM production, and results in the destabilization of the aortic wall. Moreover, secretion of cytokines/chemokines and growth factors significantly increased in *SmgGDS*$^{+/-}$ AoSMCs, which enhanced the production of ROS in an autocrine/paracrine manner.

Importantly, we found a significant increase in ROS production in the ascending aorta at day 3 after AngII treatment. In the early phase of AngII treatment, deletion of SmgGDS significantly induced ROS production in the ascending aorta. When we consider the role of ROS in the augmentation of vascular inflammation and recruitment of BM-derived cells in the adventitia, the early and enhanced production of ROS, resulting from the deletion of SmgGDS, should considerably contribute to the dilatation and dissection of the ascending aorta in SmgGDS-deficient mice. Through precise histological analyses with confocal microscopy, we found accumulation of BM-derived cells in the adventitia, and showed their migration between the elastic laminas in the ascending aorta of chimeric mice at day 3 after AngII treatment. Thus, enhanced ROS production in the aortic walls may be the initial and principal mechanism governing the secretion of cytokines/ chemokines and growth factors and subsequent recruitment of excessive BM-derived cells in the aorta of *SmgGDS*$^{+/-}$ mice. Following this process, migration of BM-derived cells in response to chemotactic factors secreted from the aortic wall leads to the destruction of the elastic lamina and induces TAA and TAD in *SmgGDS*$^{+/-}$ mice. The vicious circle through which ROS are produced by AoSMCs and inflammatory cells destabilizes the *SmgGDS*$^{+/-}$ aortas in response to AngII treatment. Taken together, SmgGDS prevents AngII-induced ROS production, which in turn inhibits inflammatory cell recruitment and aortic dissection.

**SmgGDS Deficiency Activates MMPs and ECM Remodeling**

Activation of MMPs, which degrade arterial elastin and promote destabilization of the aorta, plays a crucial role in a wide range of vascular diseases.[51,52] In patients with Marfan syndrome and bicuspid aortic valve, the expression of MMP-2 is increased in AoSMCs, which results in

Downloaded from http://circ.ahajournals.org/ by guest on June 20, 2018

their apoptosis.[53] Enhanced inflammation and ROS production directly activates MMPs,[54] promoting the development of aortic aneurysms.[55,56] Additionally, in mouse models of Marfan syndrome, MMPs play a key role in the development of TAA.[57,58] ECM affects cellular behavior in physiological and pathological processes, and provides structural support.[59] Moreover, ECM affects the inflammatory signaling in response to extracellular growth factors, and thereby, controls cell proliferation and migration.[59] In the present study, we demonstrated that the deletion of SmgGDS dramatically increased the expression of MMP-2 and MMP-9, the secretion of CyPA, and MMP activities *in vivo* and *in vitro*. Consistently, we found significant upregulation of ERK and JNK signaling, as well as an enhanced non-canonical TGF-β pathway, in *SmgGDS*$^{+/-}$ mice. ROS production was increased by SmgGDS deficiency, resulting in increased MMP activities in the ascending aorta. Thus, SmgGDS deficiency increased ascending aortic dissection and aneurysm formation *in vivo*. These results suggest that SmgGDS prevents ECM remodeling and development of TAA by downregulating the expression of MMP-2 and MMP-9, as well as decreasing CyPA secretion and TGF-β signaling.

**SmgGDS Deficiency Promotes Phenotypic Switching in AoSMCs**

The initial event leading to aortic aneurysm formation is the phenotypic switching of AoSMCs.[16] The synthetic and pro-inflammatory phenotype is the basal status for the degradation of the ECM, the weakening of the aortic wall, and TAA rupture.[16] In the present study, *SmgGDS*$^{+/-}$ AoSMCs showed reduced expression of force generation genes and increased secretion of cytokines/ chemokines and growth factors. Here, SmgGDS is one of the GEFs for RhoA and Rac1, which controls the contraction of AoSMCs.[23,28] Thus, lower expression of SmgGDS leads to reduced RhoA activity, resulting in the phenotypic switching of AoSMCs. Synthetic

Downloaded from http://circ.ahajournals.org/ by guest on June 20, 2018

and inflammatory phenotype in AoSMCs produces inflammatory cytokines, resulting in the increased recruitment of inflammatory cells, ROS production, and MMP activation. Accumulated inflammatory cells in the aortic walls also produce abundant ROS and MMPs, promoting the conversion of AoSMCs into the synthetic type.[19] These processes represent a vicious circle leading to increased ROS production and MMP activation in the ascending aorta, and the development of TAA. Importantly, the expression of *ACTA2* was significantly reduced in *SmgGDS*$^{+/-}$ aortas and AoSMCs. The expression of *ACTA2* is controlled by the transcription factors in the promoter region and is an important indicator of the normal contractile phenotype in AoSMCs.[16] Indeed, dilatation of the aortic root has been shown in *ACTA2* knockout mice.[60] Interestingly, in the present study, the incidence of AAA was not affected by the deletion of SmgGDS, suggesting a different pathogenesis involved between TAA and AAA. Thus, the development of AAA is not regulated by SmgGDS-mediated phenotypic switching of AoSMCs. Taken together, these results suggest that SmgGDS plays a protective role against the phenotypic switching of AoSMCs, and prevents the development of TAA and TAD.

Downloaded from http://circ.ahajournals.org/ by guest on June 20, 2018

**A Novel Therapeutic Target for TAA**

The present study suggests that SmgGDS plays protective roles against the development of TAA. Indeed, local delivery of SmgGDS gene construct in the aortic arch reduced the dilatation of the ascending aorta in *SmgGDS*$^{+/-}$ mice. Thus, upregulated SmgGDS in the ascending aorta may prevent aortic dilatation and the development of TAA in clinical settings. This suggests that agents that upregulate SmgGDS may represent novel drugs for TAA. Thus, it is important to explore molecules that upregulate SmgGDS in AoSMCs. The traditional approach toward developing a novel drug and bringing it to the clinical stage is costly. To solve this problem,

drug repositioning is an attractive approach. Among the drugs currently used for the treatment of other diseases, we may find a drug that upregulates SmgGDS in AoSMCs and inhibits the development of TAA. In the future, screening of agents that upregulate SmgGDS in AoSMCs may provide a novel strategy toward curing patients with TAA. Hypertension increases mechanical stress in the ascending aorta and leads to aortic dissection and rupture.[2] Thus, the present study provides a molecular mechanism for the SmgGDS-mediated protection of the ascending aorta from excessive dilatation, and may explain, in part, the importance of lower control of blood pressure toward preventing TAA and TAD.[2] Interestingly, we have previously demonstrated that administration of statins upregulates SmgGDS in the peripheral leucocytes of healthy volunteers.[31] Consistently, statins have been shown to inhibit the development of TAA and TAD.[61] However, the mechanisms for the upregulation of SmgGDS by statins remain unclear. Thus, we need to elucidate the detailed mechanisms that regulate SmgGDS expression in AoSMCs, which is downregulated by risk factors of TAA.

Downloaded from http://circ.ahajournals.org/ by guest on June 20, 2018

**Study Limitations**

The present study has several limitations. First, we were unable to directly demonstrate the mechanisms that regulate SmgGDS-mediated gene expressions of force generation proteins. Second, the number of analyses of clinical samples was not high enough to allow the assessment of SmgGDS in patients with TAA and TAD. Additional studies are needed to enable the clinical application of the present study.

**Clinical Implication and Conclusions**

Despite the rapid progress in the last decade regarding the research on TAA, only a few cures have been proposed to prevent this devastating disease.[62] TAA is a progressive disease,

developing silently, and rupture leads to a fatal outcome. Thus, early diagnosis and medical therapy are urgently needed. Previous studies showed that genetic disorders cause TAA[2], in which phenotypic switching of AoSMCs plays a crucial role. In this regard, the present study adds to the current understanding of TAA pathology, showing that mechanical stretch induces SmgGDS and downstream force generation proteins, all of which are important for mechanical support in the aortic wall. Given the severe side effects of protease inhibitors (such as broad-spectrum MMP inhibitors) in clinical trials, SmgGDS could be a promising and potentially safe drug target. Moreover, further studies are needed to use SmgGDS as a diagnostic biomarker for TAA. It is now widely accepted that epigenetic modifications are key factors in aortic diseases, following environmental stimuli (e.g., hypertension and infection).[63,64] DNA methylation is a common epigenetic modification, and the methylation status of the SmgGDS gene in TAA-AoSMCs would represent a promising research area. Furthermore, epigenetic modification can be modulated by SNPs, as clearly illustrated in several studies related to cardiovascular diseases. Thus, genome screening for the SmgGDS gene and SmgGDS-associated genes could be beneficial for TAA patients. Finally, risk factors that reduce SmgGDS expression should be confirmed to prevent TAA formation and rupture.

In conclusion, the present study demonstrates that SmgGDS in the ascending aorta plays important protective roles against excessive aortic dilatation and inflammation, thereby preventing the development of TAA and TAD.

Downloaded from http://circ.ahajournals.org/ by guest on June 20, 2018

**Acknowledgments**

We are grateful to the laboratory members in the Department of Cardiovascular Medicine of the Tohoku University for valuable technical assistance, especially to Yumi Watanabe, Ai Nishihara, and Hiromi Yamashita.

**Sources of Funding**

This work was supported in part by the grants-in-aid for Scientific Research (15H02535, 15H04816, and 15K15046) from the Ministry of Education, Culture, Sports, Science and Technology, Tokyo, Japan, the grants-in-aid for Scientific Research from the Ministry of Health, Labour, and Welfare, Tokyo, Japan (10102895), and the grants-in-aid for Scientific Research from the Japan Agency for Medical Research and Development, Tokyo, Japan (15ak0101035h0001, 16ek0109176h0001, 17ek0109227h0001).

Downloaded from http://circ.ahajournals.org/ by guest on June 20, 2018

**Disclosures**

None.

## References

1. Mallat Z, Ait-Oufella H and Tedgui A. The pathogenic transforming growth factor-β overdrive hypothesis in aortic aneurysms and dissections: A mirage? *Circ Res*. 2017;120:1718-1720. doi:10.1161/CIRCRESAHA.116.310371
2. Lu H and Daugherty A. Aortic aneurysms. *Arterioscler Thromb Vasc Biol*. 2017;37:e59-e65. doi:10.1161/ATVBAHA.117.309578
3. Sakai LY, Keene DR, Renard M and De Backer J. *FBN1*: The disease-causing gene for Marfan syndrome and other genetic disorders. *Gene*. 2016;591:279-291. doi:10.1016/j.gene.2016.07.033
4. Guo DC, Pannu H, Tran-Fadulu V, Papke CL, Yu RK, Avidan N, Bourgeois S, Estrera AL, Safi HJ, Sparks E, Amor D, Ades L, McConnell V, Willoughby CE, Abuelo D, Willing M, Lewis RA, Kim DH, Scherer S, Tung PP, Ahn C, Buja LM, Raman CS, Shete

SS and Milewicz DM. Mutations in smooth muscle α-actin (*ACTA2*) lead to thoracic aortic aneurysms and dissections. *Nat Genet*. 2007;39:1488-1493. doi:10.1038/ng.2007.6

5. Zhu L, Vranckx R, Khau Van Kien P, Lalande A, Boisset N, Mathieu F, Wegman M, Glancy L, Gasc JM, Brunotte F, Bruneval P, Wolf JE, Michel JB and Jeunemaitre X. Mutations in myosin heavy chain 11 cause a syndrome associating thoracic aortic aneurysm/aortic dissection and patent ductus arteriosus. *Nat Genet*. 2006;38:343-349. doi:10.1038/ng1721
6. Wang L, Guo DC, Cao J, Gong L, Kamm KE, Regalado E, Li L, Shete S, He WQ, Zhu MS, Offermanns S, Gilchrist D, Elefteriades J, Stull JT and Milewicz DM. Mutations in myosin light chain kinase cause familial aortic dissections. *Am J Hum Genet*. 2010;87:701-707. doi:10.1016/j.ajhg.2010.10.006
7. Boileau C, Guo DC, Hanna N, Regalado ES, Detaint D, Gong L, Varret M, Prakash SK, Li AH, d'Indy H, Braverman AC, Grandchamp B, Kwartler CS, Gouya L, Santos-Cortez RL, Abifadel M, Leal SM, Muti C, Shendure J, Gross MS, Rieder MJ, Vahanian A, Nickerson DA, Michel JB, National Heart L, Blood Institute Go Exome Sequencing P, Jondeau G and Milewicz DM. *TGFB2* mutations cause familial thoracic aortic aneurysms and dissections associated with mild systemic features of Marfan syndrome. *Nat Genet*. 2012;44:916-921. doi:10.1038/ng.2348
8. Bertoli-Avella AM, Gillis E, Morisaki H, Verhagen JM, de Graaf BM, van de Beek G, Gallo E, Kruithof BP, Venselaar H, Myers LA, Laga S, Doyle AJ, Oswald G, van Cappellen GW, Yamanaka I, van der Helm RM, Beverloo B, de Klein A, Pardo L, Lammens M, Evers C, Devriendt K, Dumoulein M, Timmermans J, Bruggenwirth HT, Verheijen F, Rodrigus I, Baynam G, Kempers M, Saenen J, Van Craenenbroeck EM, Minatoya K, Matsukawa R, Tsukube T, Kubo N, Hofstra R, Goumans MJ, Bekkers JA, Roos-Hesselink JW, van de Laar IM, Dietz HC, Van Laer L, Morisaki T, Wessels MW and Loeys BL. Mutations in a TGF-β ligand, *TGFB3*, cause syndromic aortic aneurysms and dissections. *J Am Coll Cardiol*. 2015;65:1324-1336. doi:10.1016/j.jacc.2015.01.040
9. Bart L. Loeys MD, Ph.D.,, Ulrike Schwarze MD, Tammy Holm MD, Bert L. Callewaert MD, George H. Thomas PD, Hariyadarshi Pannu PD, Julie F. De Backer MD, Gretchen L. Oswald MS, Sofie Symoens BS, Sylvie Manouvrier MD, Ph.D.,, Amy E. Roberts MD, Francesca Faravelli MD, M. Alba Greco MD, Reed E. Pyeritz MD, Ph.D.,, Dianna M. Milewicz MD, Ph.D.,, Paul J. Coucke PD, Duke E. Cameron MD, Alan C. Braverman MD, Peter H. Byers MD, Anne M. De Paepe MD, Ph.D., and Harry C. Dietz MD. Aneurysm syndromes caused by mutations in the TGF-β receptor. *N Engl J Med*. 2006;355:788-798. doi:10.1056/NEJMoa055695
10. Mizuguchi T, Collod-Beroud G, Akiyama T, Abifadel M, Harada N, Morisaki T, Allard D, Varret M, Claustres M, Morisaki H, Ihara M, Kinoshita A, Yoshiura K, Junien C, Kajii T, Jondeau G, Ohta T, Kishino T, Furukawa Y, Nakamura Y, Niikawa N, Boileau C and Matsumoto N. Heterozygous *TGFBR2* mutations in Marfan syndrome. *Nat Genet*. 2004;36:855-860. doi:10.1038/ng1392
11. Pannu H, Fadulu VT, Chang J, Lafont A, Hasham SN, Sparks E, Giampietro PF, Zaleski C, Estrera AL, Safi HJ, Shete S, Willing MC, Raman CS and Milewicz DM. Mutations in transforming growth factor-β receptor type II cause familial thoracic aortic aneurysms and dissections. *Circulation*. 2005;112:513-520. doi:10.1161/CIRCULATIONAHA.105.537340
12. Guo DC, Regalado E, Casteel DE, Santos-Cortez RL, Gong L, Kim JJ, Dyack S, Horne

Downloaded from http://circ.ahajournals.org/ by guest on June 20, 2018

SG, Chang G, Jondeau G, Boileau C, Coselli JS, Li Z, Leal SM, Shendure J, Rieder MJ, Bamshad MJ, Nickerson DA, Gen TACRC, National Heart L, Blood Institute Grand Opportunity Exome Sequencing P, Kim C and Milewicz DM. Recurrent gain-of-function mutation in *PRKG1* causes thoracic aortic aneurysms and acute aortic dissections. *Am J Hum Genet*. 2013;93:398-404. doi:10.1016/j.ajhg.2013.06.019

13. Milewicz DM, Trybus KM, Guo DC, Sweeney HL, Regalado E, Kamm K and Stull JT. Altered smooth muscle cell force generation as a driver of thoracic aortic aneurysms and dissections. *Arterioscler Thromb Vasc Biol*. 2017;37:26-34. doi:10.1161/ATVBAHA.116.303229
14. Schaheen B, Downs EA, Serbulea V, Almenara CC, Spinosa M, Su G, Zhao Y, Srikakulapu P, Butts C, McNamara CA, Leitinger N, Upchurch GR, Jr., Meher AK and Ailawadi G. B-cell depletion promotes aortic infiltration of immunosuppressive cells and is protective of experimental aortic aneurysm. *Arterioscler Thromb Vasc Biol*. 2016;36:2191-2202. doi:10.1161/ATVBAHA.116.307559
15. Ailawadi G, Moehle CW, Pei H, Walton SP, Yang Z, Kron IL, Lau CL and Owens GK. Smooth muscle phenotypic modulation is an early event in aortic aneurysms. *J Thorac Cardiovasc Surg*. 2009;138:1392-1399. doi:10.1016/j.jtcvs.2009.07.075
16. Liu R, Lo L, Lay AJ, Zhao Y, Ting KK, Robertson EN, Sherrah AG, Jarrah SR, Li H, Zhou Z, Hambly BD, Richmond DR, Jeremy RW, Bannon PG, Vadas MA and Gamble J. ARHGAP18 protects against thoracic aortic aneurysm formation by mitigating the synthetic and pro-inflammatory smooth muscle cell phenotype. *Circ Res*. 2017;121:512-524. doi:10.1161/CIRCRESAHA.117.310692
17. Weiser-Evans MCM. Smooth muscle differentiation control comes full circle: The circular noncoding RNA, circ*ACTA2*, functions as a miRNA sponge to fine-tune α-SMA expression. *Circ Res*. 2017;121:591-593. doi:10.1161/CIRCRESAHA.117.311722
18. Fan LM, Douglas G, Bendall JK, McNeill E, Crabtree MJ, Hale AB, Mai A, Li JM, McAteer MA, Schneider JE, Choudhury RP and Channon KM. Endothelial cell-specific reactive oxygen species production increases susceptibility to aortic dissection. *Circulation*. 2014;129:2661-2672. doi:10.1161/CIRCULATIONAHA.113.005062
19. Liu R, Leslie KL and Martin KA. Epigenetic regulation of smooth muscle cell plasticity. *Biochim Biophys Acta*. 2015;1849:448-453. doi:10.1016/j.bbagrm.2014.06.004
20. Sawada H, Rateri DL, Moorleghen JJ, Majesky MW and Daugherty A. Smooth muscle cells derived from second heart field and cardiac neural crest reside in spatially distinct domains in the media of the ascending aorta. *Arterioscler Thromb Vasc Biol*. 2017;37:1722-1726. doi:10.1161/ATVBAHA.117.309599
21. de Carcer G, Wachowicz P, Martinez-Martinez S, Oller J, Mendez-Barbero N, Escobar B, Gonzalez-Loyola A, Takaki T, El Bakkali A, Camara JA, Jimenez-Borreguero LJ, Bustelo XR, Canamero M, Mulero F, de Los Angeles Sevilla M, Montero MJ, Redondo JM and Malumbres M. Plk1 regulates contraction of postmitotic smooth muscle cells and is required for vascular homeostasis. *Nat Med*. 2017;23:964-974. doi:10.1038/nm.4364
22. Satoh K, Kikuchi N, Kurosawa R and Shimokawa H. PDE1C negatively regulates growth factor receptor degradation and promotes VSMC proliferation. *Circ Res*. 2015;116:1098-1100. doi:10.1161/CIRCRESAHA.115.306139
23. Mack CP, Somlyo AV, Hautmann M, Somlyo AP and Owens GK. Smooth muscle differentiation marker gene expression is regulated by RhoA-mediated actin polymerization. *J Biol Chem*. 2001;276:341-347. doi:10.1074/jbc.M005505200

Downloaded from http://circ.ahajournals.org/ by guest on June 20, 2018

24. Isomura M, Kaibuchi K, Yamamoto T, Kawamura S, Katayama M and Takai Y. Partial purification and characterization of GDP dissociation stimulator (GDS) for the Rho proteins from bovine brain cytosol. *Biochem and Biophys Res Commun*. 1990;169:652-659. doi:10.1016/0006-291X/90
25. Hideaki Y, Takuya S and Yoshimi T. The Dbl oncogene product as a GDP/GTP exchange protein for the Rho family: its properties in comparison with those of SmgGDS. *Biochem Biophys Res Commun*. 1994;198:811-817. doi:0006-291X/94
26. Telikicherla D, Maharudraiah J, Pawar H, Marimuthu A, Kashyap MK, Ramachandra YL, Roa JC and Pandey A. Overexpression of kinesin associated protein 3 (*KIFAP3*) in breast cancer. *J Proteomics Bioinform*. 2012;5:122-126. doi:10.4172/jpb.1000223
27. Haris G V, Scott S and Kun-Liang G. SmgGDS displays differential binding and exchange activity towards different Ras isoforms. *Oncogene*. 2002;21:2425-2432. doi:10.1038/sj/onc/1205306
28. Berg TJ, Gastonguay AJ, Lorimer EL, Kuhnmuench JR, Li R, Fields AP and Williams CL. Splice variants of SmgGDS control small GTPase prenylation and membrane localization. *J Biol Chem*. 2010;285:35255-35266. doi:10.1074/jbc.M110.129916
29. Williams CL. The polybasic region of Ras and Rho family small GTPases: a regulator of protein interactions and membrane association and a site of nuclear localization signal sequences. *Cell Signal*. 2003;15:1071-1080. doi:10.1016/s0898-6568(03)00098-6
30. Rashid M, Tawara S, Fukumoto Y, Seto M, Yano K and Shimokawa H. Importance of Rac1 signaling pathway inhibition in the pleiotropic effects of HMG-CoA reductase inhibitors. *Circ J*. 2009;73:361-370. doi:10.1253/circj.CJ-08-0817
31. Tanaka S, Fukumoto Y, Nochioka K, Minami T, Kudo S, Shiba N, Takai Y, Williams CL, Liao JK and Shimokawa H. Statins exert the pleiotropic effects through small GTP-binding protein dissociation stimulator upregulation with a resultant Rac1 degradation. *Arterioscler Thromb Vasc Biol*. 2013;33:1591-1600. doi:10.1161/ATVBAHA.112.300922
32. Minami T, Satoh K, Nogi M, Kudo S, Miyata S, Tanaka S and Shimokawa H. Statins up-regulate SmgGDS through β1-integrin/Akt1 pathway in endothelial cells. *Cardiovasc Res*. 2016;109:151-161. doi:10.1093/cvr/cvv253
33. Kudo S, Satoh K, Nogi M, Suzuki K, Sunamura S, Omura J, Kikuchi N, Kurosawa R, Satoh T, Minami T, Ikeda S, Miyata S and Shimokawa H. SmgGDS as a crucial mediator of the inhibitory effects of statins on cardiac hypertrophy and fibrosis: novel mechanism of the pleiotropic effects of statins. *Hypertension*. 2016;67:878-889. doi:10.1161/HYPERTENSIONAHA.115.07089
34. Ayumi T, Jun M, Hiroyoshi I, Miki T, Atsushi T, Yasuko N, Hisahiro Y, Shin-ichi N and Yoshimi T. Involvement of a small GTP-binding protein (G protein) regulator, small G protein GDP dissociation stimulator, in antiapoptotic cell survival signaling. *Mol Biol Cell*. 2000;11:1875-1886. doi:10.1091/mbc.11.5.1875
35. Rateri DL, Davis FM, Balakrishnan A, Howatt DA, Moorleghen JJ, O'Connor WN, Charnigo R, Cassis LA and Daugherty A. Angiotensin II induces region-specific medial disruption during evolution of ascending aortic aneurysms. *Am J Pathol*. 2014;184:2586-2595. doi:10.1016/j.ajpath.2014.05.014
36. Satoh K. AMPKα2 regulates hypoxia-inducible factor-1α stability and neutrophil survival to promote vascular repair after ischemia. *Circ Res*. 2017;120:8-10. doi:10.1161/CIRCRESAHA.116.310217


Downloaded from http://circ.ahajournals.org/ by guest on June 20, 2018

37. Holm. TM, Habashi. JP, Doyle. JJ, Bedja. D, Chen. Y, Erp. Cv, Lindsay. ME, Kim. D, Schoenhoff. F, Cohn. RD, Loeys. BL, Thomas. CJ, Patnaik. S, Marugan. JJ, Judge. DP and Dietz. HC. Noncanonical TGFβ signaling contributes to aortic aneurysm progression in Marfan syndrome mice. *Science*. 2011;332:358-361. doi:10.1126/science.1192149
38. Yoshimura K, Aoki H, Ikeda Y, Fujii K, Akiyama N, Furutani A, Hoshii Y, Tanaka N, Ricci R, Ishihara T, Esato K, Hamano K and Matsuzaki M. Regression of abdominal aortic aneurysm by inhibition of c-Jun N-terminal kinase. *Nat Med*. 2005;11:1330-1338. doi:10.1038/nm1335
39. Jennifer PH, Daniel P. Judge, Tammy M. Holm, Ronald D. Cohn, Bart L. Loeys, Timothy K. Cooper, Loretha Myers, Erin C. Klein, Guosheng Liu, Carla Calvi, Megan Podowski, Enid R. Neptune, Marc K. Halushka, Djahida Bedja, Kathleen Gabrielson, Daniel B. Rifkin, Luca Carta, Francesco Ramirez, David L. Huso and Dietz HC. Losartan, an AT1 antagonist, prevents aortic aneurysm in a mouse model of Marfan syndrome. *Science*. 2006;312:117-121. doi:10.1126/science.1124287
40. Satoh K, Nigro P, Matoba T, O'Dell MR, Cui Z, Shi X, Mohan A, Yan C, Abe J, Illig KA and Berk BC. Cyclophilin A enhances vascular oxidative stress and the development of angiotensin II-induced aortic aneurysms. *Nat Med*. 2009;15:649-656. doi:10.1038/nm.1958
41. Satoh K, Nigro P and Berk BC. Oxidative stress and vascular smooth muscle cell growth: A mechanistic linkage by Cyclophilin A. *Antioxid Redox Signal*. 2010;12:675-682. doi:10.1089=ars.2009.2875
42. Satoh K, Satoh T, Kikuchi N, Omura J, Kurosawa R, Suzuki K, Sugimura K, Aoki T, Nochioka K, Tatebe S, Miyamichi-Yamamoto S, Miura M, Shimizu T, Ikeda S, Yaoita N, Fukumoto Y, Minami T, Miyata S, Nakamura K, Ito H, Kadomatsu K and Shimokawa H. Basigin mediates pulmonary hypertension by promoting inflammation and vascular smooth muscle cell proliferation. *Circ Res*. 2014;115:738-750. doi:10.1161/CIRCRESAHA.115.304563
43. Suzuki K, Satoh K, Ikeda S, Sunamura S, Otsuki T, Satoh T, Kikuchi N, Omura J, Kurosawa R, Nogi M, Numano K, Sugimura K, Aoki T, Tatebe S, Miyata S, Mukherjee R, Spinale FG, Kadomatsu K and Shimokawa H. Basigin promotes cardiac fibrosis and failure in response to chronic pressure overload in mice. *Arterioscler Thromb Vasc Biol*. 2016;36:636-646. doi:10.1161/ATVBAHA.115.306686
44. Sakai LY, Keene DR, Renard M and De Backer J. *FBN1*: The disease-causing gene for Marfan syndrome and other genetic disorders. *Gene*. 2016;591:279-291. doi:10.1016/j.gene.2016.07.033
45. LeMaire SA, McDonald ML, Guo DC, Russell L, Miller CC, 3rd, Johnson RJ, Bekheirnia MR, Franco LM, Nguyen M, Pyeritz RE, Bavaria JE, Devereux R, Maslen C, Holmes KW, Eagle K, Body SC, Seidman C, Seidman JG, Isselbacher EM, Bray M, Coselli JS, Estrera AL, Safi HJ, Belmont JW, Leal SM and Milewicz DM. Genome-wide association study identifies a susceptibility locus for thoracic aortic aneurysms and aortic dissections spanning *FBN1* at 15q21.1. *Nat Genet*. 2011;43:996-1000. doi:10.1038/ng.934
46. Elizabeth N, Patrick G, Ellen LL, Andrew DH, Nathan S, Donna M, Balaraman K, Michael BD, John AA and Carol LW. An adenosine-mediated signaling pathway suppresses prenylation of the GTPase Rap1B and promotes cell scattering. *Sci Signal*. 2013;6:ra39. doi:10.1126/scisignal.2003374

Downloaded from http://circ.ahajournals.org/ by guest on June 20, 2018

47. Moon MY, Kim HJ, Kim JG, Lee JY, Kim J, Kim SC, Choi IG, Kim PH and Park JB. Small GTPase Rap1 regulates cell migration through regulation of small GTPase RhoA activity in response to transforming growth factor-β1. *J Cell Physiol*. 2013;228:2119-2126. doi:10.1002/jcp.24383
48. Carta L, Smaldone S, Zilberberg L, Loch D, Dietz HC, Rifkin DB and Ramirez F. p38 MAPK is an early determinant of promiscuous Smad2/3 signaling in the aortas of Fibrillin-1 (*FBN1*)-null mice. *J Biol Chem*. 2009;284:5630-5636. doi:10.1074/jbc.M806962200
49. Yang HHC, van Breemen C and Chung AWY. Vasomotor dysfunction in the thoracic aorta of Marfan syndrome is associated with accumulation of oxidative stress. *Vascul Pharmacol*. 2010;52:37-45. doi:10.1016/j.vph.2009.10.005
50. Cheng G, Diebold BA, Hughes Y and Lambeth JD. Nox1-dependent reactive oxygen generation is regulated by Rac1. *J Biol Chem*. 2006;281:17718-17726. doi:10.1074/jbc.M512751200
51. Shogo K, Yasunori O, Yoshikatsu O, Kazushi I and Isao N. Matrix metalloproteinase-9 (92-kd gelatinase/type IV collagenase equals gelatinase B) can degrade arterial elastin. *Am J Pathol*. 1994;145:1208-1218.
52. Galis ZS, Sukhova GK, Lark MW and Libby P. Increased expression of matrix metalloproteinases and matrix degrading activity in vulnerable regions of human atherosclerotic plaques. *J Clin Invest*. 1994;94:2493-2503. doi:10.1172/JCI117619
53. Nataatmadja M, West M, West J, Summers K, Walker P, Nagata M and Watanabe T. Abnormal extracellular matrix protein transport associated with increased apoptosis of vascular smooth muscle cells in Marfan syndrome and bicuspid aortic valve thoracic aortic aneurysm. *Circulation*. 2003;108 Suppl 1:II329-II334. doi:10.1161/01.cir.0000087660.82721.15
54. Rajagopalan S, Meng XP, Ramasamy S, Harrison DG and Galis ZS. Reactive oxygen species produced by macrophage-derived foam cells regulate the activity of vascular matrix metalloproteinases in vitro. Implications for atherosclerotic plaque stability. *J Clin Invest*. 1996;98:2572-2579. doi:10.1172/JCI119076
55. Thompson RW, Holmes DR, Mertens RA, Liao S, Botney MD, Mecham RP, Welgus HG and Parks WC. Production and localization of 92-kilodalton gelatinase in abdominal aortic aneurysms. An elastolytic metalloproteinase expressed by aneurysm-infiltrating macrophages. *J Clin Invest*. 1995;96:318-326. doi:10.1172/JCI118037
56. Sakalihasan N DP, Nusgens BV, Limet R, Lapière CM. Activated forms of MMP2 and MMP9 in abdominal aortic aneurysms. *J Vasc Surg*. 1996;24:127-133. doi:10.1016/S0741-5214(96)70153-2
57. Xiong W, Meisinger T, Knispel R, Worth JM and Baxter BT. MMP-2 regulates Erk1/2 phosphorylation and aortic dilatation in Marfan syndrome. *Circ Res*. 2012;110:e92-e101. doi:10.1161/CIRCRESAHA.112.268268
58. Chung AW, Yang HH, Radomski MW and van Breemen C. Long-term doxycycline is more effective than atenolol to prevent thoracic aortic aneurysm in Marfan syndrome through the inhibition of matrix metalloproteinase-2 and -9. *Circ Res*. 2008;102:e73-e85. doi:10.1161/CIRCRESAHA.108.174367
59. Hynes R. The extracellular matrix: not just pretty fibrils. *Science*. 2009;326:1216-1219. doi:10.1126/science.1176009
60. Chen J, Peters A, Papke CL, Villamizar C, Ringuette LJ, Cao J, Wang S, Ma S, Gong L,

Downloaded from http://circ.ahajournals.org/ by guest on June 20, 2018

Byanova KL, Xiong J, Zhu MX, Madonna R, Kee P, Geng YJ, Brasier AR, Davis EC, Prakash S, Kwartler CS and Milewicz DM. Loss of smooth muscle α-actin leads to NF-κB-dependent increased sensitivity to angiotensin II in smooth muscle cells and aortic enlargement. *Circ Res*. 2017;120:1903-1915. doi:10.1161/CIRCRESAHA.117.310563

61. Angeloni E, Vitaterna A, Pirelli M and Refice S. Effects of statin therapy on ascending aorta aneurysms growth: A propensity-matched analysis. *Int J Cardiol*. 2015;191:52-55. doi:10.1016/j.ijcard.2015.05.001
62. Forteza A, Evangelista A, Sanchez V, Teixido-Tura G, Sanz P, Gutierrez L, Gracia T, Centeno J, Rodriguez-Palomares J, Rufilanchas JJ, Cortina J, Ferreira-Gonzalez I and Garcia-Dorado D. Efficacy of losartan vs. atenolol for the prevention of aortic dilation in Marfan syndrome: a randomized clinical trial. *Eur Heart J*. 2016;37:978-985. doi:10.1093/eurheartj/ehv575
63. Krishna SM, Dear AE, Norman PE and Golledge J. Genetic and epigenetic mechanisms and their possible role in abdominal aortic aneurysm. *Atherosclerosis*. 2010;212:16-29. doi:10.1016/j.atherosclerosis.2010.02.008
64. Krishna SM, Seto SW, Jose RJ, Li J, Morton SK, Biros E, Wang Y, Nsengiyumva V, Lindeman JH, Loots GG, Rush CM, Craig JM and Golledge J. Wnt signaling pathway inhibitor sclerostin inhibits angiotensin II-induced aortic aneurysm and atherosclerosis. *Arterioscler Thromb Vasc Biol*. 2017;37:553-566. doi:10.1161/ATVBAHA.116.308723

Downloaded from http://circ.ahajournals.org/ by guest on June 20, 2018

Circulation

## Figure Legends

**Figure 1. Deletion of SmgGDS Induces thoracic aortic aneurysm (TAA) and rupture**

(**A**) Death due to TAA rupture in *Apoe*$^{-/-}$ (*n*=13) and *Apoe*$^{-/-}$*SmgGDS*$^{+/-}$ mice (*n*=15) during AngII infusion for 4 weeks. (**B**) Death due to abdominal aortic aneurysm (AAA) rupture in *Apoe*$^{-/-}$ and *Apoe*$^{-/-}$*SmgGDS*$^{+/-}$ mice during AngII infusion for 4 weeks. (**C**) TAA incidence in *Apoe*$^{-/-}$ and *Apoe*$^{-/-}$*SmgGDS*$^{+/-}$ mice during AngII infusion for 4 weeks. (**D**) AAA incidence in *Apoe*$^{-/-}$ and *Apoe*$^{-/-}$*SmgGDS*$^{+/-}$ mice during AngII infusion for 4 weeks. (**E**) Left, maximal diameter of ascending aorta assessed by ultrasound imaging in *Apoe*$^{-/-}$ and *Apoe*$^{-/-}$*SmgGDS*$^{+/-}$ mice during AngII infusion for 4 weeks. **P*<0.05 (*Apoe*$^{-/-}$ vs. *Apoe*$^{-/-}$*SmgGDS*$^{+/-}$ at each week). Right, maximal diameters of ascending aorta in *Apoe*$^{-/-}$ and *Apoe*$^{-/-}$*SmgGDS*$^{+/-}$ mice before and after AngII infusion for 4 weeks. (**F**) Left, maximal diameter of abdominal aorta assessed by ultrasound imaging in *Apoe*$^{-/-}$ and *Apoe*$^{-/-}$*SmgGDS*$^{+/-}$ mice during AngII infusion for 4 weeks. Right, maximal diameter of abdominal aorta in *Apoe*$^{-/-}$ and *Apoe*$^{-/-}$*SmgGDS*$^{+/-}$ mice before and after the AngII infusion for 4 weeks. (**G**) Representative Elastica-Masson staining of aorta in *Apoe*$^{-/-}$ and *Apoe*$^{-/-}$*SmgGDS*$^{+/-}$ mice after infusion of AngII or saline for 4 weeks. Scale bars, 100 μm. (**H**) Elastin degradation grade of ascending aorta in *Apoe*$^{-/-}$ and *Apoe*$^{-/-}$ *SmgGDS*$^{+/-}$ mice after infusion of AngII or saline for 4 weeks (*n*=5 each). Comparisons of parameters were performed with two-way ANOVA, followed by Tukey's HSD test for multiple comparisons. (**I**) Schematic representation of SmgGDS-mediated prevention of elastin degradation and aortic dilatation. **P*<0.05.

Downloaded from http://circ.ahajournals.org/ by guest on June 20, 2018

**Figure 2. Deletion of SmgGDS induces thoracic aortic dissection (TAD) at day 3 after angiotensin II (AngII) infusion**

(**A**) Representative pictures of whole aortas of *Apoe*$^{-/-}$ (*n*=6) and *Apoe*$^{-/-}$*SmgGDS*$^{+/-}$ (*n*=7) mice at day 3 after AngII infusion. **P*<0.05. (**B**) Representative pictures of staining for Elastica-Masson and ACTA2 in ascending aortas of *Apoe*$^{-/-}$ mice at day 3 after AngII infusion. (**C**–**E**) Representative pictures of Elastica-Masson staining in the aortas of *Apoe*$^{-/-}$ *SmgGDS*$^{+/-}$ mice at day 3 after AngII infusion. (**F**–**H**) Representative pictures of ACTA2 staining in aortas of *Apoe*$^{-/-}$ *SmgGDS*$^{+/-}$ mice at day 3 after AngII infusion. Scale bars, 100 μm.

Downloaded from http://circ.ahajournals.org/ by guest on June 20, 2018

**Figure 3. Deletion of SmgGDS induces phenotypic switching in AoSMCs**

(**A**) Representative immunofluorescence staining for ACTA2 (red, Alexa flour 546) and CD45 (green, Alexa flour 488) in the ascending aortas of *Apoe*$^{-/-}$ and *Apoe*$^{-/-}$*SmgGDS*$^{+/-}$ mice at day 3 after angiotensin II (AngII) infusion. Scale bars, 50 μm. (**B**) Representative immunostaining for Fibrillin-1 (Fbn1) in ascending aortas of *Apoe*$^{-/-}$ and *Apoe*$^{-/-}$*SmgGDS*$^{+/-}$ mice. Scale bars, 100 μm. (**C**) mRNA expression of *Fbn1* in ascending aortas of *Apoe*$^{-/-}$ and *Apoe*$^{-/-}$*SmgGDS*$^{+/-}$ mice (*n*=10 each). (**D**) Immunofluorescence staining for Fbn1 (green, Alexa flour 488) and Tubulin (red, Alexa flour 546) in *Apoe*$^{-/-}$ and *Apoe*$^{-/-}$*SmgGDS*$^{+/-}$ AoSMCs after treatment with saline or AngII (100 nM) for 24 hours. Scale bars, 10 μm. (**E**) RT-PCR analysis of *Fbn1* mRNA in *Apoe*$^{-/-}$ and *Apoe*$^{-/-}$*SmgGDS*$^{+/-}$ AoSMCs (*n*=6 each). (**F**) RT-PCR of *Acta2, Mlk, Myh11, and Prkg1* mRNA in *Apoe*$^{-/-}$ and *Apoe*$^{-/-}$*SmgGDS*$^{+/-}$ AoSMCs after treatment with saline or AngII (100 nM) for 4 hours (*n*=6 each). (**G**) Western blot analysis of SmgGDS, Acta2 and calponin in *Apoe*$^{-/-}$ and *Apoe*$^{-/-}$*SmgGDS*$^{+/-}$ AoSMCs after treatment with saline or AngII (100

nM) for 24 hours ($n$=4 each). (**H**) Migration ($n$=4 each) assays in *Apoe*$^{-/-}$ and *Apoe*$^{-/-}$ S*mgGDS*$^{+/-}$ AoSMCs in response to 10% fetal bovine serum (FBS). (**I**) Activity assays for RhoA and Rap1 in *Apoe*$^{-/-}$ and *Apoe*$^{-/-}$ S*mgGDS*$^{+/-}$ AoSMCs ($n$=4 each). (**J**) Activity assays for RhoC in *Apoe*$^{-/-}$ and *Apoe*$^{-/-}$ S*mgGDS*$^{+/-}$ AoSMCs in response to AngII and cyclic stretch ($n$=3 each). (**K**) Schematic representation of the SmgGDS-mediated prevention of phenotype switching in AoSMCs. (**L**) Western blot analysis of SmgGDS, RhoA, ROCK1, and ROCK2 in AoSMCs after treatment with cyclic stretch (1 Hz) for 0, 3, 24 hours ($n$=3 each). (**M**) Western blot analysis of ratio (phosphorylated Smad2/3 per total Smad2/3), Smad4 and TGF-β in *Apoe*$^{-/-}$ or *Apoe*$^{-/-}$*SmgGDS*$^{+/-}$ AoSMCs treated with saline or AngII (100 nM) for 24 hours. Data represent the mean ± s.e.m. *$P$<0.05. Comparisons of parameters were performed with Tukey's honest significant difference test for multiple comparisons.

Downloaded from http://circ.ahajournals.org/ by guest on June 20, 2018

American Heart Association.

Circulation

**Figure 4. SmgGDS deficiency in the aortic walls augments migration of bone marrow (BM)-derived cells**

(**A**) Levels of cytokines and chemokines in aortas from *Apoe*$^{-/-}$ and *Apoe*$^{-/-}$*SmgGDS*$^{+/-}$ mice after treatment with saline or angiotensin II (AngII, 1000 ng/kg/min) for 3 days ($n$=5 each). (**B**) Western blot analysis of phosphorylated ERK, total ERK, phosphorylated JNK, total JUNK and TGFβ1 proteins in aortas of *Apoe*$^{-/-}$ and *Apoe*$^{-/-}$*SmgGDS*$^{+/-}$ mice after treatment with AngII for 3 days ($n$=5 each). Data represent the mean ± SEM. *$P$<0.05. Comparisons of parameters were performed with the unpaired Student's $t$-test. (**C**) The protocols for BM transplantation experiments. (**D**) Representative *en face* aortic immunostaining for GFP (green) and CD31 (red, Alexa flour 546) in ascending aortas of *Apoe*$^{-/-}$ and *Apoe*$^{-/-}$*SmgGDS*$^{+/-}$ chimeric mice after

infusion of AngII for 4 weeks. (**E**) Representative immunostaining for GFP (green), ACTA2 (Cy3, red), and DAPI (blue) in ascending aortas of *Apoe*$^{-/-}$ and *Apoe*$^{-/-}$*SmgGDS*$^{+/-}$ chimeric mice after infusion of AngII for 4 weeks. (**F**) Assessment of the number of GFP-positive cells in *Apoe*$^{-/-}$ and *Apoe*$^{-/-}$*SmgGDS*$^{+/-}$ mice after AngII treatment. (**G**) Representative immunostaining for GFP (green), CD45 (red, Alexa flour 546), and DAPI (blue) in ascending aortas of *Apoe*$^{-/-}$ and *Apoe*$^{-/-}$*SmgGDS*$^{+/-}$ chimeric mice after infusion of AngII for 4 weeks. (**H**) Representative immunostaining for GFP (green), cyclophilin A (CyPA, red, Alexa flour 546), and DAPI (blue) in ascending aortas of *Apoe*$^{-/-}$ and *Apoe*$^{-/-}$*SmgGDS*$^{+/-}$ chimeric mice after infusion of AngII for 4 weeks. Scale bars, 100 μm.

Downloaded from http://circ.ahajournals.org/ by guest on June 20, 2018

American Heart Association.

**Figure 5. Deletion of SmgGDS increases ROS production in the ascending aorta**

(**A**) Representative images of CellROX staining in *Apoe*$^{-/-}$ and *Apoe*$^{-/-}$*SmgGDS*$^{+/-}$ AoSMCs after treatment with saline or angiotensin II (AngII, 100 nM) for 4 hours. Scale bars, 10 μm. (**B**) Quantitative analysis of CellROX fluorescence intensity in *Apoe*$^{-/-}$ and *Apoe*$^{-/-}$*SmgGDS*$^{+/-}$ AoSMCs after treatment with saline or AngII (100 nM) for 4 hours (*n*=8 each). (**C**–**E**) Quantitative analysis of fluorescence intensities for 2,7-dichlorodihydrofluorescein (DCF, **C**), dihydroethidium (DHE, **D**), and MitoSOX (**E**) in *Apoe*$^{-/-}$ and *Apoe*$^{-/-}$*SmgGDS*$^{+/-}$ AoSMCs after treatment with saline or AngII (100 nM) for 4 hours (*n*=8 each). (**F**) RT-PCR for *Nox1*, *Nox2*, *and Nox4* in ascending aortas of *Apoe*$^{-/-}$ and *Apoe*$^{-/-}$*SmgGDS*$^{+/-}$mice at day 3 after AngII infusion (*n*=6 each). (**G**) Western blot analysis of Rac1 and Nrf2 in *Apoe*$^{-/-}$ and *Apoe*$^{-/-}$*SmgGDS*$^{+/-}$ AoSMCs after treatment with saline or AngII (100 nM) for 24 hours. (**H**) Lucigenin assay for NADPH oxidase activity in *Apoe*$^{-/-}$ and *Apoe*$^{-/-}$*SmgGDS*$^{+/-}$ AoSMCs after treatment with saline

or AngII (100 nM) for 24 hours (*n*=6 each). (**I**) Representative images of DHE staining in ascending aortas of *Apoe*$^{-/-}$ and *Apoe*$^{-/-}$*SmgGDS*$^{+/-}$ mice after treatment with saline or AngII (1000 ng/min/kg) for 3 days. Scale bars, 10 μm. (**J**) Densitometric analysis of DHE fluorescence in ascending aortas relative to controls (*n*=5 each). (**K**) Western blot analysis of Rac1 protein in ascending aortas of *Apoe*$^{-/-}$ and *Apoe*$^{-/-}$*SmgGDS*$^{+/-}$ mice after treatment with AngII (1000 ng/kg/min) for 3 days. Data represent the mean ± s.e.m. **P*<0.05. Comparisons of parameters were performed with Tukey's honest significant difference test for multiple comparisons.

Downloaded from http://circ.ahajournals.org/ by guest on June 20, 2018

American Heart Association.

**Figure 6. SmgGDS inhibits MMP activation in AoSMCs**

(**A**) RT-PCR analysis of *Mmp9* and *Mmp2* mRNA expression in *Apoe*$^{-/-}$ and *Apoe*$^{-/-}$ *SmgGDS*$^{+/-}$ AoSMCs after treatment with saline or angiotensin II (AngII, 100 nM) for 4 hours (*n*=6 each). (**B**) Representative immunofluorescence images of *in situ* zymography (DQ gelatin) and immunostaining for tubulin (red, Alexa flour 546) in *Apoe*$^{-/-}$ and *Apoe*$^{-/-}$*SmgGDS*$^{+/-}$ AoSMCs after treatment with saline or AngII (100 nM) for 24 hours. Scale bars, 10 μm. (**C**) Quantitative analysis of fluorescence intensity in *Apoe*$^{-/-}$ and *Apoe*$^{-/-}$*SmgGDS*$^{+/-}$ AoSMCs after treatment with saline or AngII (100 nM) for 24 hours (*n*=8 each). (**D**) Western blot analysis of cyclophilin A (CyPA) in conditioned medium (CM) prepared from *Apoe*$^{-/-}$ and *Apoe*$^{-/-}$ *SmgGDS*$^{+/-}$ AoSMCs after treatment with saline or AngII for 24 hours (*n*=4 each). (**E**) Representative immunofluorescence images of *in situ* zymography (DQ gelatin, green) and immunostaining for CyPA (red, Alexa flour 546), and DAPI (blue) in *Apoe*$^{-/-}$ and *Apoe*$^{-/-}$ *SmgGDS*$^{+/-}$ ascending aortas after treatment with saline or AngII (1000 ng/kg/min) for 7 days.

Circulation

Scale bars, 100 μm. (**F**) Densitometric analysis of MMP activities in ascending aortas assessed by DQ gelatin (*n*=5 each). (**G**) Gelatin zymography to detect proMMP-9, MMP-9, proMMP-2 and MMP-2 in the ascending aortas of *Apoe*$^{-/-}$ and *Apoe*$^{-/-}$*SmgGDS*$^{+/-}$ after treatment with AngII (1000 ng/kg/min) for 7 days (*n*=5 each). (**H**) Western blot analysis of MMP-12 (43kDa activated form) in conditioned medium from *Apoe*$^{-/-}$ and *Apoe*$^{-/-}$*SmgGDS*$^{+/-}$ ascending aortas after treatment with AngII (1000 ng/kg/min) for 7 days (*n*=5 each). (**I**) Schematic representation of the SmgGDS-mediated inhibition of reactive oxygen species (ROS) production and matrix metalloproteinases (MMPs) activation via suppression of CyPA secretion from AoSMCs. Data represent the mean ± s.e.m. **P*<0.05. Comparisons of parameters were performed with Tukey's honest significant difference test for multiple comparisons.

Downloaded from http://circ.ahajournals.org/ by guest on June 20, 2018

**Figure 7. Downregulation of SmgGDS in ascending aorta in patients with TAA**

(**A**) Representative immunofluorescence images of *in situ* zymography (DQ gelatin, green) and immunostaining for SmgGDS (red, Alexa flour 546) in ascending aortas of patients with thoracic aortic aneurysm (TAA). Scale bars, 200 μm (left) and 20 μm (right). (**B**) Western blot analysis of cyclophilin A (CyPA) in conditioned medium (CM) prepared from control and TAA-AoSMCs (*n*=6 each). (**C**) Plasma levels of CyPA (ng/mL) in controls (*n*=25) and patients with TAA (*n*=52) or abdominal aortic aneurysm (AAA, *n*=16). **P*<0.05 by Dunnett's test. (**D**) Representative immunofluorescence images of *in situ* zymography (DQ gelatin) in control AoSMCs and TAA-AoSMCs after treatment with saline or AngII (100 nM) for 24 hours. Scale bars, 10 μm. (**E**) Quantitative analyses of fluorescence intensities for 2,7-dichlorodihydrofluorescein (DCF), dihydroethidium (DHE), and MitoSOX in control and TAA-

AoSMCs after treatment with saline or angiotensin II (AngII, 100 nM) for 4 hours (*n*=8 each). (**F**) Western blot analyses of ACTA2 and Calponin in control and TAA-AoSMCs after treatment with saline or AngII for 3 days. (**G**) Western blot analysis of SmgGDS in control and TAA-AoSMCs after treatment with AngII for 0, 1, 3, and 5 days.

**Figure 8. SmgGDS transfection rescues *Apoe*$^{-/-}$*SmgGDS*$^{+/-}$ mice from thoracic aortic dissection (TAD) and rupture**

(**A**) Protocols for local delivery of SmgGDS plasmid around the ascending aorta. (**B**) Western blot analysis of SmgGDS levels in ascending aortas after SmgGDS overexpression. (**C**) Representative immunostaining for SmgGDS (red, Alexa flour 546) and DAPI (blue) in the ascending aortas of *Apoe*$^{-/-}$*SmgGDS*$^{+/-}$ mice after treatment with AngII (1000 ng/min/kg) for 3 days. Scale bars, 10 μm. (**D**) Representative images of dihydroethidium (DHE) staining (red) in ascending aortas of *Apoe*$^{-/-}$*SmgGDS*$^{+/-}$ mice after treatment with AngII (1000 ng/min/kg) for 3 days. Scale bars, 10 μm. (**E**) Representative immunofluorescence images of *in situ* zymography (DQ gelatin, green) and DAPI (blue) in *Apoe*$^{-/-}$*SmgGDS*$^{+/-}$ ascending aortas after treatment with AngII (1000 ng/min/kg) for 3 days. Scale bars, 50 μm. (**F**) Elastin degradation grade of the ascending aorta in *Apoe*$^{-/-}$*SmgGDS*$^{+/-}$ mice after infusion of AngII for 4 weeks. **P*<0.05 (SmgGDS plasmid vs. control plasmid, *n*=11 each). Comparisons of parameters were performed with two-way ANOVA, followed by Tukey's HSD test for multiple comparisons. (**G**) Death due to TAA rupture in control plasmid group versus SmgGDS plasmid group (*n*=11 each). (**H**) Death due to AAA rupture in control plasmid group versus SmgGDS plasmid group (*n*=11 each). (**I**) Maximal diameters of the ascending aorta assessed by ultrasound imaging in

Downloaded from http://circ.ahajournals.org/ by guest on June 20, 2018

*Apoe*$^{-/-}$*SmgGDS*$^{+/-}$ mice during AngII infusion for 4 weeks (*n*=11 each). **P*<0.05 (SmgGDS plasmid vs. control plasmid at each week). (**J**) Maximal diameters of the abdominal aorta assessed by ultrasound imaging in *Apoe*$^{-/-}$*SmgGDS*$^{+/-}$ mice during AngII infusion for 4 weeks (*n*=11 each).

Downloaded from http://circ.ahajournals.org/ by guest on June 20, 2018

American Heart Association.
Circulation

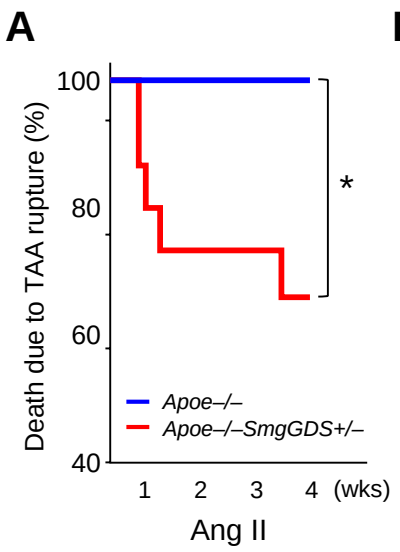


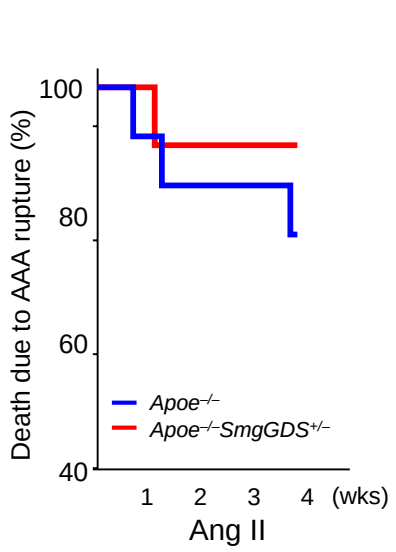


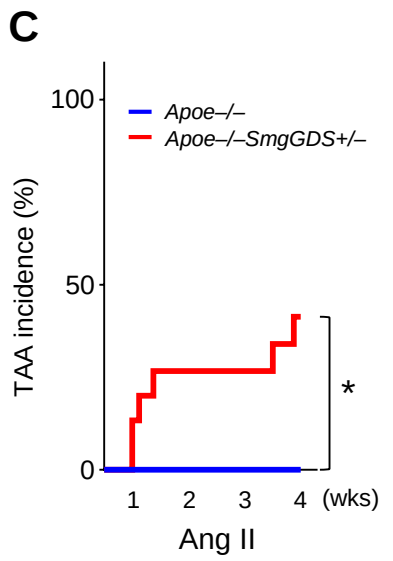


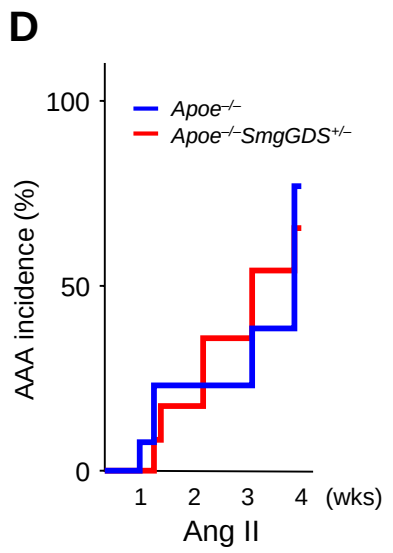


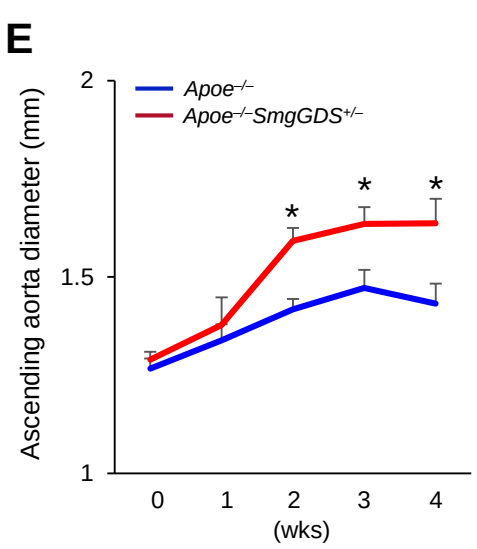


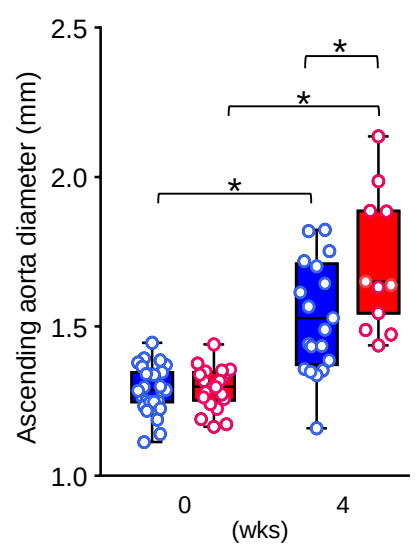


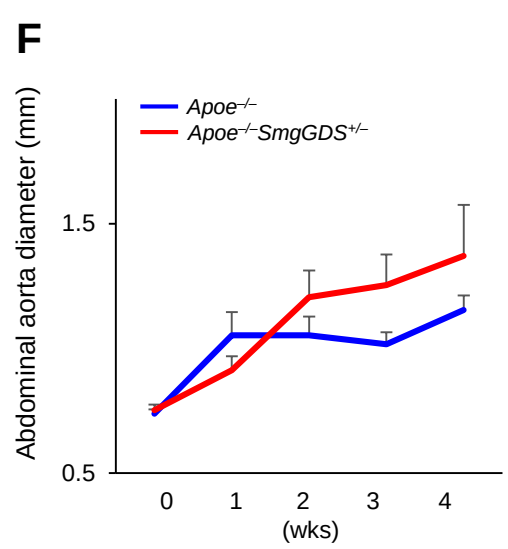


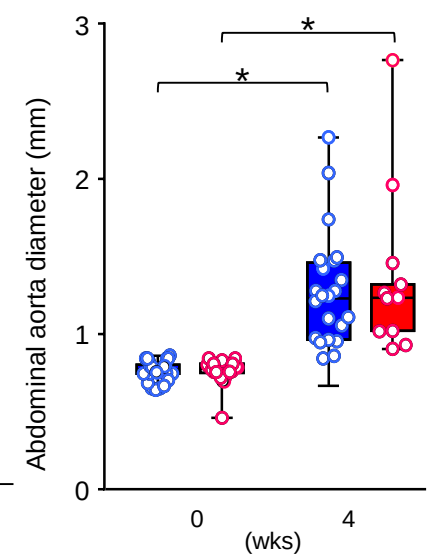


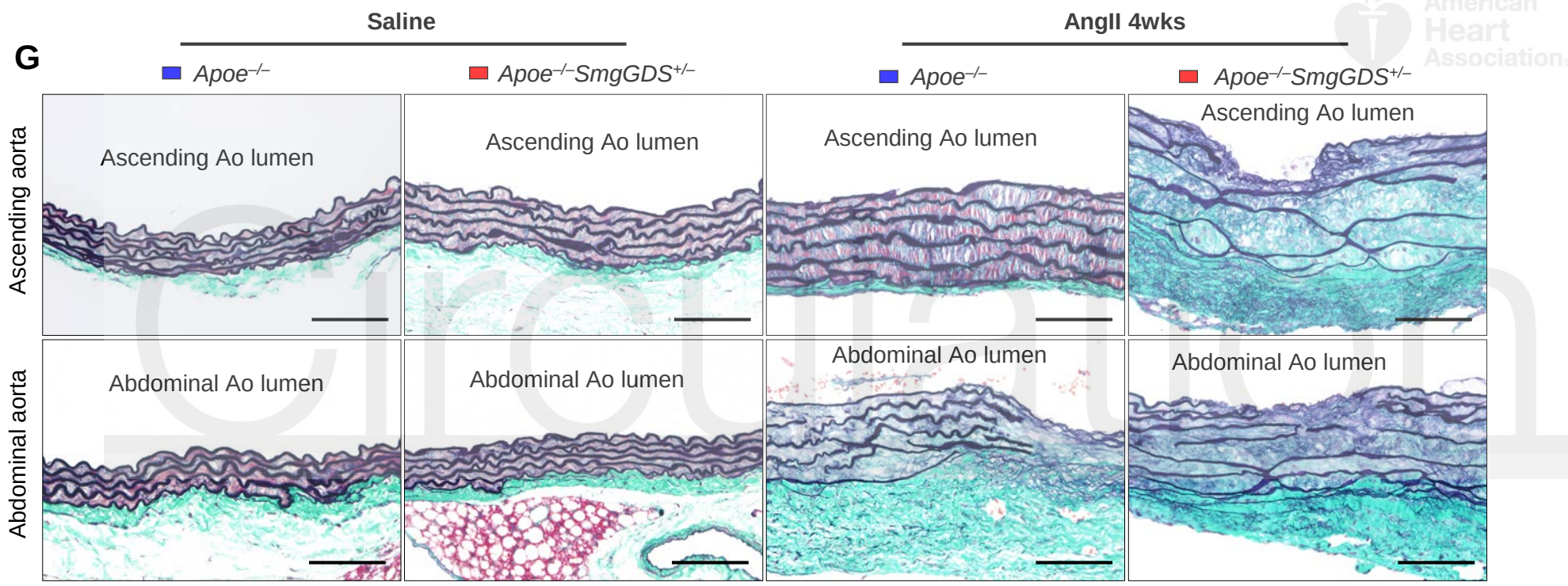


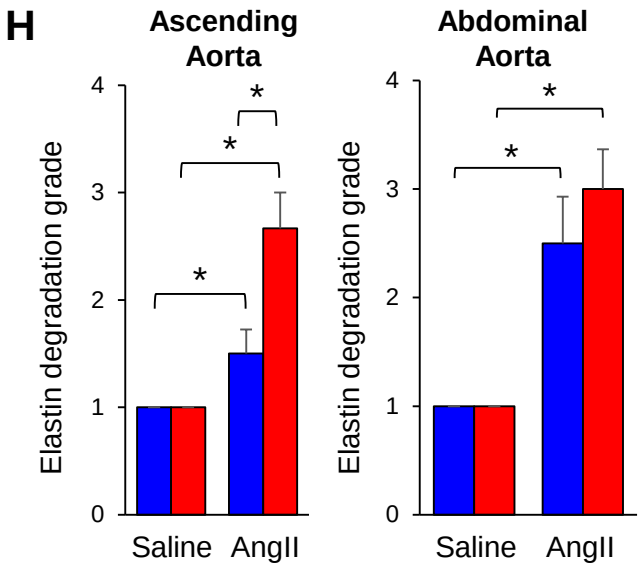


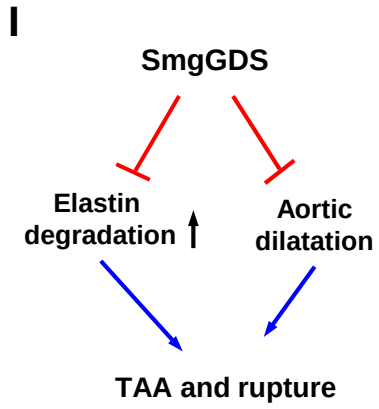


Downloaded from http://circ.ahajournals.org/ by guest on June 20, 2018

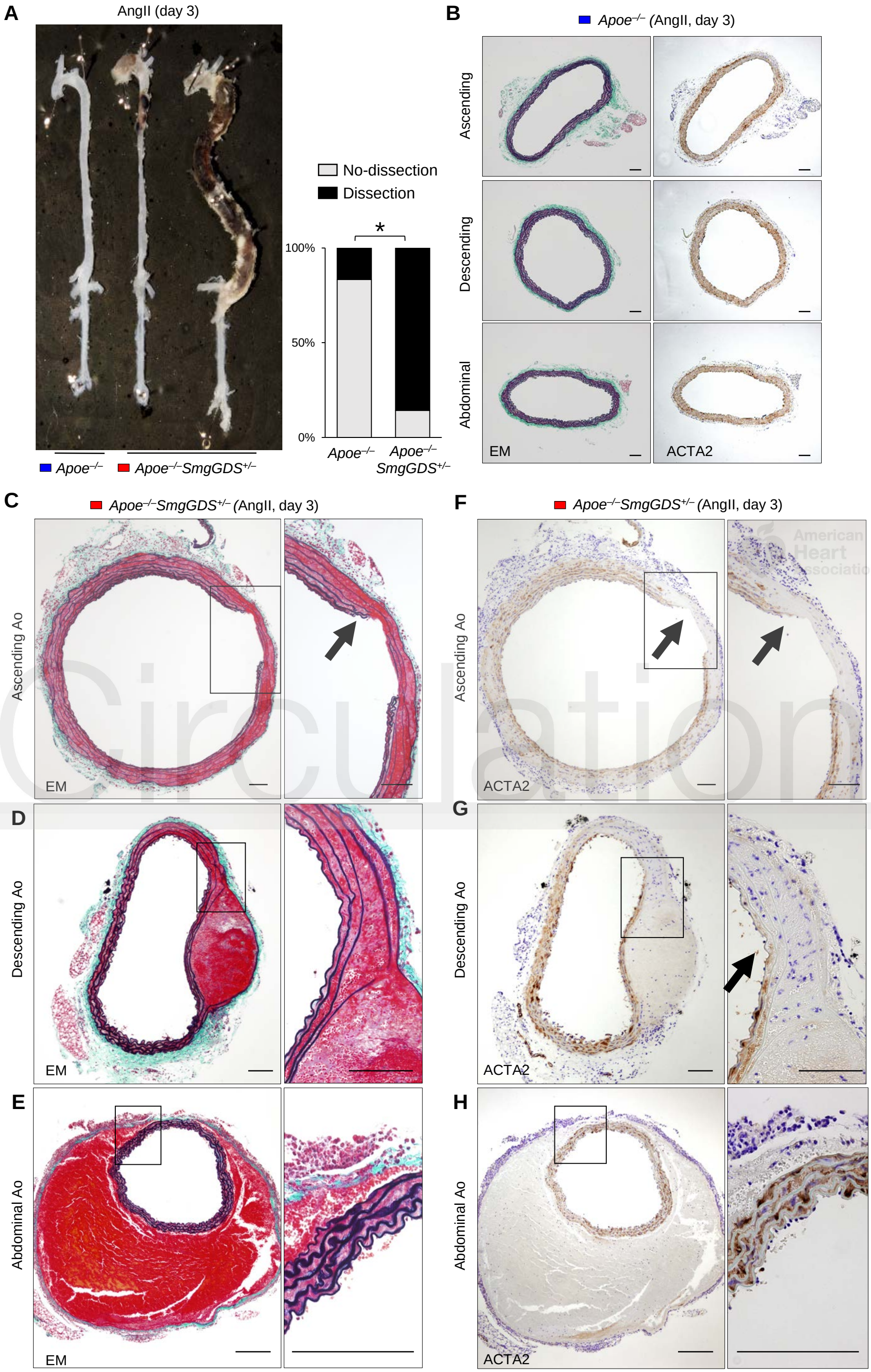


Downloaded from http://circ.ahajournals.org/ by guest on June 20, 2018

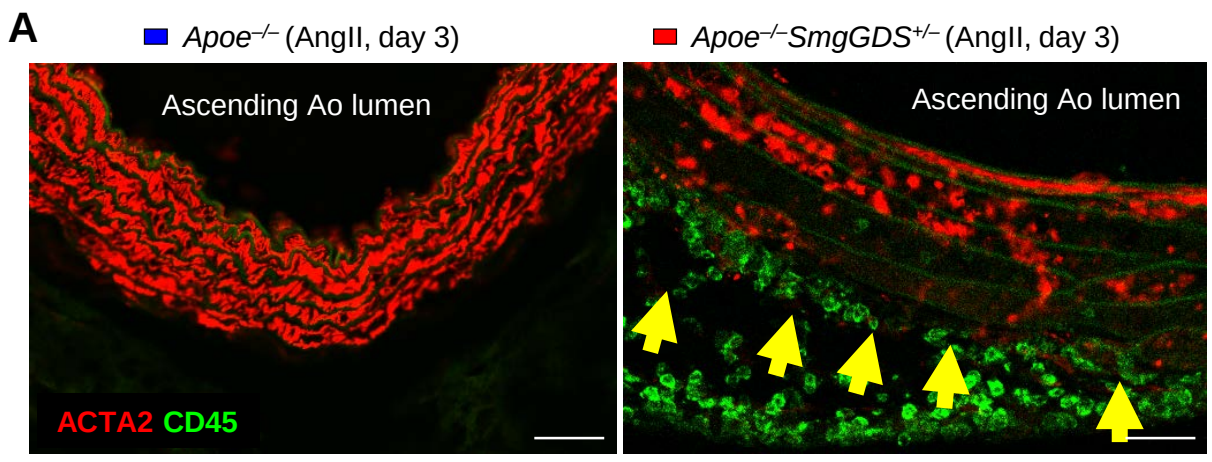


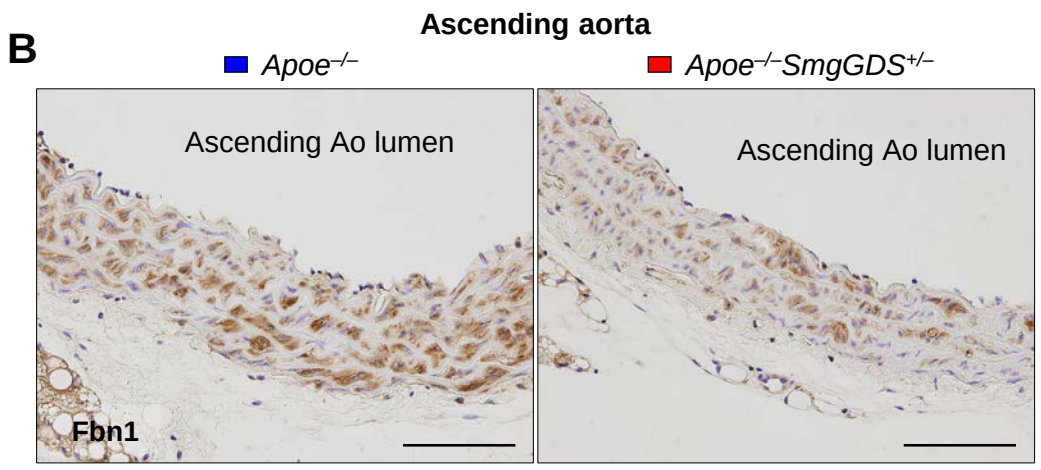


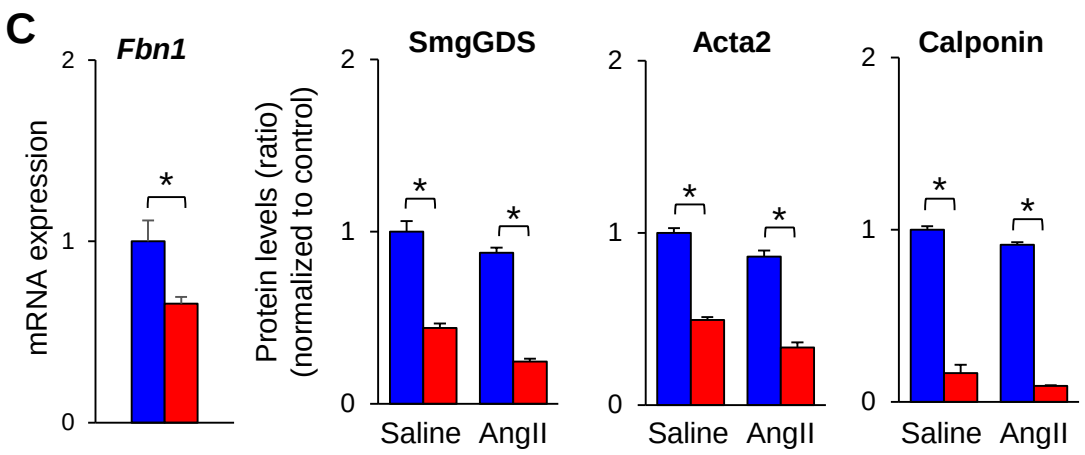


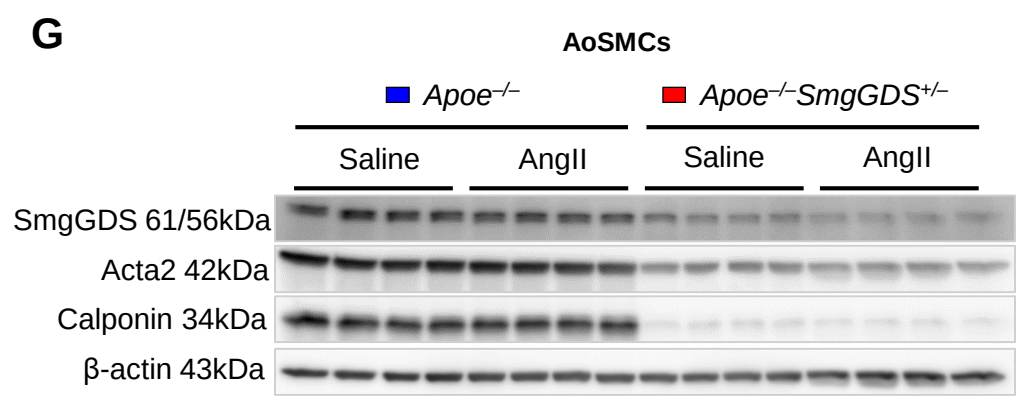


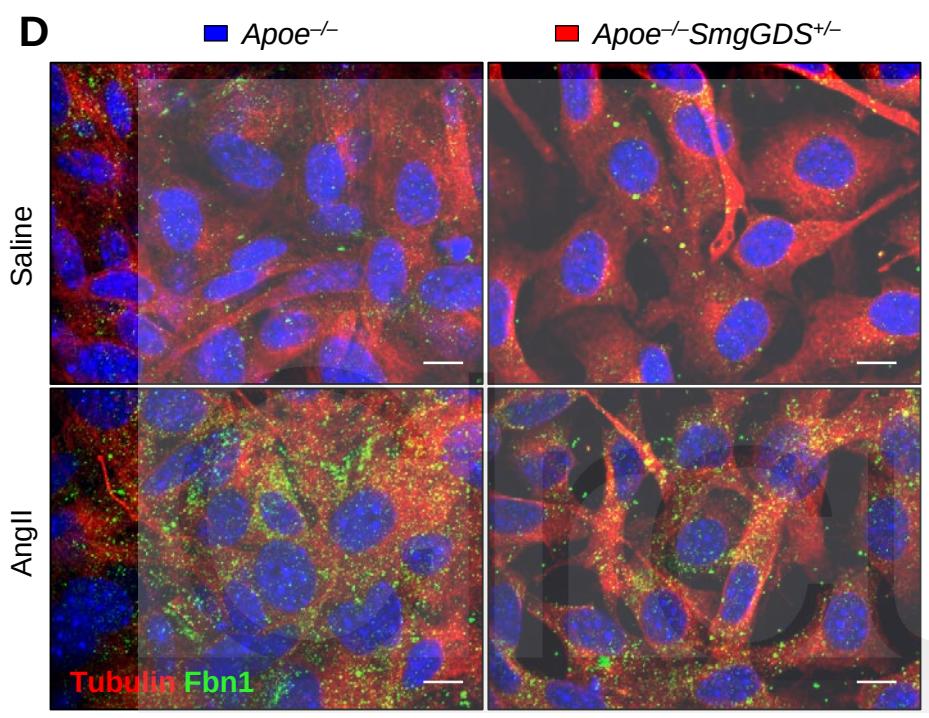


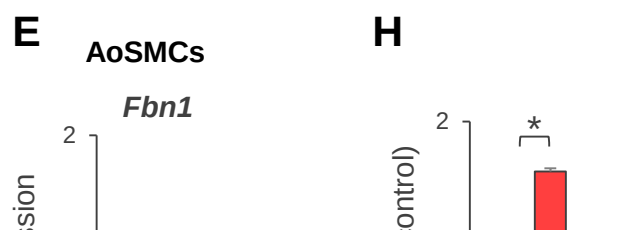





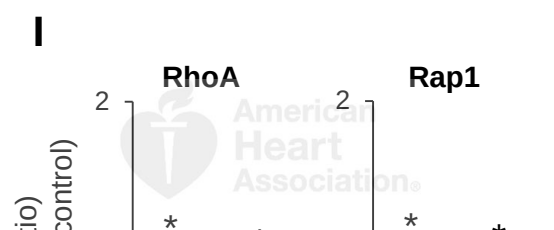


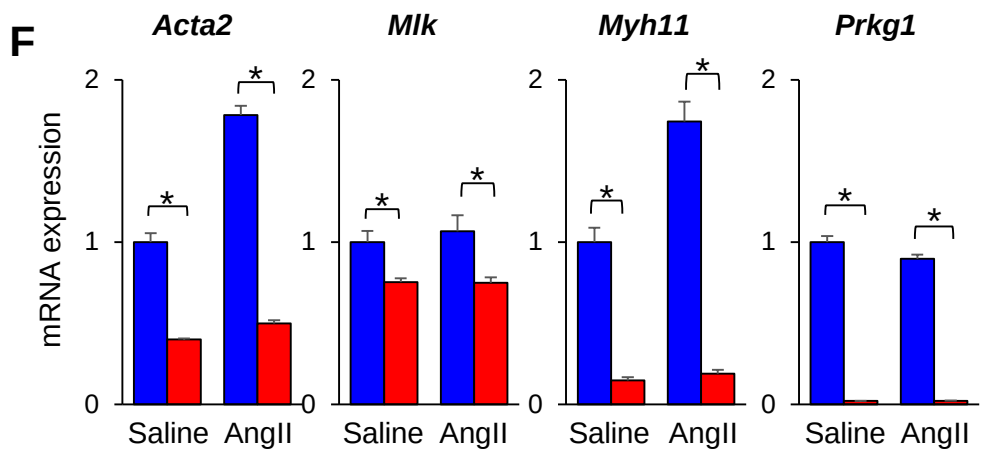


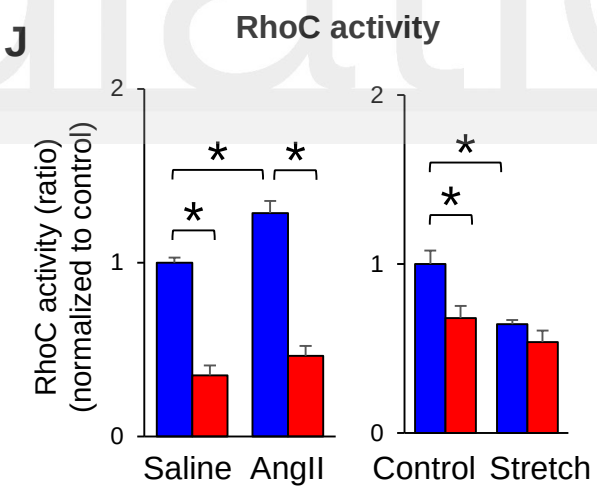


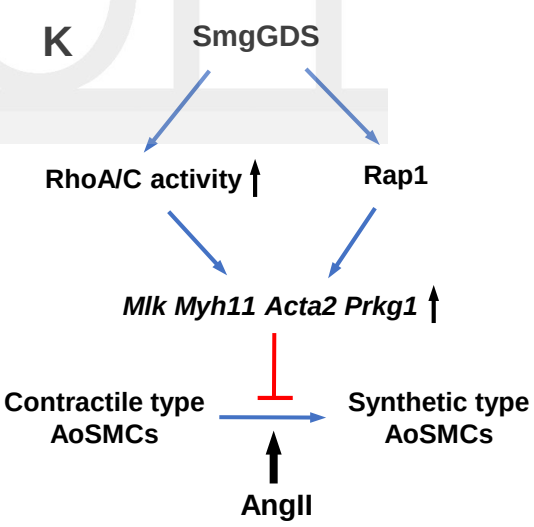


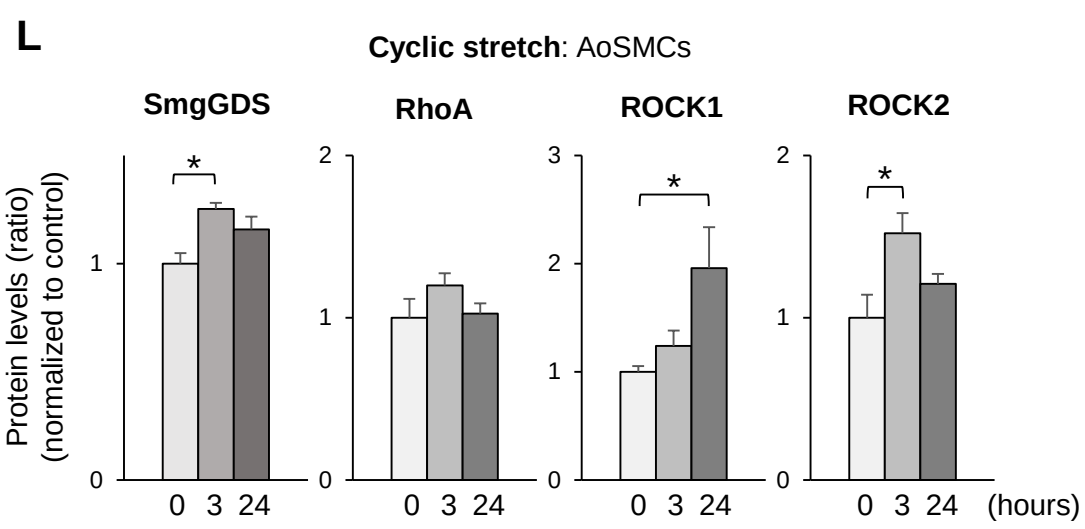


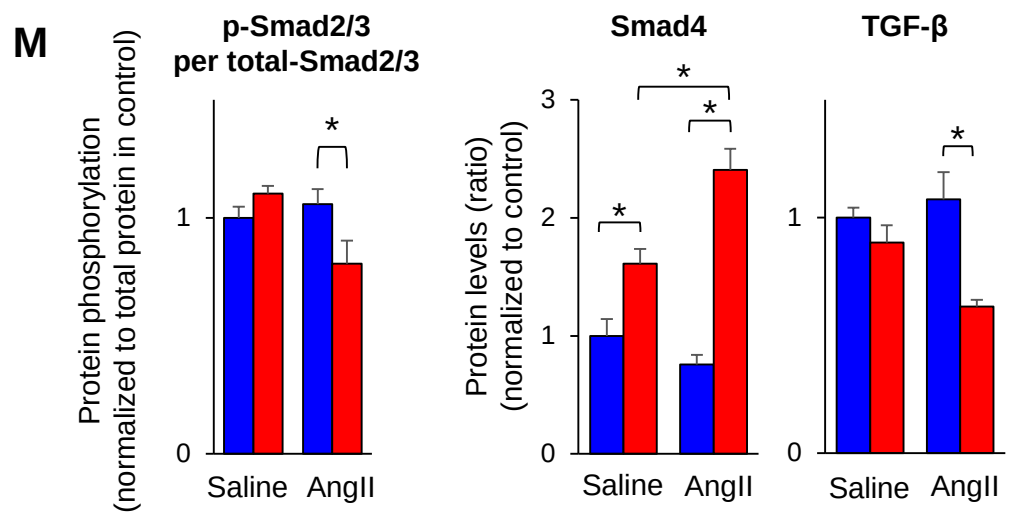


Downloaded from http://circ.ahajournals.org/ by guest on June 20, 2018

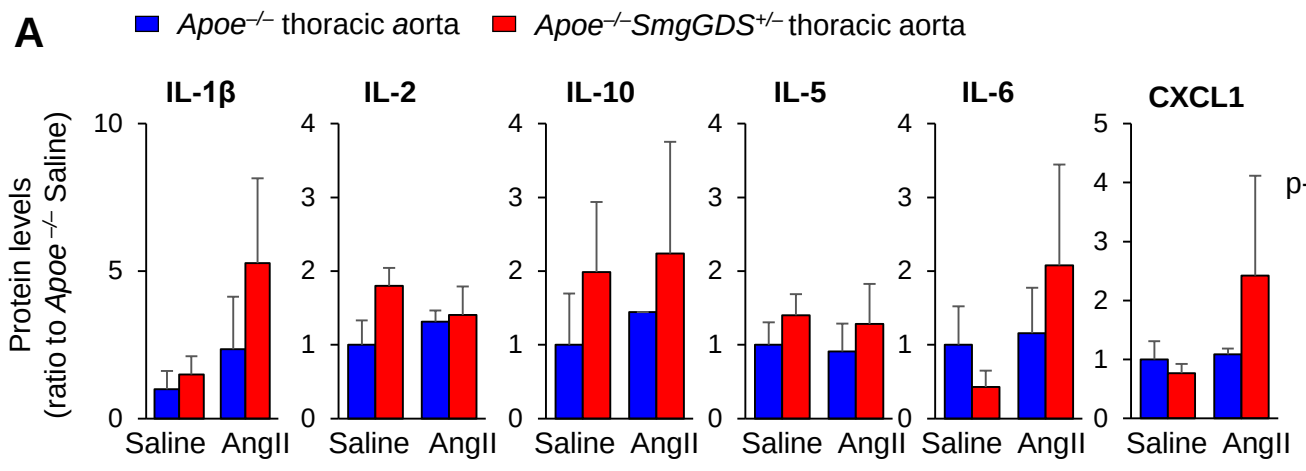


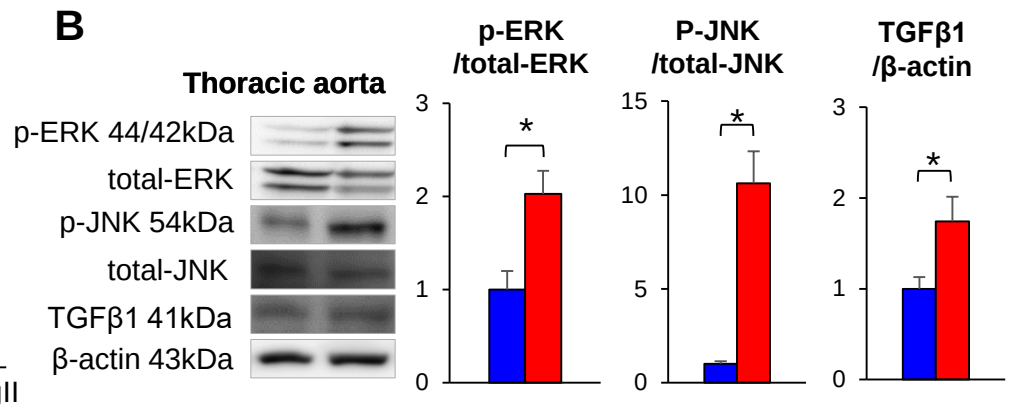


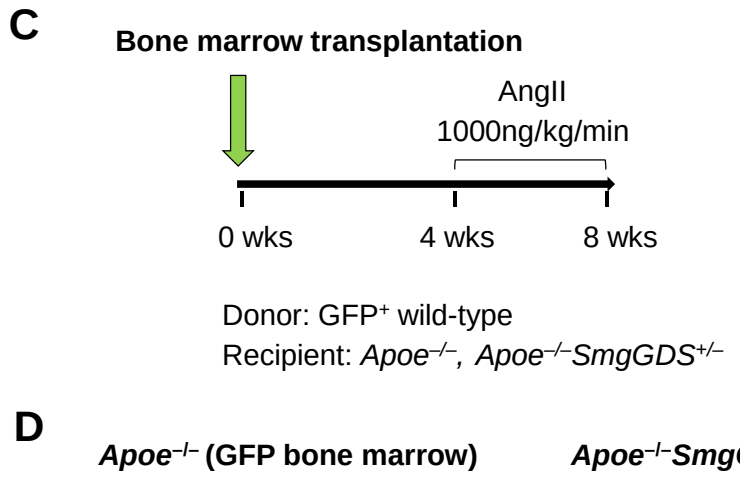


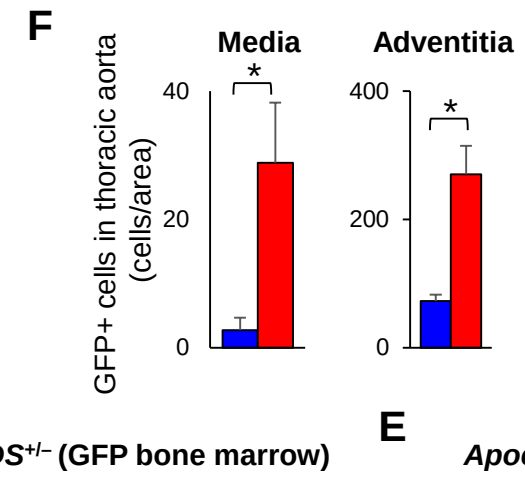


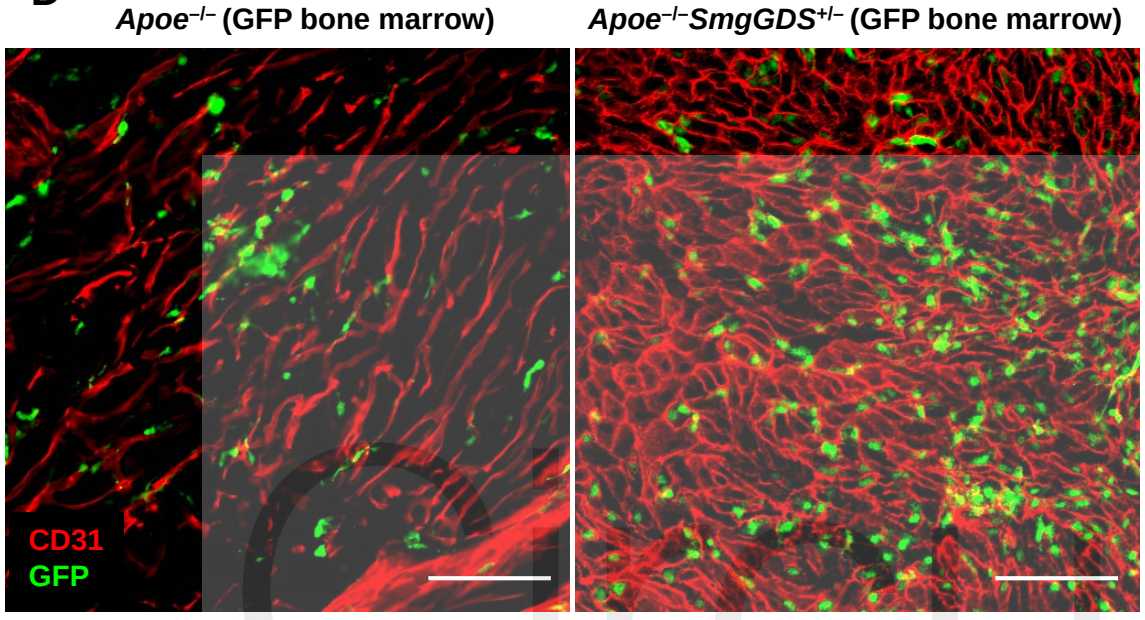


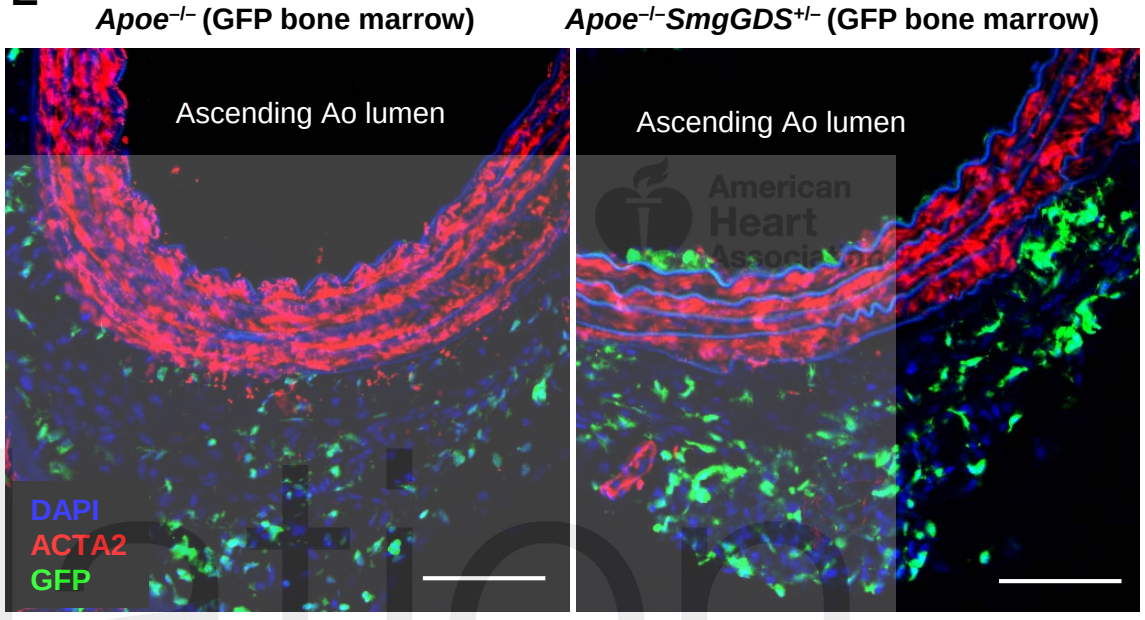


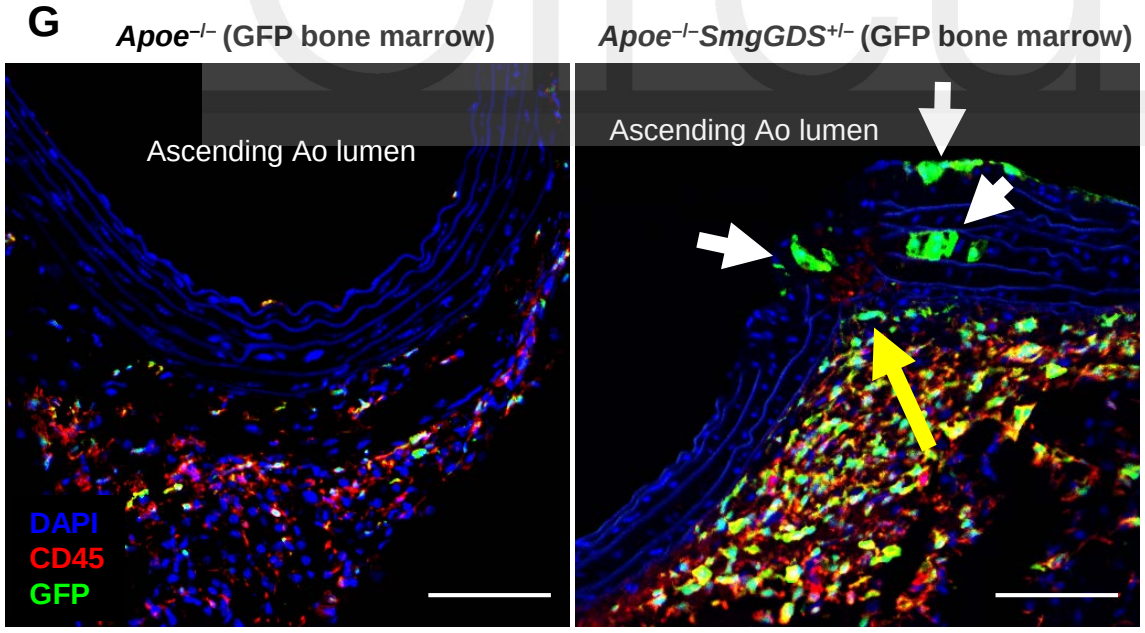


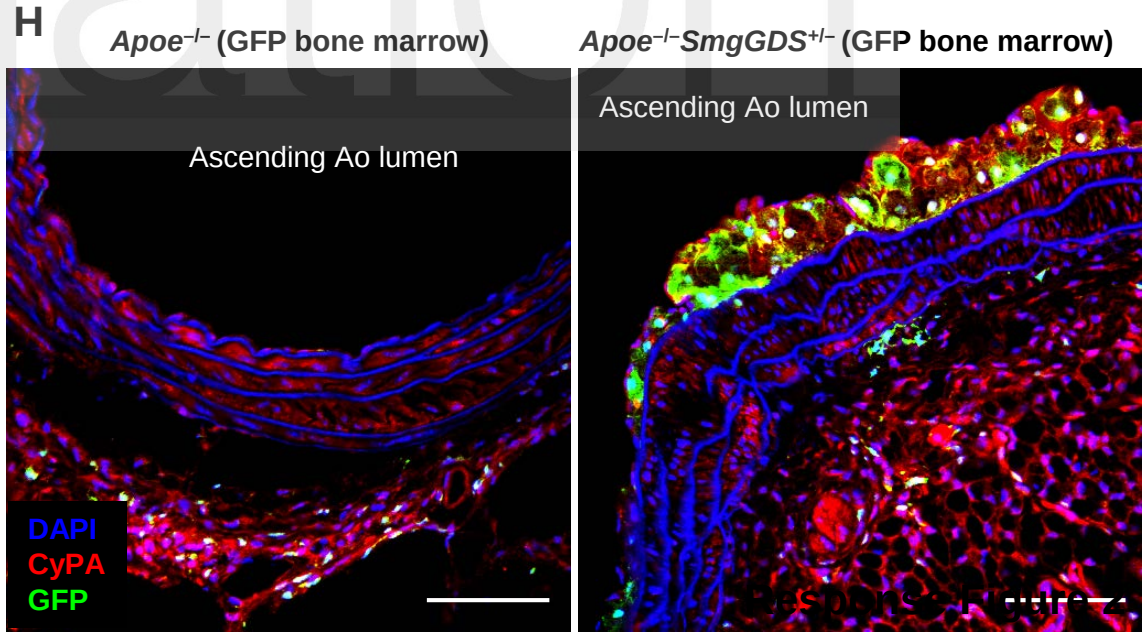


Downloaded from http://circ.ahajournals.org/ by guest on June 20, 2018

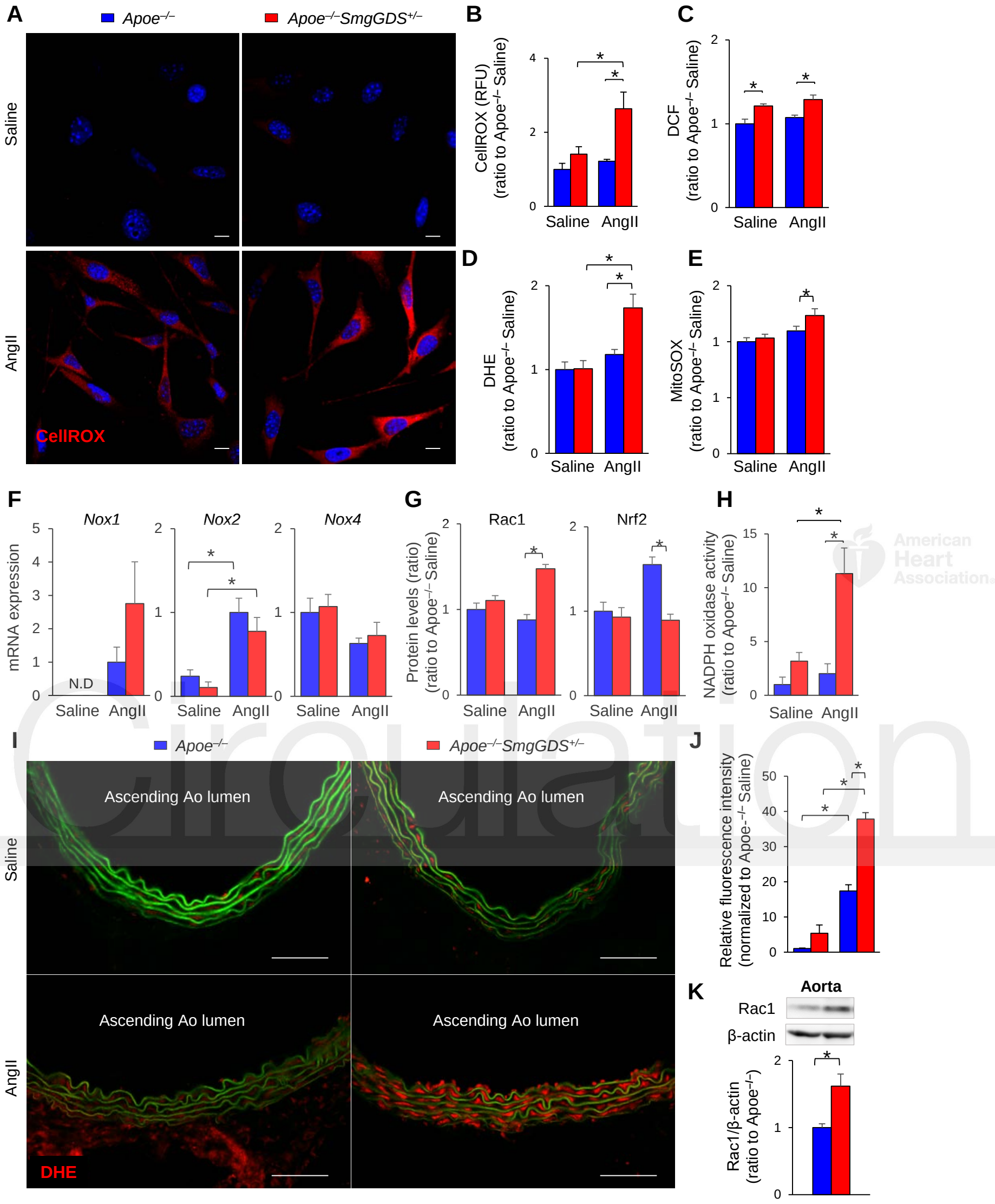


Downloaded from http://circ.ahajournals.org/ by guest on June 20, 2018

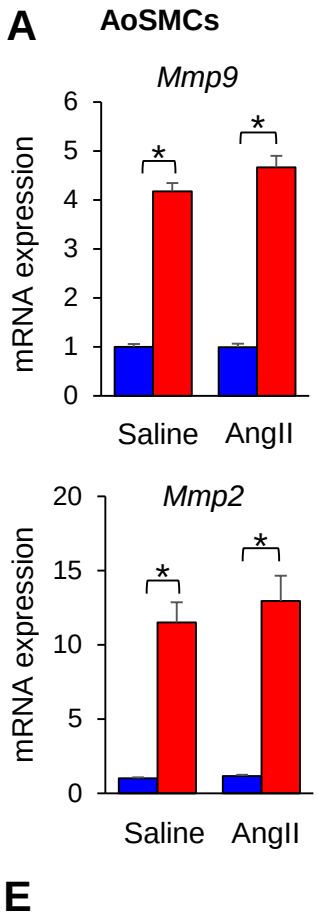


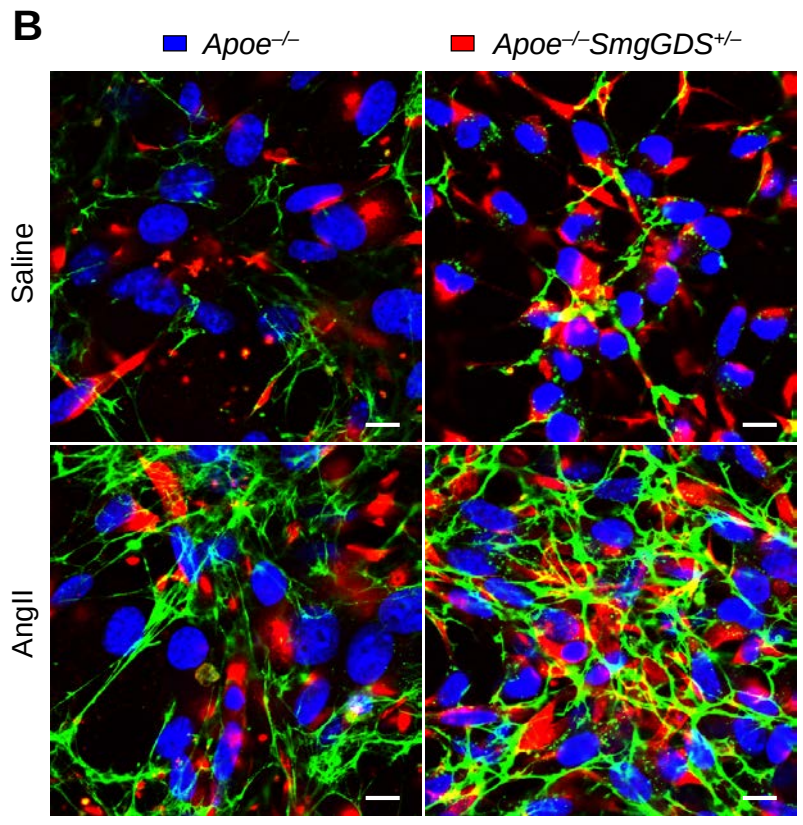


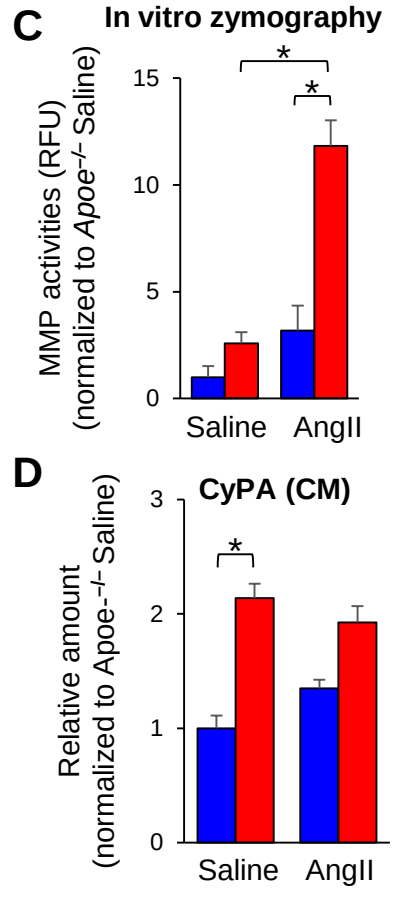


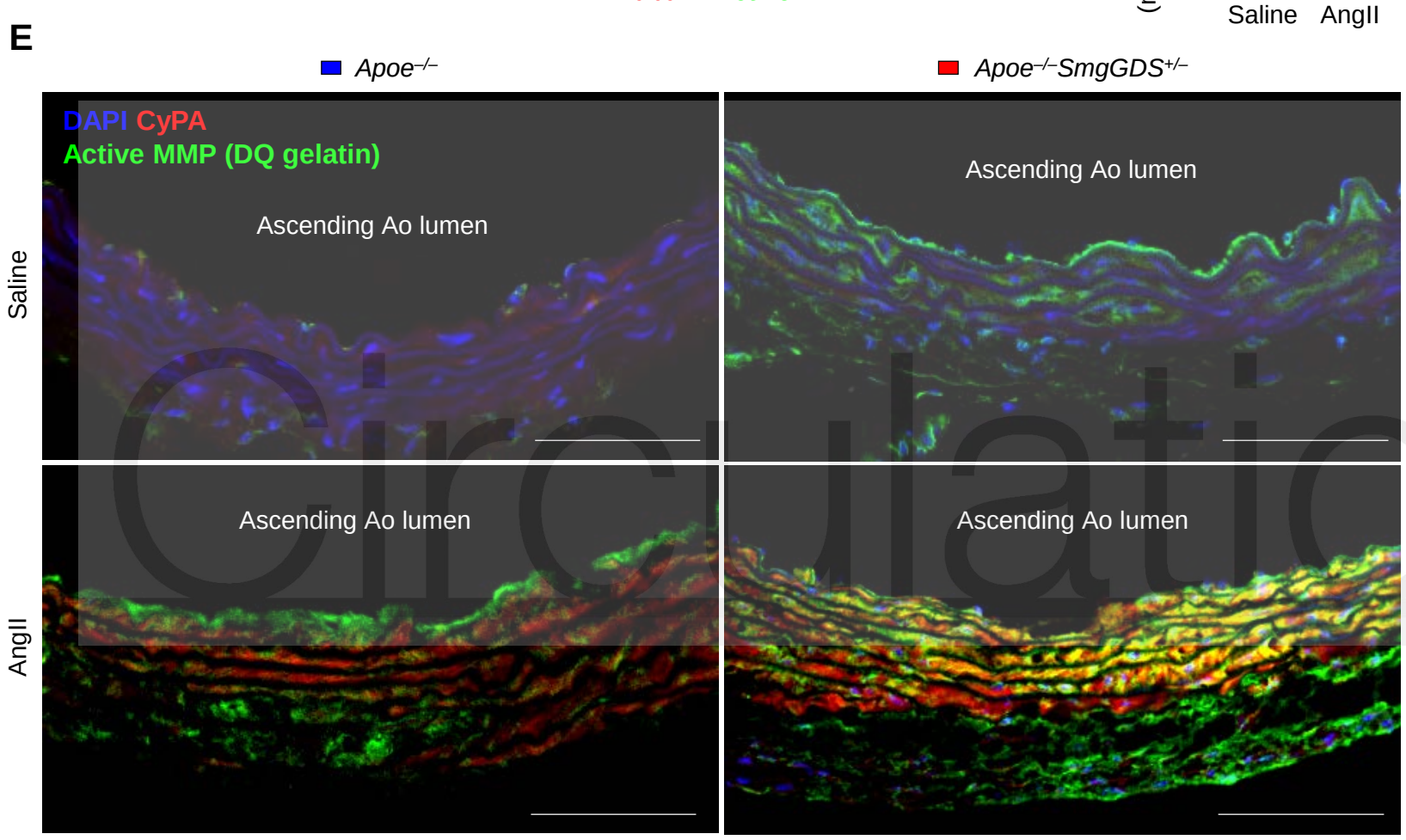


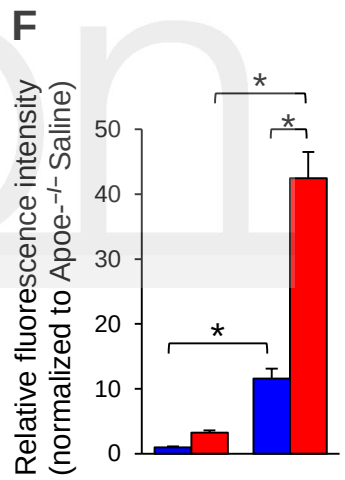


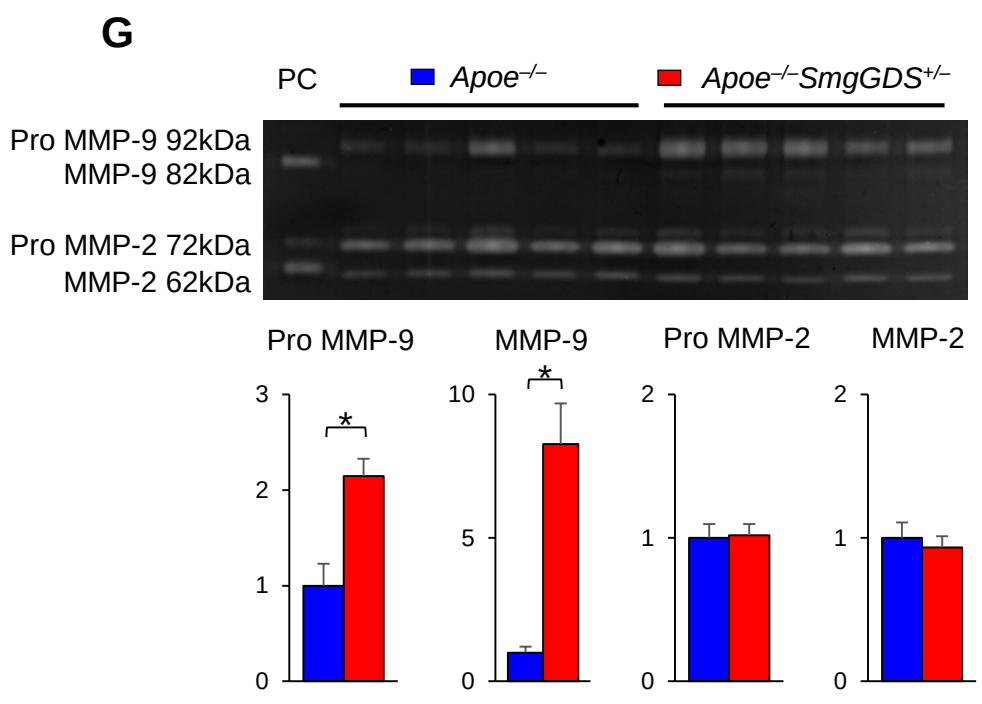


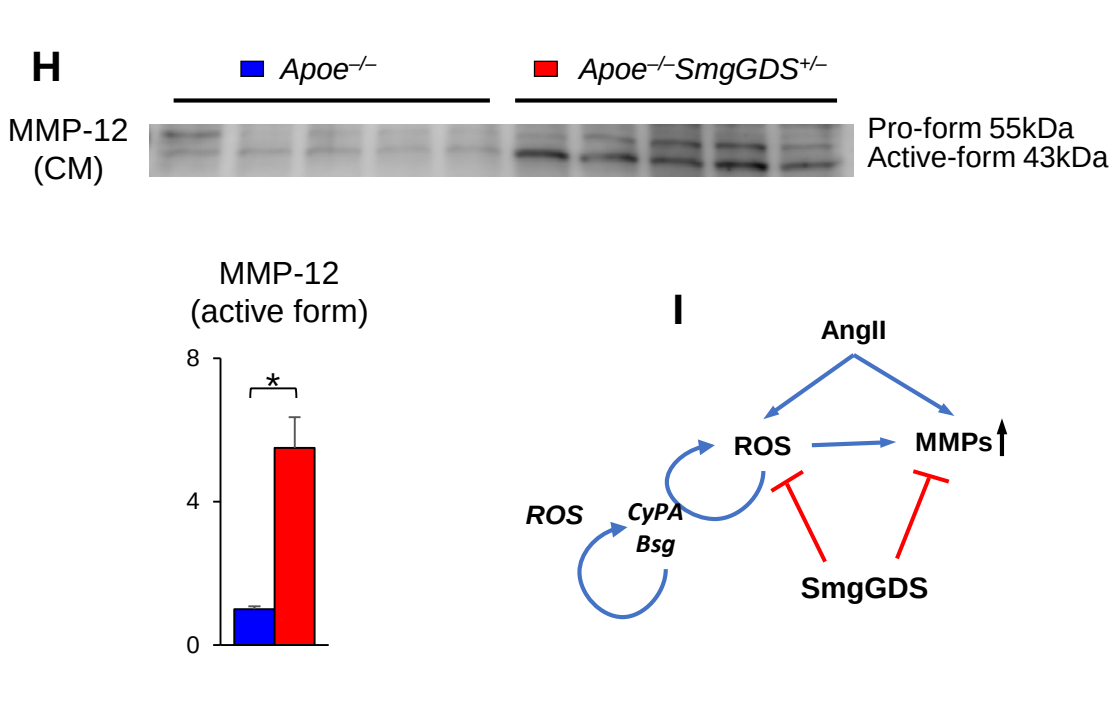


Downloaded from http://circ.ahajournals.org/ by guest on June 20, 2018

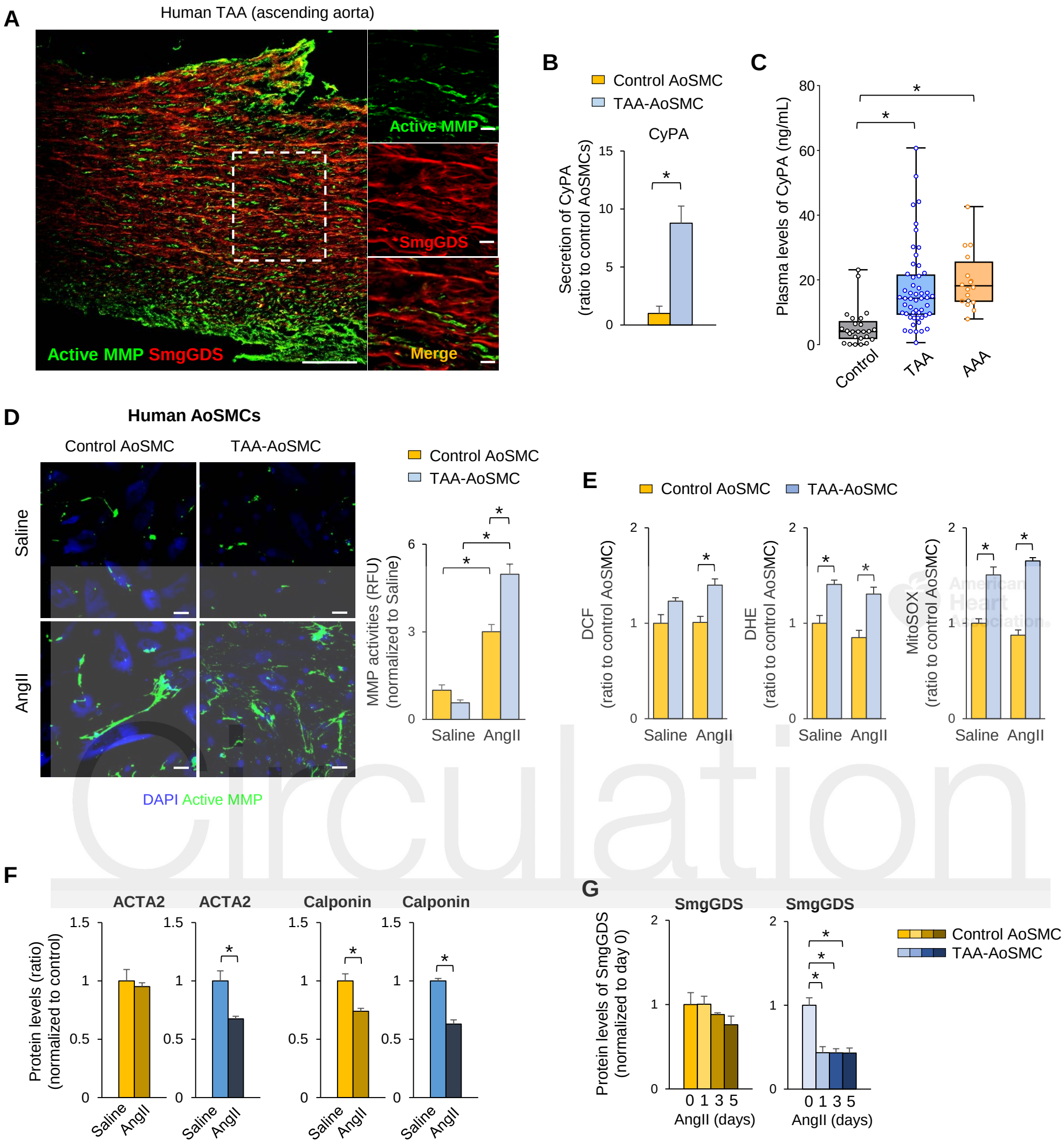


Downloaded from http://circ.ahajournals.org/ by guest on June 20, 2018

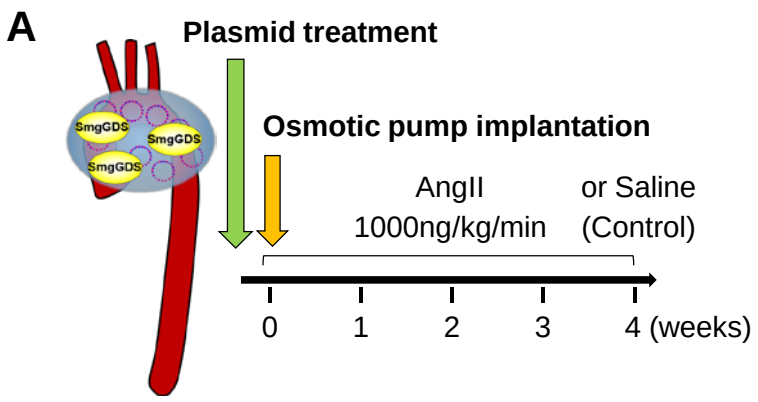


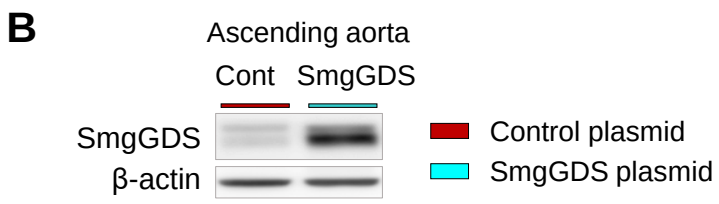


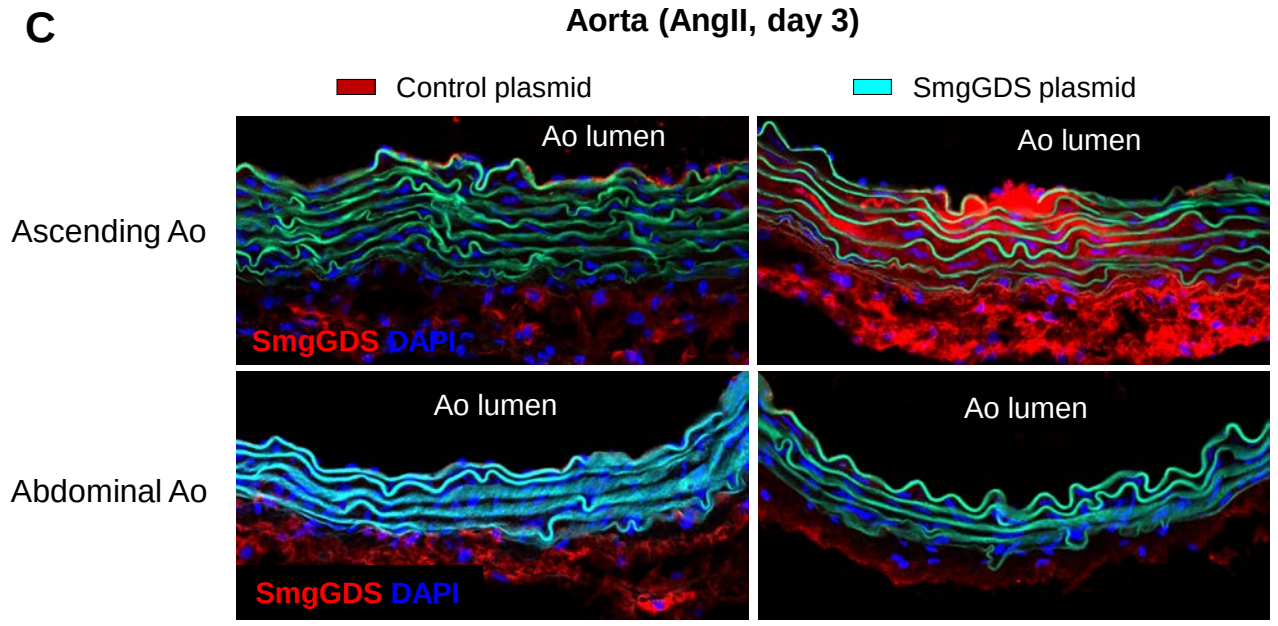


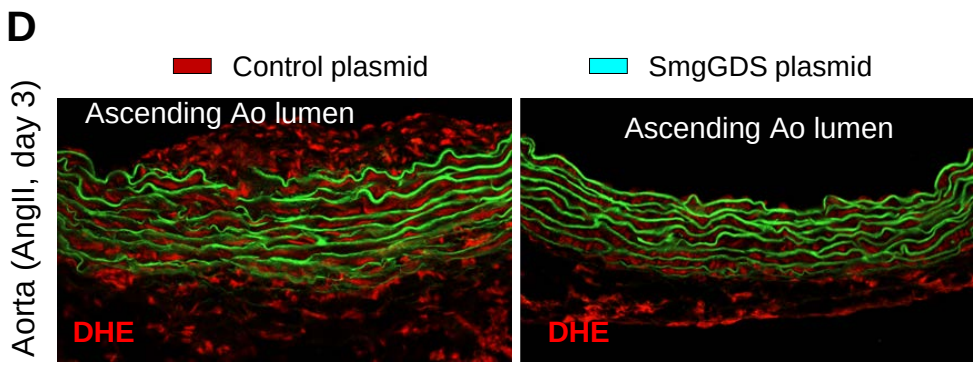


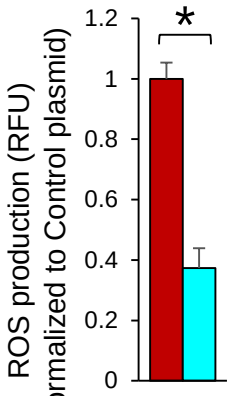


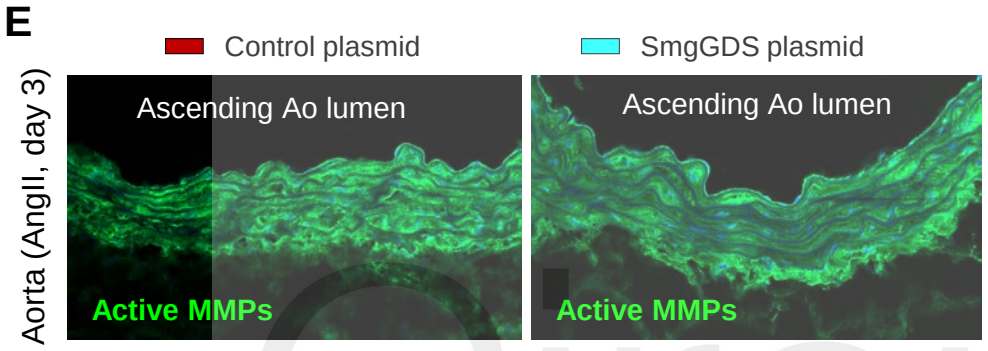


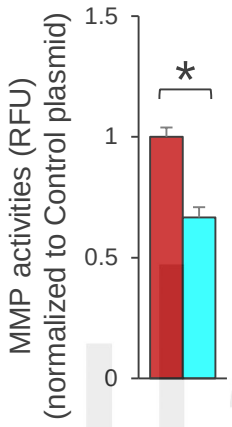


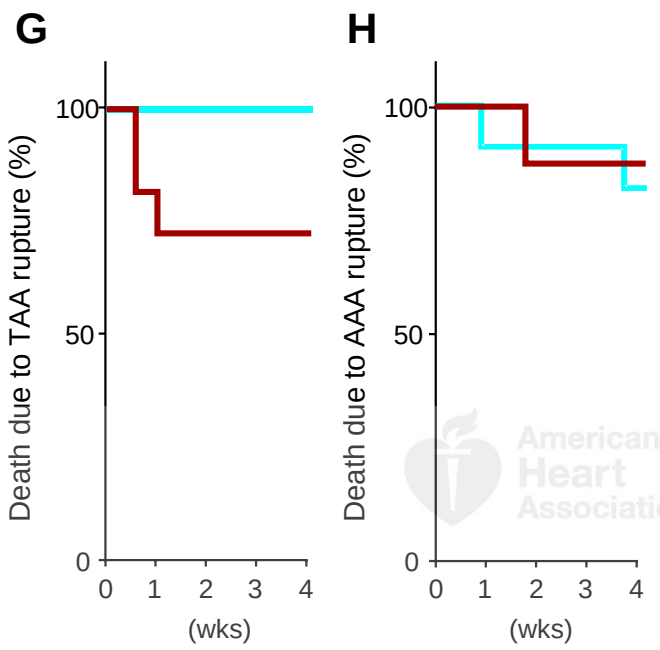





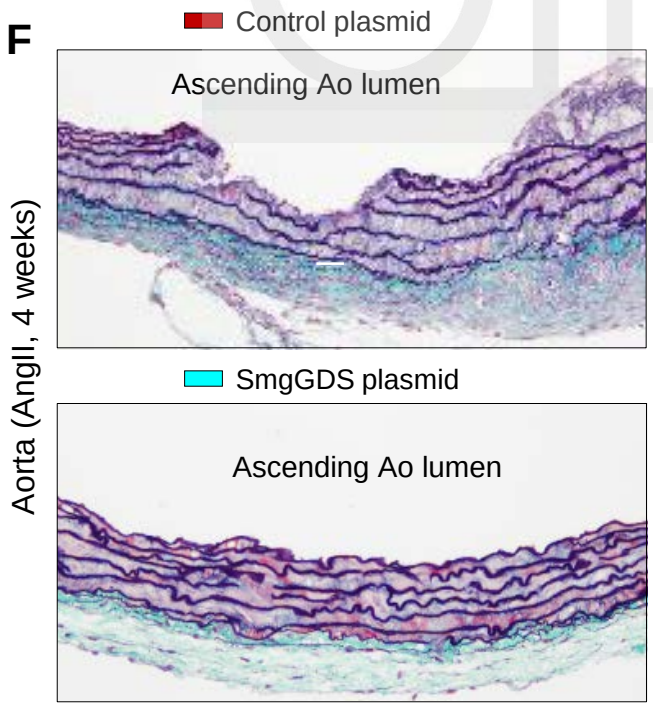


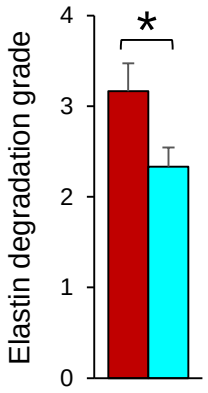


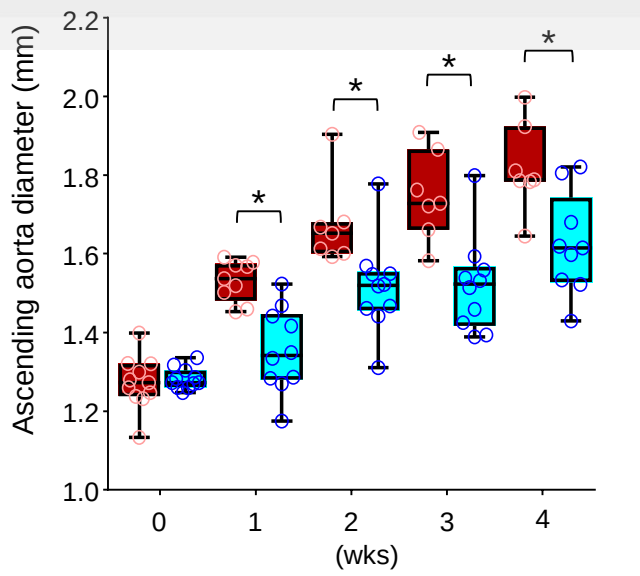


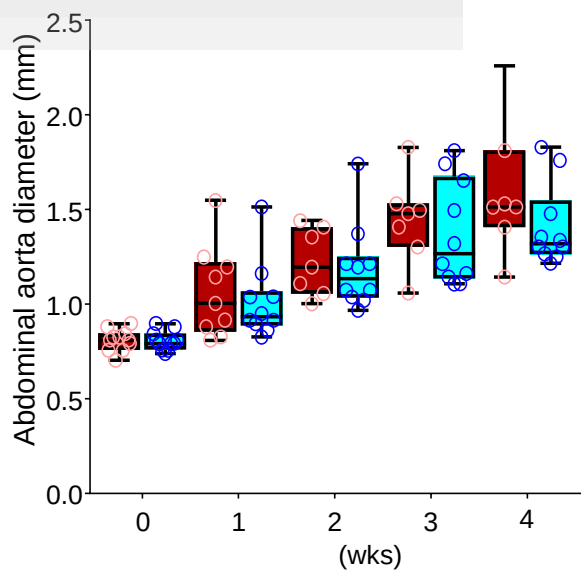


Downloaded from http://circ.ahajournals.org/ by guest on June 20, 2018

Circulation

American Heart Association®

# SmgGDS Prevents Thoracic Aortic Aneurysm Formation and Rupture by Phenotypic Preservation of Aortic Smooth Muscle Cells

Masamichi Nogi, Kimio Satoh, Shinichiro Sunamura, Nobuhiro Kikuchi, Taijyu Satoh, Ryo Kurosawa, Junichi Omura, Md. Elias Al-Mamun, Mohammad Abdul Hai Siddique, Kazuhiko Numano, Shun Kudo, Satoshi Miyata, Masatoshi Akiyama, Kiichiro Kumagai, Shunsuke Kawamoto, Yoshikatsu Saiki and Hiroaki Shimokawa

*Circulation.* published online June 19, 2018;
*Circulation* is published by the American Heart Association, 7272 Greenville Avenue, Dallas, TX 75231
Copyright © 2018 American Heart Association, Inc. All rights reserved.
Print ISSN: 0009-7322. Online ISSN: 1524-4539

The online version of this article, along with updated information and services, is located on the World Wide Web at:
http://circ.ahajournals.org/content/early/2018/06/13/CIRCULATIONAHA.118.035648

Data Supplement (unedited) at:
http://circ.ahajournals.org/content/suppl/2018/06/18/CIRCULATIONAHA.118.035648.DC1

**Permissions:** Requests for permissions to reproduce figures, tables, or portions of articles originally published in *Circulation* can be obtained via RightsLink, a service of the Copyright Clearance Center, not the Editorial Office. Once the online version of the published article for which permission is being requested is located, click Request Permissions in the middle column of the Web page under Services. Further information about this process is available in the Permissions and Rights Question and Answer document.

**Reprints:** Information about reprints can be found online at:
http://www.lww.com/reprints

**Subscriptions:** Information about subscribing to *Circulation* is online at:
http://circ.ahajournals.org//subscriptions/

Downloaded from http://circ.ahajournals.org/ by guest on June 20, 2018

# SUPPLEMENTAL MATERIAL

# SmgGDS Prevents Thoracic Aortic Aneurysm Formation and Rupture by Phenotypic Preservation of Aortic Smooth Muscle Cells

Masamichi Nogi, MD[1]; Kimio Satoh, MD, PhD[1]; Shinichiro Sunamura, MD[1]; Nobuhiro Kikuchi, MD, PhD[1]; Taijyu Satoh, MD, PhD[1]; Ryo Kurosawa, MD[1]; Junichi Omura, MD, PhD[1]; Md. Elias-Al-Mamun, PhD[1]; Mohammad Abdul Hai Siddique, PhD[1]; Kazuhiko Numano MD[1]; Shun Kudo, MD, PhD[1]; Satoshi Miyata, PhD[1]; Masatoshi Akiyama, MD, PhD[2]; Kiichiro Kumagai, MD, PhD[2]; Shunsuke Kawamoto, MD, PhD[2]; Yoshikatsu Saiki, MD, PhD[2]; Hiroaki Shimokawa, MD, PhD[1]

[1]Department of Cardiovascular Medicine, Tohoku University Graduate School of Medicine, Sendai, Japan. [2]Department of Cardiovascular Surgery, Tohoku University Graduate School of Medicine, Sendai, Japan

[1]Department of Cardiovascular Medicine, Tohoku University Graduate School of Medicine, Sendai, Japan. [2]Department of Cardiovascular Surgery, Tohoku University Graduate School of Medicine, Sendai, Japan

# Supplementary Methods

## Microarray

Total RNA was extracted from the primary cultured AoSMCs obtained from TAA patients (TAA-AoSMCs) and non-TAA controls undergoing bypass surgery, and was quantified using NanoDrop 2000C (Thermo Fisher Scientific). For microarray expression profiling, samples were processed using the Agilent SurePrint G3 Mouse GE 8x60K Microarray Kit (Agilent Technologies, Santa Clara, CA) according to the manufacturer's instructions. The statistical computing software R (version 3.3.2.) and samr (version 2.0) package of R were used for preprocessing and statistical analysis. Differentially expressed genes were considered significant at SAM *t*-test P values of $< 0.05$. Genes with significant changes were further subjected to pathway analysis using Ingenuity Pathway Analysis (IPA) (http://www.ingenuity.com) to identify gene sets representing specific biological processes or functions.

## Blood Pressure and Metabolic Measurements

Blood pressure at baseline was measured by the tail-cuff system (Muromachi Kikai Co, Ltd, MK-2000ST NP-NIBP Monitor, Tokyo, Japan) without anesthesia as described previously.[1] Blood samples were obtained from the mice before sacrifice. The blood was collected from the abdominal vena cava at sacrifice. Serum cholesterol and triglyceride were determined by a commercially available enzymatic assay kit (FUJIFILM, DRI-CHEM 7000V).

## Elastin Degradation Analysis

Degradation of medial elastic lamina were analyzed as described previously.[1] Briefly, based on elastin degradation-grading (no degradation, mild degradation, severe degradation and aortic rupture), degradation of medial elastic lamina was scored.

## Histological Analyses

After ultrasound imaging, animals were anesthetized with isoflurane (1.0%). For morphological analysis, aortas were perfused with cold phosphate-buffered saline (PBS) and fixed with 10% phosphate-buffered formalin at physiological pressure for 5 minutes. The whole aortas were harvested, fixed for 24 hours, embedded in paraffin, and cross-sections (3 μm) were prepared. The whole heart and lungs were embedded in paraffin, and cross-sections (3 μm) were prepared.

Paraffin sections were stained with Elastica-Masson (EM) or used for immunostaining. The antibody to ACTA2 (1:400, Sigma-Aldrich), Fibrillin-1, phosphorylated and total ERK, JNK, and TGFβ1 were used. As a negative control, species- and isotype-matched IgG were used in place of the primary antibodies.

**Transmission Electron Microscopy**

The ultrastructures of mouse aortic walls were visualized using transmission electron microscopy (TEM). For TEM assessment, aortas were perfused with cocktail consisting of 4% paraformaldehyde and 25% glutaraldehyde. The whole aortas were harvested and fixed with this cocktail for 3 hours. Ultrathin sections were made using Leica EM UC7 (Leica Microsystems, Wetzlar, Germany) and observed with a H-7600 transmission electron microscope (Hitachi High-Technologies Co., Tokyo, Japan).

**Immunofluorescence Staining**

Aortic tissues were embedded in optimum cutting temperature compound and quickly frozen. The tissues were cut into 10 μm thick slices. AoSMCs were plated on glass based dishes (AGC Techno Glass, Shizuoka, Japan) maintained in DMEM containing 10% FBS at 37°C in a humidified atmosphere. After AngII or saline treatment, cells were washed by cold PBS and added 4% *paraformaldehyde* phosphate buffer solution. Antibodies used were as follows: ACTA2, CD45, Fibrillin-1, SmgGDS, and Cyclophilin A. Slides and dishes were viewed with a fluorescence confocal microscopy (LSM 780, Carl Zeiss, Oberkochen, Germany).[4]

**Bone Marrow Transplantation**

Bone marrow (BM) transplantation was performed as previously described.[1,5] Briefly, recipient mice were lethally irradiated and received an intravenous injection of $5\times10^6$ donor $GFP^+$ BM cells suspended in 100 μL calcium-and magnesium-free PBS with 2% FBS. After transplantation, the mice were placed on a regular chow diet for 4 weeks followed by AngII infusion (1000 ng/kg/min) for 4 weeks. Transgenic mice ubiquitously expressing GFP were obtained from the Jackson Laboratory.

**Bone Marrow-derived Cell Recruitment Assays**

Analyses of leukocyte migration were performed 4 weeks after AngII infusion. Migrating GFP positive cells were analyzed by using a confocal microscopy (Zeiss, LSM780).

**Harvest of Mouse AoSMCs**

*Apoe*$^{-/-}$ and *Apoe*$^{-/-}$*SmgGDS*$^{+/-}$ AoSMCs were cultured from the aortas of male mice (23–26g BW) and maintained in DMEM containing 10% FBS at 37°C in a humidified atmosphere with 5% $CO_2$ as previously described.[1] AoSMCs of passages 4–7 at 70–80% confluence were used for experiments.

**Preparation of Conditioned Medium**

Conditioned medium (CM) from *Apoe*$^{-/-}$ and *Apoe*$^{-/-}$*SmgGDS*$^{+/-}$ AoSMCs incubated for 24 hours in DMEM were collected and filtered to remove cell debris. The collected medium was concentrated 100-fold with an Amicon ultra filter (Merck Millipore, Billerica, MA) to yield concentrated CM.[6,7]

**Cell Proliferation Assay**

For the assessment of cell proliferation, AoSMCs were seeded in 96-well plates (3,000 cells/well) in DMEM with 10% FBS and were incubated with compounds at each concentration for 48 hours. Cell proliferation was measured by the Cell-Titer 96 AQueous One Solution Cell Proliferation Assay kit (Promega, Madison, USA).[8]

**Measurements of Reactive Oxygen Species,**

AoSMCs were plated on 96-well plate in 3,000 cells/well concentration maintained in DMEM containing 10% FBS at 37°C in a humidified atmosphere with 5% $CO_2$. AoSMCs were allowed to adhere for 24 hours and treated with vehicle or AngII (1 μM) for 4 hours. After the treatment, 2,7-dichlorofluorescin diacetate (DCF, final concentration 10 μM, Sigma-Aldrich), CellROX Deep Red (final concentration 5 μM, Thermo Fisher Scientific), dihydroethidium (DHE, final concentration 2 μM, SIGMA), or MitoSOX Deep Red Reagent for oxidative stress detection (final concentration 5 μM, Thermo Fisher Scientific) were added to the culture medium according to the manufacturer's instruction. After the incubation for 30 min at 37℃, cells were washed twice with warmed PBS, and the fluorescence intensity was measured with SpectraMax i3 (Molecular Devices, Sunnyvale, CA).

**NADPH Oxidase Activity Assay**

NADPH oxidase activity was measured by a lucigenin-enhanced luminescence assay as described

previously.[9,10] Briefly, AoSMCs that had been treated with AngII (1 μM) or saline for 4 hours were washed, and cells were scraped from the plate. These cells were washed with cold PBS and lysed with cell lysis buffer (Cell Signaling) and protease inhibitor cocktail (Sigma-Aldrich) after the incubation period. Protein content was standardized for total protein content using the BCA Protein Assay kit (Thermo Scientific).[5] NADH/NADPH oxidase activity was measured in a luminescence assay with 500 μM lucigenin as the electron acceptor and either 100 μM NADH or 100 μM NADPH as the substrate. The reaction was started by the addition of 100 μL of homogenate (100–200 μg protein). Luminescence intensity was measured with SpectraMaxi3 (Molecular Devices, Sunnyvale, CA).

**Confocal Microscopy**

AoSMCs were plated on glass based dishes (AGC Techno Glass, Shizuoka, Japan) maintained in DMEM containing 10% FBS at 37°C in a humidified atmosphere with 5% $CO_2$. AoSMCs were allowed to adhere for 24 hours and treated with saline or AngII (1 μM) for 12 hours. After the treatment, AoSMCs were stained using prewarmed (37°C) staining solution containing CellROX Deep Red in DMEM according to the manufacturer's instruction. Cells on dishes were rinsed in warmed PBS and then fixed in 3.7% formaldehyde and PBS for 30 min. Cells were mounted using ProLong Diamond Antifade Mountant with DAPI (Thermo Fisher Scientific) and was visualized on a LSM780 confocal microscope (Carl Zeiss, Oberkochen, Germany).

**Measurement of Cytokines/Chemokines and Growth Factors**

Protein levels of cytokines/chemokines and growth factors in the conditioned medium (CM) or the aortas were measured with a Bioplex system (Bio-Rad, Tokyo, Japan) according to the manufacturer's instructions. We measured cytokines/chemokines and growth factors in CM from AoSMCs after treatment with saline or AngII (1μM, 100-mm dish, 10 mL DMEM). To analyze the plasma levels of cytokines/chemokines, we collected the blood from the abdominal vena cava at sacrifice, which were added with EDTA and centrifuged (4°C, 10,000g, 15 min). Thoracic aortas were perfused with cold PBS and the circulating blood was completely removed. Aortic tissues were homogenized with tissue protein extraction reagent (Pierce, Rockford, America) and centrifuged (4°C, 15,000g, 15 min), and thereafter, clear supernatants were standardized for total protein content using the BCA Protein Assay kit (Pierce, Rockford, America). [5,11,12] Mouse cytokines/chemokines and growth factors were measured with commercially available kits (Bio-Rad, 9-Plex, MD0-00000EL and 23-Plex, M60-009RDPD).

**RNA Isolation and Real-time PCR**

Isolation of total RNA from human PASMCs were performed using the RNeasy Plus Mini Kit (Qiagen) according to the manufacturer's protocol. Total RNA was converted to cDNA using PrimeScript RT Master Mix (Takara Bio Inc., Kusatsu). Human primers (*FBN1*, *ACTA2*, *MYLK*, *MYH11*, *PRKG1*, and *NRF2*) and mouse primers (*Fbn1*, *Mlk*, *Myh11*, *Acta2*, *Prkg1*, *Nox1*, *Nox2*, *Nox4*, *Mmp2*, and *Mmp9*) were purchased from Life Technologies (TaqMan assays, Applied Biosystems, US). After reverse transcription, quantitative real-time PCR on the CFX 96 Real-Time PCR Detection System (Bio-Rad) was performed using either SsoFast Probes Supermix (Bio-Rad) for TaqMan probes. The Ct value determined by CFX Manager Software (version2.0, Bio-Rad) for all samples was normalized to housekeeping gene *Gapdh* and the relative fold change was computed by the ΔΔCt method.[13]

**Western Blot Analysis**

Human AoSMCs were seeded in 100-mm dishes in DMEM with 10% FBS. AoSMCs were allowed to adhere for 24 hours, washed two times and starved in serum-free medium for 24 hours. PASMCs were then treated with AngII (1 μM) for 24 hours. After the incubation period, these cells were washed with cold PBS and lysed with cell lysis buffer (Cell Signaling, Beverley, MA) and protease inhibitor cocktail (Sigma-Aldrich). Total cell lysates and the aorta homogenates were loaded on the sodium dodecyl sulfate-polyacrylamide gel electrophoresis (SDS-PAGE) and transferred to polyvinylidene difluoride (PVDF) membranes (GE Healthcare, Buckinghamshire, UK), following blocking for 1 hour at room temperature in 5% bovine serum albumin (BSA) or 5% skim milk in tris-buffered saline with Tween 20 (TBST).[13] The primary antibodies were as follows; β-actin (1:3000, Abcam, Cambridge, UK), SmgGDS (1:500, BD Biosciences), Cyclophilin A (1:1000, Enzo) phosphorylated-JNK (1:500, Cell Signaling), total-JNK (1:1000, Cell signaling), Rac1 (1000:1, Millipore), RhoA (500:1, Cell Signaling), RhoC (500:1, Cell Signaling), phosphorylated-ERK1/2 (1:1000, Cell Signaling), total-ERK1/2 (1:1000, Cell Signaling), ACTA2 (1:1000, Abcam), Calponin (1:1000, Abcam), ROCK1 (1:1000, BD Biosciences), ROCK2 (1:1000, BD Biosciences), RhoA (1:1000, Cell Signaling), phosphorylated-Smad2/3 (1:1000, Abcam), total-Smad2/3 (1:1000, Cell signaling), Smad4 (1:1000, Cell signaling) and TGF-β (1:1000, NOVUS). The regions containing proteins were visualized by the enhanced chemiluminescence system (ECL Prime Western Blotting Detection

Reagent, GE Healthcare). Densitometric analysis was performed by the Image J Software (NIH, Bethesda, MD).

**RhoC Activity**

Measurement of active RhoC levels was determined by the GLISA assay (Cytoskeleton #BK121). Active RhoC was determined using the RhoC activation assay kit with a rabbit monoclonal anti-RhoC (Cell Signaling) antibody at 1:100 concentration. Active RhoC levels were normalized to total Rho GTPase levels determined by immunoblotting.

**ROS Analysis**

Aortas were perfused with PBS (pH7.4) at 100 mmHg for 5 min at 4°C. Aortas were perfused with PBS (pH 7.4) at 100 mmHg for 5 min at 4°C. Aortic tissue was harvested, and the abdominal aorta were embedded in OCT and snap-frozen. Dihydroethidine hydrochloride (5 μM, Molecular Probes) was topically applied to the freshly cut frozen aortic sections (10 μm) for 30 min at 37°C to reveal the presence of ROS as red fluorescence (585 nm) by confocal microscopy (LSM780, Carl Zeiss, Oberkochen, Germany). All sections are shown with the luminal aspect facing upwards and the adventitia facing downwards.

**MMP Activity**

The evaluation of MMP activities in response to AngII was performed as described previously[1]. To verify the role of SmgGDS in AngII-induced MMP activation, AoSMCs were treated with AngII (1 μM) in culture medium. For *in situ* and *in vitro* zymography, freshly cut frozen aortic sections (10 μm) and AoSMCs were incubated with a fluorogenic gelatin substrate (DQ gelatin, Molecular Probes) dissolved to 25 mg/mL in zymography buffer (50 mmol/L Tris-HCl pH 7.4 and 15 mmol/L $CaCl_2$) according to the manufacturer's protocol. Proteolytic activity was detected as green fluorescence (530 nm) by confocal microscopy (LSM780, Carl Zeiss, Oberkochen, Germany). All sections are shown with the luminal aspect facing upwards and the adventitia facing downwards.

**Overexpression of SmgGDS in Mice and Human AoSMCs**

The human SmgGDS (*RAP1GDS1*)-overexpressing plasmid were provided by Dr. Williams.[14] The human SmgGDS plasmid was cloned into the pcDNA3.1(+) vector, and control plasmid DNA was also produced. We coated the ascending aorta and transverse aorta with special gel

containing SmgGDS-overexpressing plasmid, which enables to release SmgGDS gene continuously. We anesthetized the mice with isoflurane (1.0%), exposed the ascending and transverse aorta, and applied the atelocollagen (AteloGene Local Use "Quick Gelation", KOKEN, Japan) with SmgGDS or control plasmid DNA according to the manufacturer's instructions. After the transfection, we infused 6–8 weeks old male *Apoe*$^{-/-}$*SmgGDS*$^{+/-}$ mice with 1000 ng/lg/min AngII (MP Biomedicals) for 4 weeks. The human *SmgGDS* gene was transfected to human AoSMCs with Lipofectamine 3000 reagent (Thermo Fisher Scientific) according to the manufacturer's instructions.

**Measurements of Plasma Levels of Cyclophilin A**

The Ethical Review Board of Tohoku University approved the study protocol, and written informed consent was obtained from all patients (No. 2008-470). Patients with hypertension were regarded as being at risk if their blood pressure was ≥140/90 mmHg or if they had a history of antihypertensive drug use. Patients with diabetes mellitus were regarded as being at risk if their fasting glucose level was ≥126 mg/dL or if they had a history of hypoglycemic drug or insulin use. Patients with dyslipidemia were regarded as being at risk if their LDL cholesterol level was ≥140 mg/dL or their HDL cholesterol level was ≤40 mg/dL, or if they were taking a lipid-lowering drug. Fasting blood samples were collected for measurement of CyPA concentration from the antecubital vein in the supine position. Plasma samples were collected using EDTA and were centrifuged for 10 min at 2,500 g within 30 min of blood collection, and aliquots were stored at -80°C. Plasma CyPA levels were measured using an immunoassay based on the sandwich technique according to the manufacturer's protocol (Human Cyclophilin A ELISA Kit, CSB-E09920h, Cusabio).

# Supplementary Table 1

**Baseline Characteristics (Related to Supplementary Figures 1 and 8)**

| | Controls (*n*=4) | TAA (*n*=6) |
|---|---|---|
| Age — years | 55 ± 13 | 61 ± 6 |
| Female sex — no. (%) | 1 (25) | 3 (50) |
| Body-mass index | 21 ± 4 | 22 ± 2 |
| Medication — no. (%) | | |
| ACE inhibitor/ARB | 2 (50) | 6 (100) |
| Ca channel blocker | 0 (0) | 3 (50) |
| β-blocker | 3 (75) | 3 (50) |
| Statin | 2 (50) | 3 (50) |
| Aortic diameter (mm) | | |
| Maximum thoracic aorta | 30 ± 7 | 50 ± 8 |

# Supplementary Table 2

**Top 10 Significant Canonical Pathways in TAA-AoSMCs**

| No. | Top canonical pathways |
|---|---|
| 1 | Aryl hydrocarbon receptor signaling |
| 2 | Role of BRCA1 in DNA damage response |
| 3 | Hereditary breast cancer signaling |
| 4 | Unfolded protein response |
| 5 | Glucose and glucose-1-phosphate degradation |
| 6 | Growth arrest and DNA damage 45 (GADD45) signaling |
| 7 | DNA damage-induced 14-3-3σ signaling |
| 8 | Death receptor signaling |
| 9 | Tumor necrosis factor (TNF) R1 signaling |
| 10 | Ataxia telangiectasia-mutated (ATM) signaling |

## Supplementary Table 3

| | Baseline Characteristics | | |
|---|---|---|---|
| | *Apoe*$^{-/-}$ | *Apoe*$^{-/-}$*SmgGDS*$^{+/-}$ | p |
| Body weight | 25 ± 2 | 24 ± 2 | NS |
| Total cholesterol | 507 ± 93 | 514 ± 85 | NS |
| Triglyceride | 150 ± 50 | 149 ± 38 | NS |

NS, no significant difference. Results are mean ± SD.

## Supplementary Table 4

**Baseline Characteristics (Related to Figure 8)**

| | Controls (*n*=25) | TAA (*n*=52) | AAA (*n*=16) |
|---|---|---|---|
| Age — years | 56 ± 12 | 74 ± 9 | 72 ± 8 |
| Female sex — no. (%) | 13 (52) | 8 (15) | 1 (4) |
| Body-mass index | 24 ± 3 | 22 ± 4 | 24 ± 3 |
| Medication — no. (%) | | | |
| ACE inhibitor/ARB | 9 (36) | 33 (63) | 8 (50) |
| Ca channel blocker | 7 (28) | 31 (60) | 9 (56) |
| β-blocker | 3 (12) | 19 (37) | 4 (25) |
| Statin | 9 (36) | 18 (35) | 12 (75) |
| Smoking | 6 (24) | 11 (21) | 9 (56) |

## Supplementary Figure 1

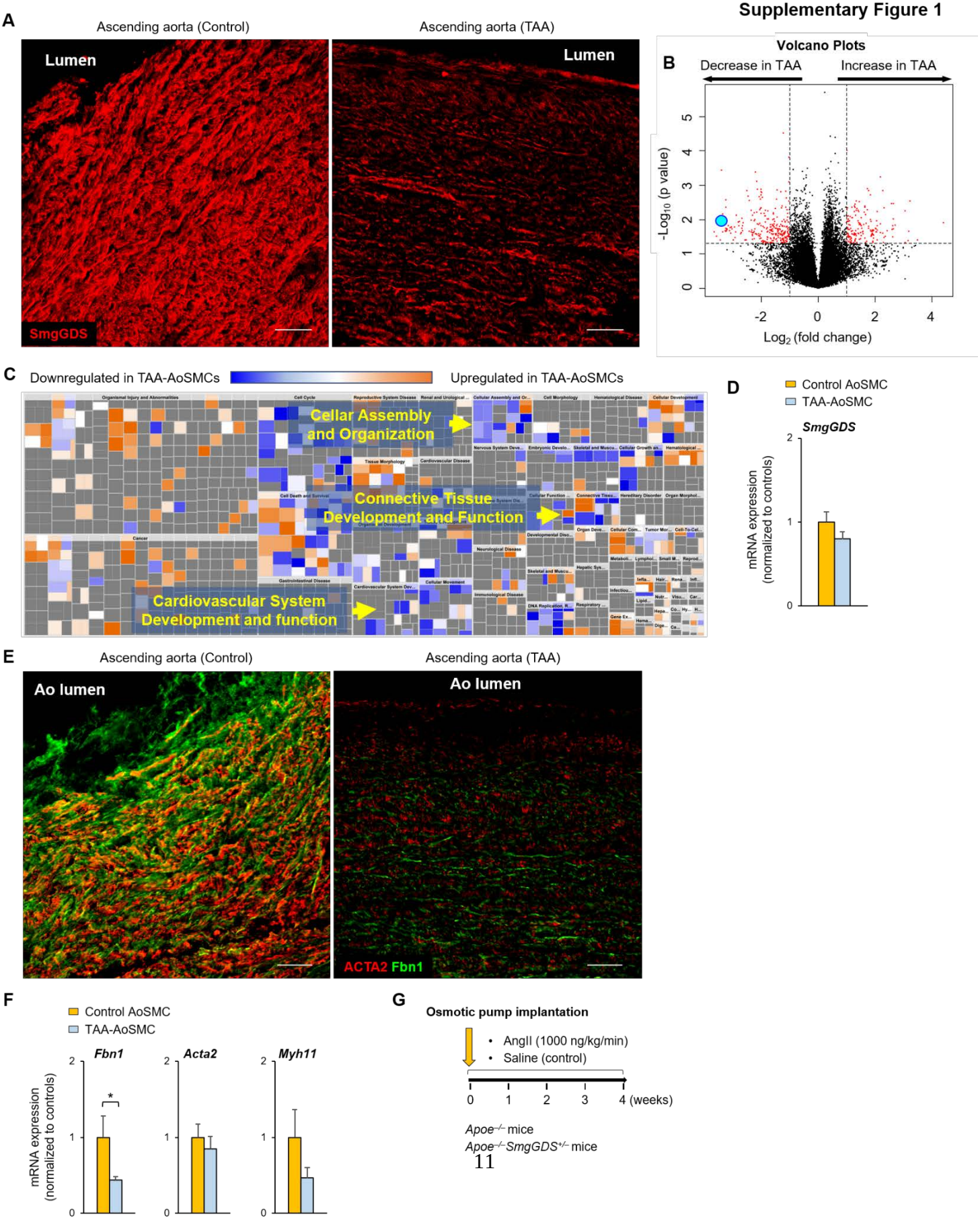

**Supplementary Figure 1. Expressions of SmgGDS, Fibrillin-1, and contractile genes in ascending aortas of patients with thoracic aortic aneurysm (TAA)**

(**A**) Representative immunostaining for SmgGDS (red, Alexa flour 546) in ascending aortas of control and TAA patients. (**B**) Volcano plots of gene expression variations in primary cultured AoSMCs obtained from TAA patients (TAA-AoSMCs) and control AoSMCs. Blue plots represent probes for SmgGDS. Dashed lines represent an adjusted P value of 0.05 and ± 1-fold change. (**C**) Heat map analysis of gene microarray analyses by Ingenuity Pathway Analysis software. (**D**) RT-PCR analysis of SmgGDS mRNA in control ($n$=4) and TAA-AoSMCs ($n$=6). (**E**) Representative double-immunostaining for Fbn1 (green, Alexa flour 488) and ACTA2 (red, Alexa flour 546) in ascending aortas of control and TAA patients. (**F**) RT-PCR analysis of *Fbn1*, *Acta2*, *Myh11* mRNA in control ($n$=4) and TAA-AoSMCs ($n$=6). (**G**) Schematic protocol of AngII (1000 ng/kg/min) infusion in $Apoe^{-/-}$ ($n$=13) and $Apoe^{-/-}SmgGDS^{+/-}$ ($n$=15) mice by osmotic pump implantation for 4 weeks. Scale bars, 100 μm. Data represent the mean ± SEM. *$P$<0.05. Comparisons of parameters were performed with the unpaired Student's $t$-test.

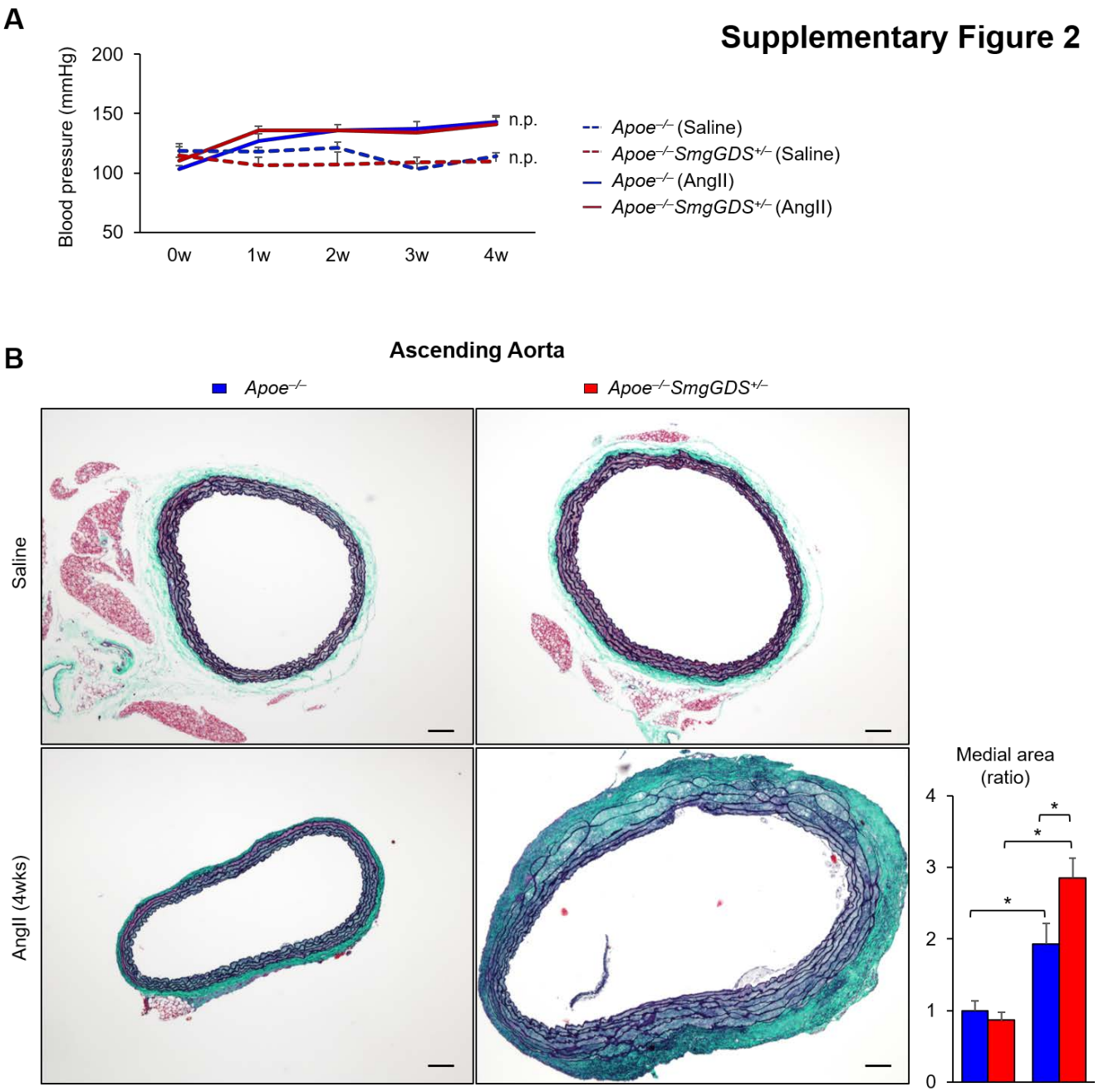


**Supplementary Figure 2. Blood pressure measurement and elastin degradation of the aortic walls after angiotensin II (AngII) treatment**

(**A**) Blood pressure measurement of *Apoe*$^{-/-}$ and *Apoe*$^{-/-}$*SmgGDS*$^{+/-}$ mice during the treatment with saline or AngII (1000 ng/kg/min) (saline, *n*=5 each; AngII; *n*=13–15). (**B**) Representative Elastica-Masson staining and assessment of ascending aortas from *Apoe*$^{-/-}$ and *Apoe*$^{-/-}$ *SmgGDS*$^{+/-}$ mice after treatment with saline or AngII for 4 weeks (saline, *n*=5 each; AngII, *n*=13–15). Scale bars, 100 μm. Data represent the mean ± SEM. **P*<0.05.

**Supplementary Figure 3**

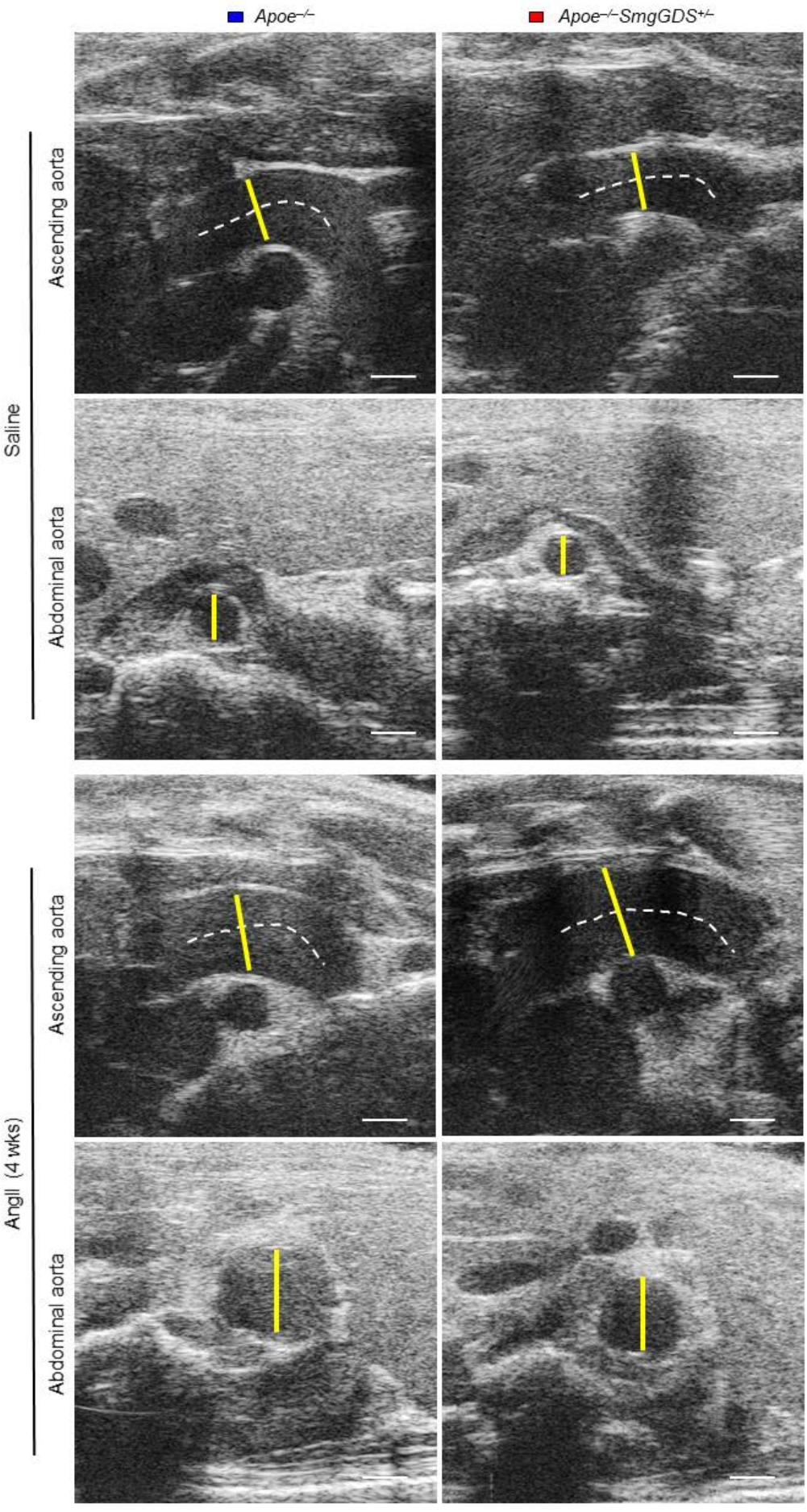

**Supplementary Figure 3. Aortic dilatation in response to angiotensin II (AngII) treatment**
Representative ultrasound imaging of ascending aortas and abdominal aortas after treatment with saline or AngII (1000 ng/kg/min) for 4 weeks. Yellow bars show the maximum diameters of ascending and abdominal aortas. White scale bars, 1 cm.

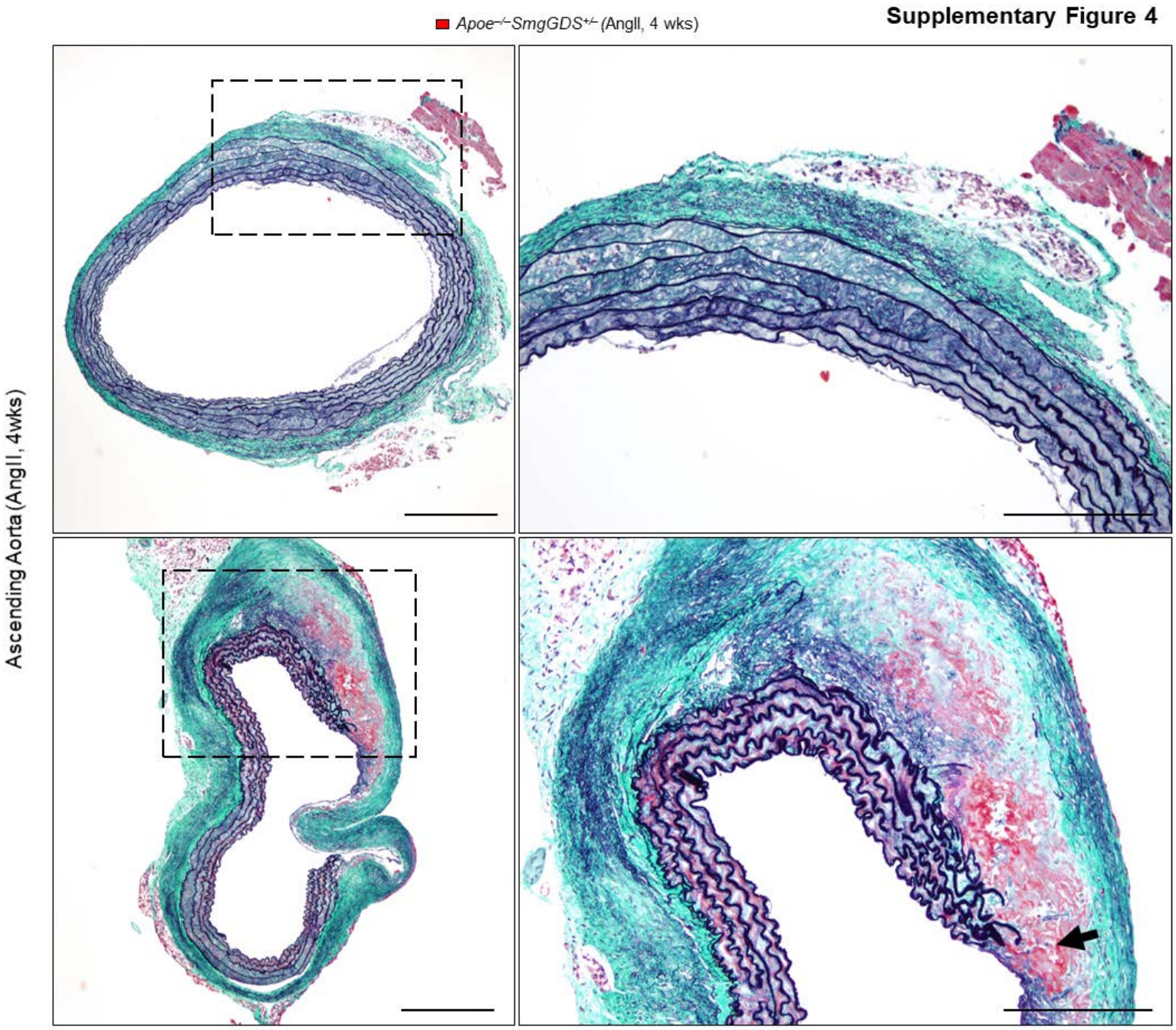


**Supplementary Figure 4. Elastin degradation in ascending aorta of *Apoe*$^{-/-}$*SmgGDS*$^{+/-}$ mice in response to angiotensin II (AngII) treatment**

Representative Elastica-Masson staining of ascending aortas from *Apoe*$^{-/-}$*SmgGDS*$^{+/-}$ mice after treatment with AngII (1000 ng/kg/min) for 4 weeks. Scale bars, 200 μm.

**Supplementary Figure 5**

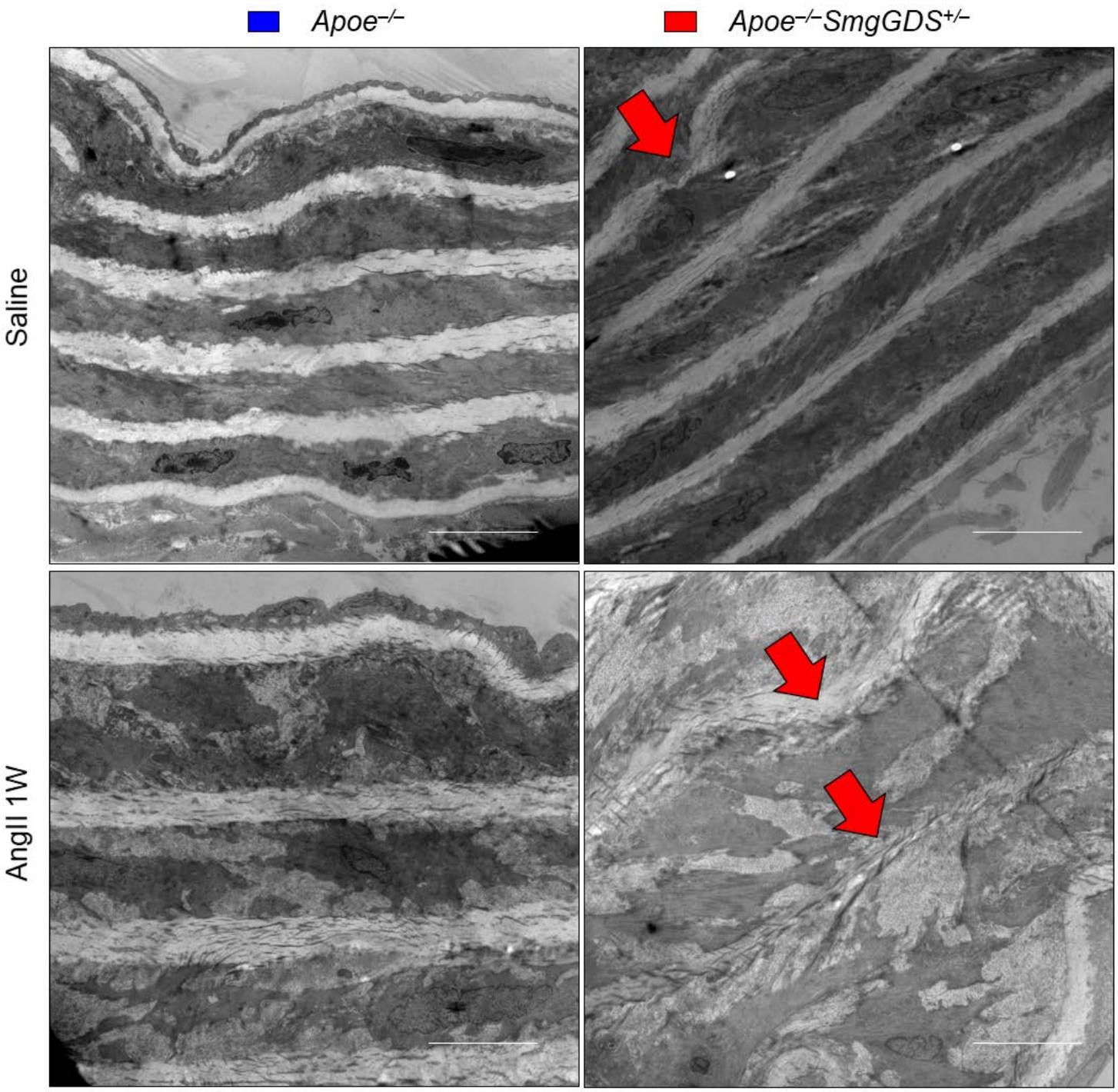


**Supplementary Figure 5. Electron microscopic analysis**
Representative electron microscopic images of ascending aortas from *Apoe*$^{-/-}$ and *Apoe*$^{-/-}$ *SmgGDS*$^{+/-}$ mice after treatment with saline or AngII (1000 ng/kg/min) for 7days. Scale bars, 10μm

**Supplementary Figure 6**

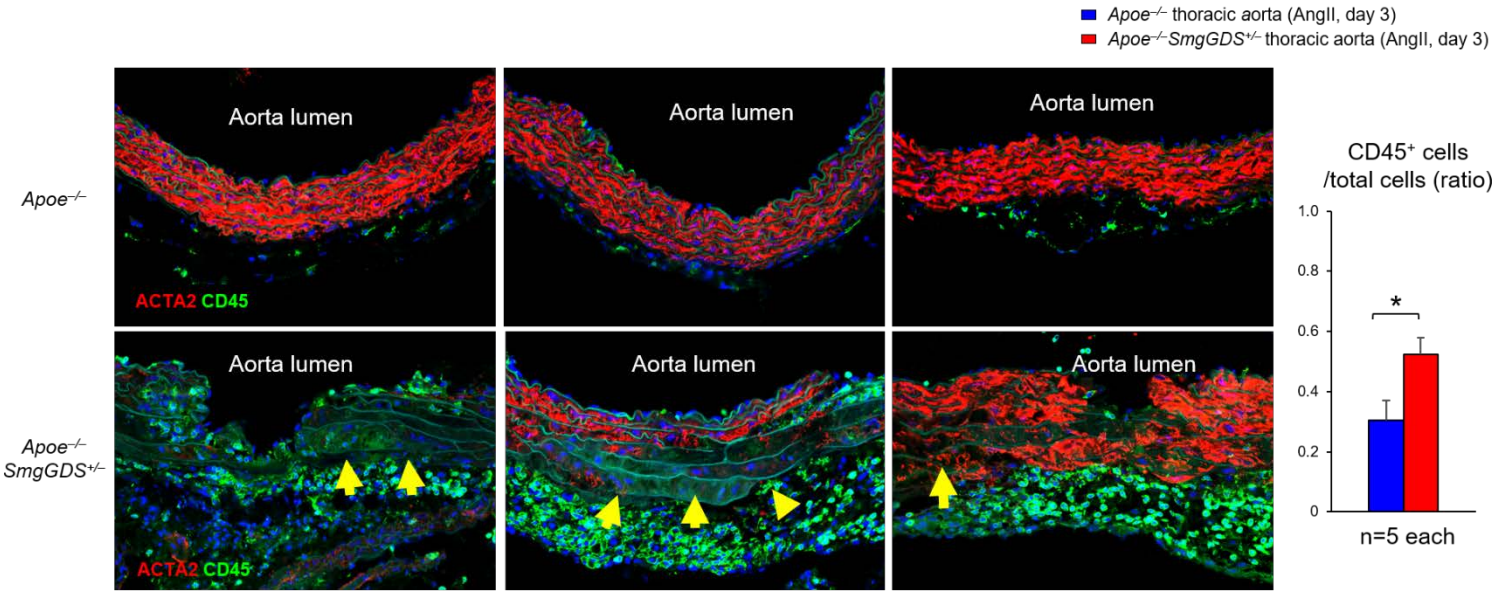


**Supplementary Figure 6. Expression of ACTA2 and migrating CD45$^+$ leucocytes**

Representative immunofluorescence staining of ACTA2 (red) and CD45 (green) in the ascending aortas of *Apoe*$^{-/-}$ and *Apoe*$^{-/-}$*SmgGDS*$^{+/-}$ mice treated with angiotensin II (AngII, 1000 ng/kg/min) for 3 days (*n*=5 each). Scale bars, 100 μm. Data represent the mean ± SEM. **P*<0.05.

**Supplementary Figure 7**

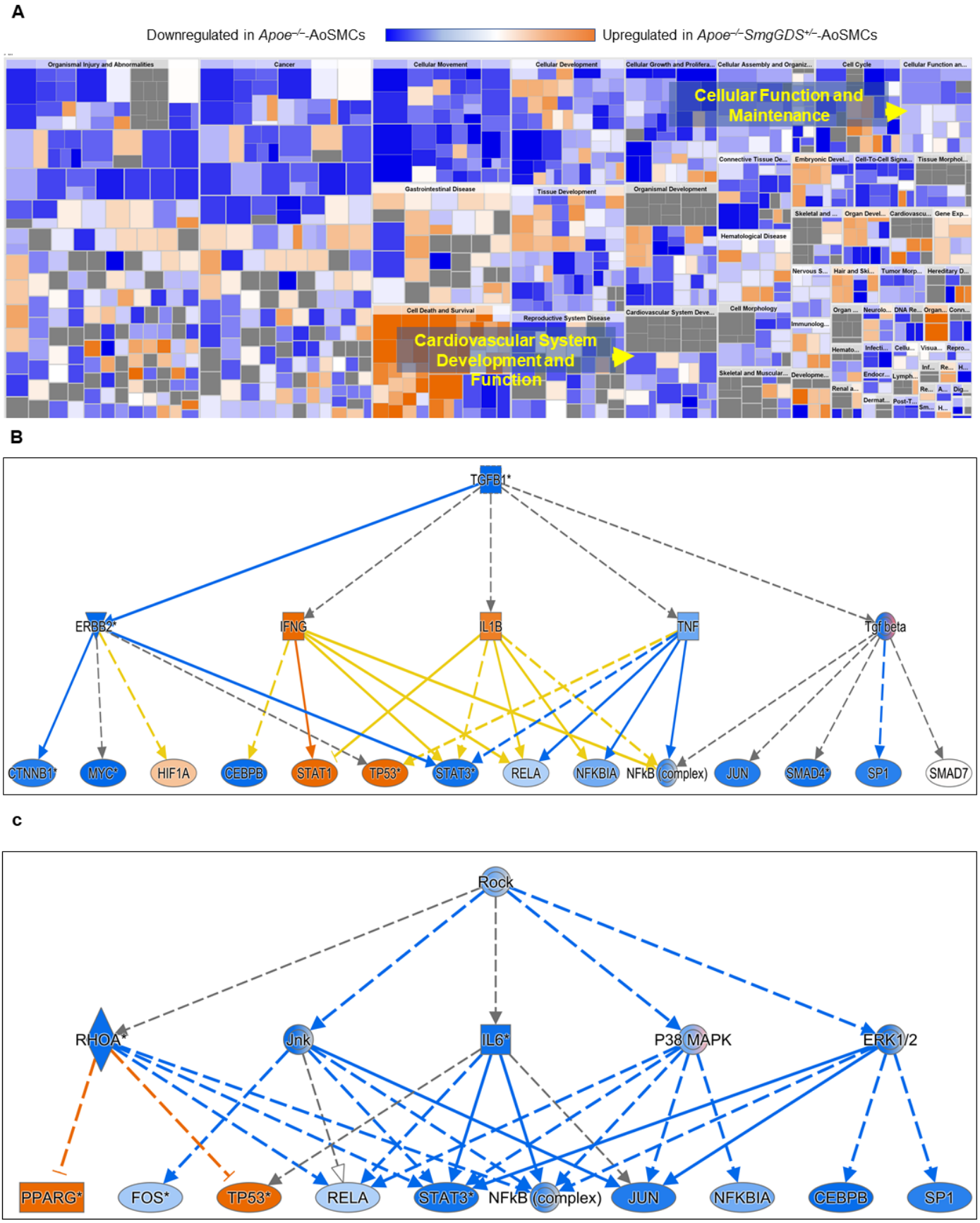

**Supplementary Figure 7. Gene microarray analyses in *Apoe*$^{-/-}$ and *Apoe*$^{-/-}$*SmgGDS*$^{+/-}$ AoSMCs**

(**A**) Heat map analysis of gene microarray analyses by Ingenuity Pathway Analysis software. (**B**) TGFB1 pathway was downregulated in *Apoe*$^{-/-}$*SmgGDS*$^{+/-}$ AoSMCs. (**C**) ROCK pathway was downregulated in *Apoe*$^{-/-}$*SmgGDS*$^{+/-}$ AoSMCs.

**Supplementary Figure 8**

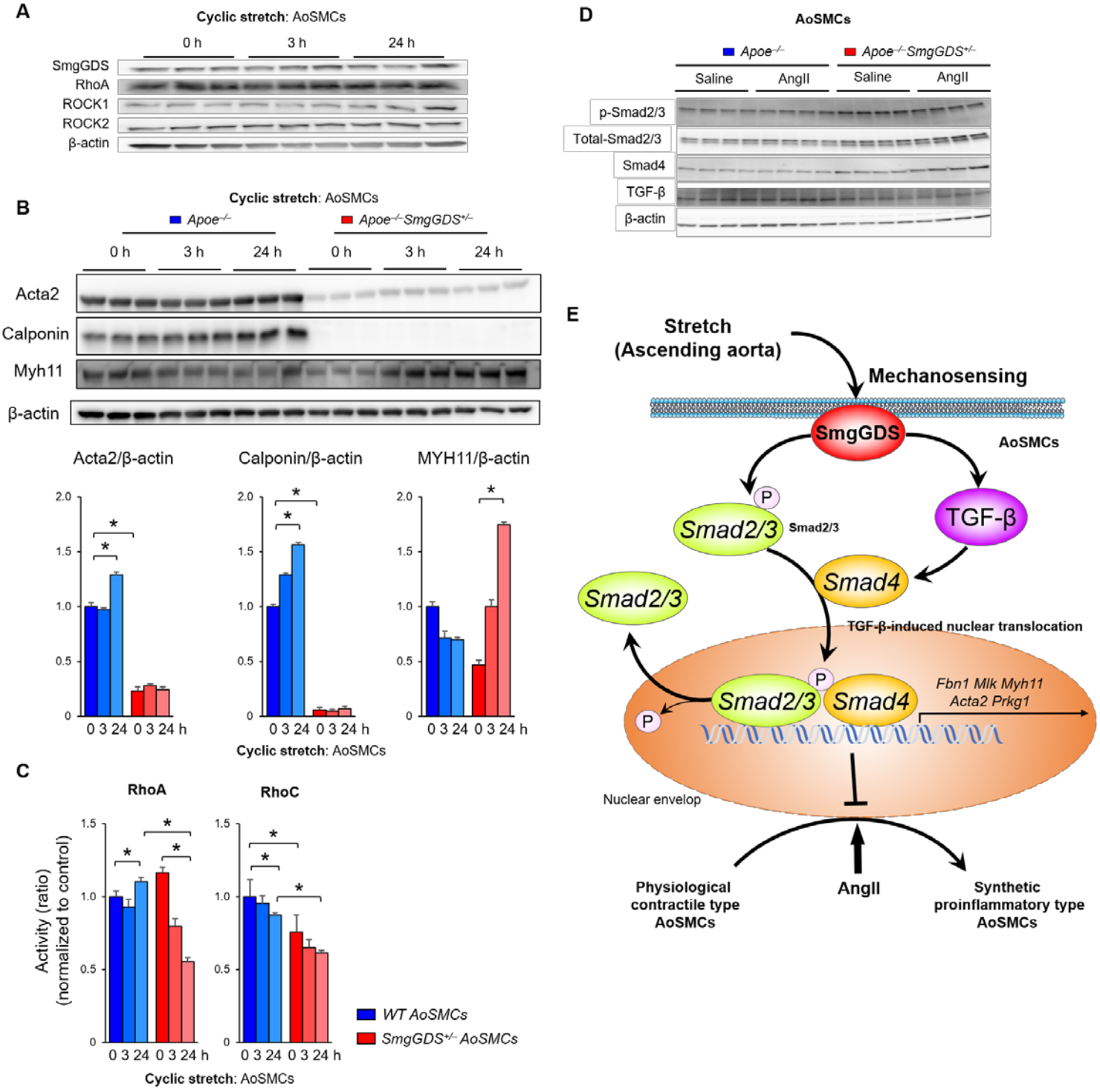

**Supplementary Figure 8. Mechanical stretch upregulates SmgGDS and downstream signaling**

(**A**) Western blot analysis of SmgGDS, RhoA, ROCK1, and ROCK2 in AoSMCs after treatment with cyclic stretch (1 Hz) for 0, 3, 24 hours (*n*=3 each). (**B**) Western blot analysis of phosphorylated Smad2/3, total Smad2/3, Smad4 and TGF-β in *Apoe*$^{-/-}$ or *Apoe*$^{-/-}$*SmgGDS*$^{+/-}$ AoSMCs treated with saline or AngII (100 nM) for 24 hours. (**C**) Western blot analysis of Acta2, Calponin, Myh11, and β-actin in *Apoe*$^{-/-}$ or *Apoe*$^{-/-}$*SmgGDS*$^{+/-}$ AoSMCs after treatment with cyclic stretch (1 Hz) for 0, 3, 24 hours (*n*=3 each). (**D**) Activity assays for RhoA and RhoC in S*mgGDS*$^{+/+}$ (*wild-type*) and S*mgGDS*$^{+/-}$ AoSMCs after treatment with cyclic stretch (1 Hz) for 0, 3, and 24 hours (*n*=3 each). (**E**) Schematic representation of the SmgGDS-mediated protection of AoSMCs from phenotypic switching protective role against mechanical stress and AngII. Mechanical stretch induces SmgGDS, which activates downstream signaling of RhoA/Rho-kinase and TGF-β/Smad2/3/4 in AoSMCs. Data represent the mean ± SEM. **P*<0.05.

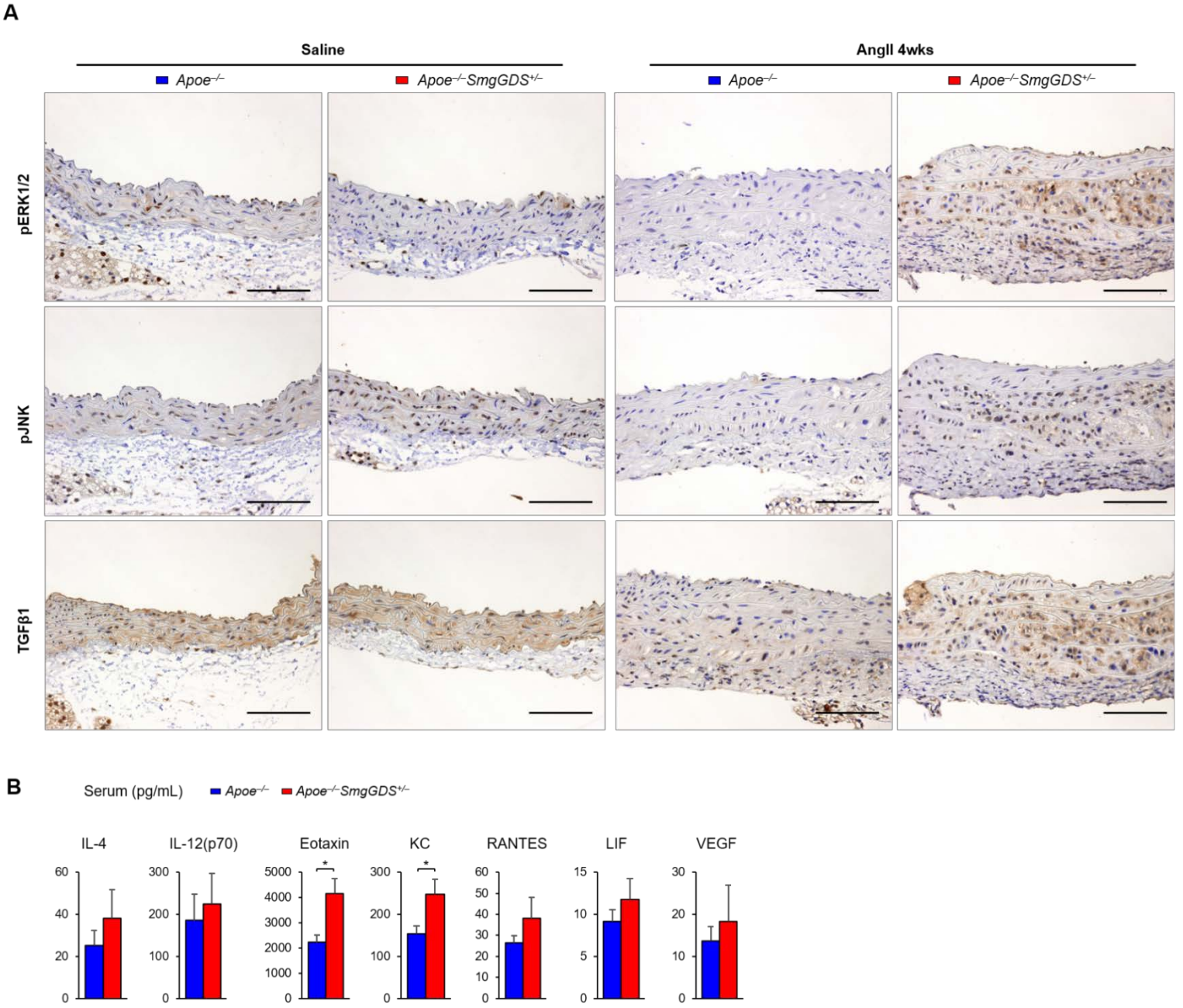


**Supplementary Figure 9. SmgGDS deletion augments inflammation in the ascending aortas**

(**A**) Representative immunostaining of phosphorylated ERK, phosphorylated JNK, and TGFβ1 in ascending aortas of *Apoe*$^{-/-}$ and *Apoe*$^{-/-}$*SmgGDS*$^{+/-}$ mice after treatment with saline or angiotensin II (AngII) for 4 weeks. Scale bars, 100 μm. (**B**) Serum levels of cytokines/chemokines and growth factors in *Apoe*$^{-/-}$ ($n$=14) and *Apoe*$^{-/-}$*SmgGDS*$^{+/-}$ ($n$=18) mice after infusion of AngII for 4 weeks. Data represent the mean ± SEM. *$P$<0.05.

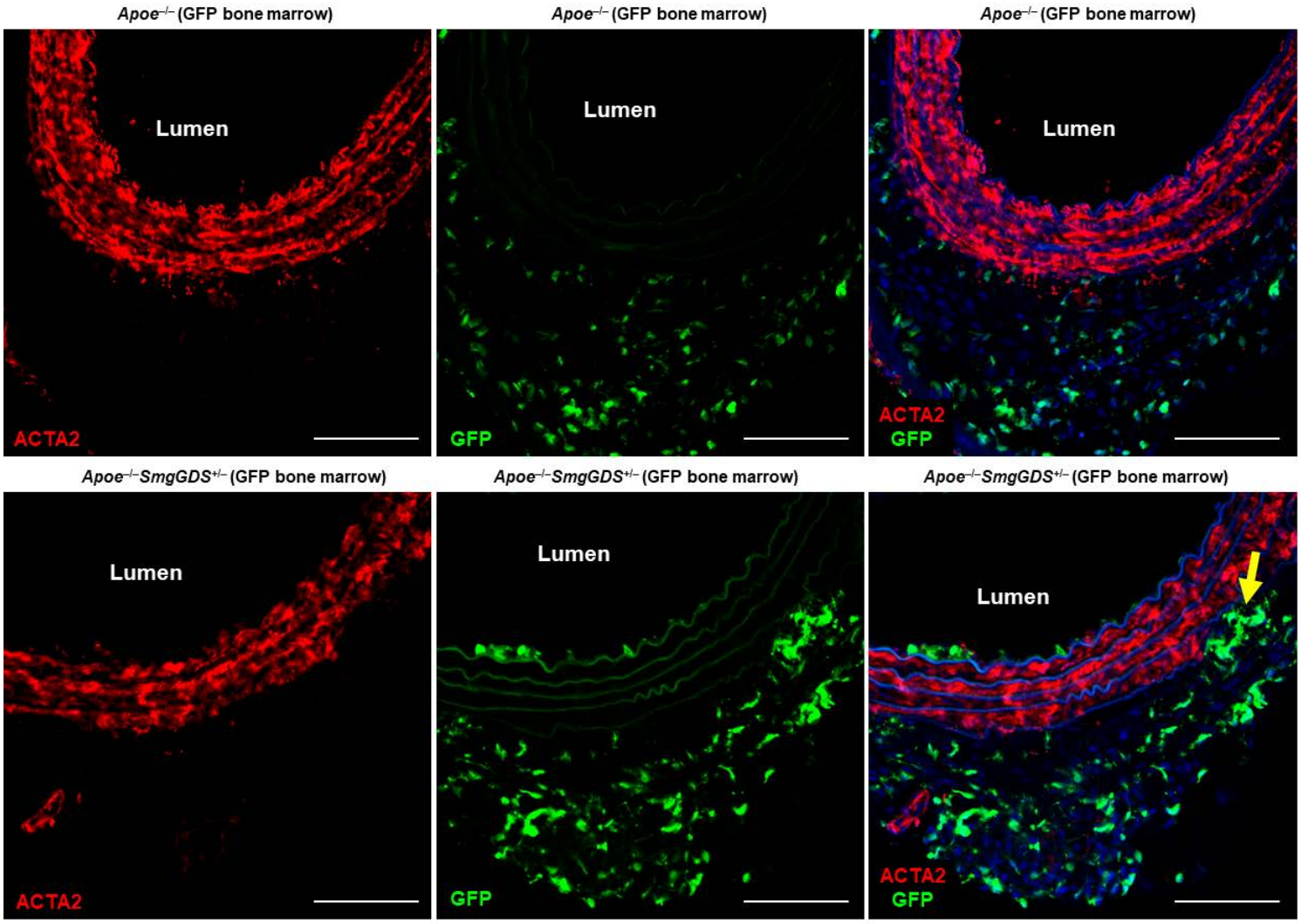


**Supplementary Figure 10. Expression of ACTA2 and migration of GFP$^+$ bone marrow (BM)-derived cells**

Representative immunostaining for GFP (green), ACTA2 (Cy3, red), and DAPI (blue) in ascending aortas from *Apoe*$^{-/-}$ and *Apoe*$^{-/-}$*SmgGDS*$^{+/-}$ chimeric mice after treatment with angiotensin II (AngII, 1000 ng/kg/min) for 4 weeks. Yellow bar indicates the migration of GFP$^+$ BM-derived cells into the aortic walls in *Apoe*$^{-/-}$*SmgGDS*$^{+/-}$ mice. Scale bars, 100 μm.

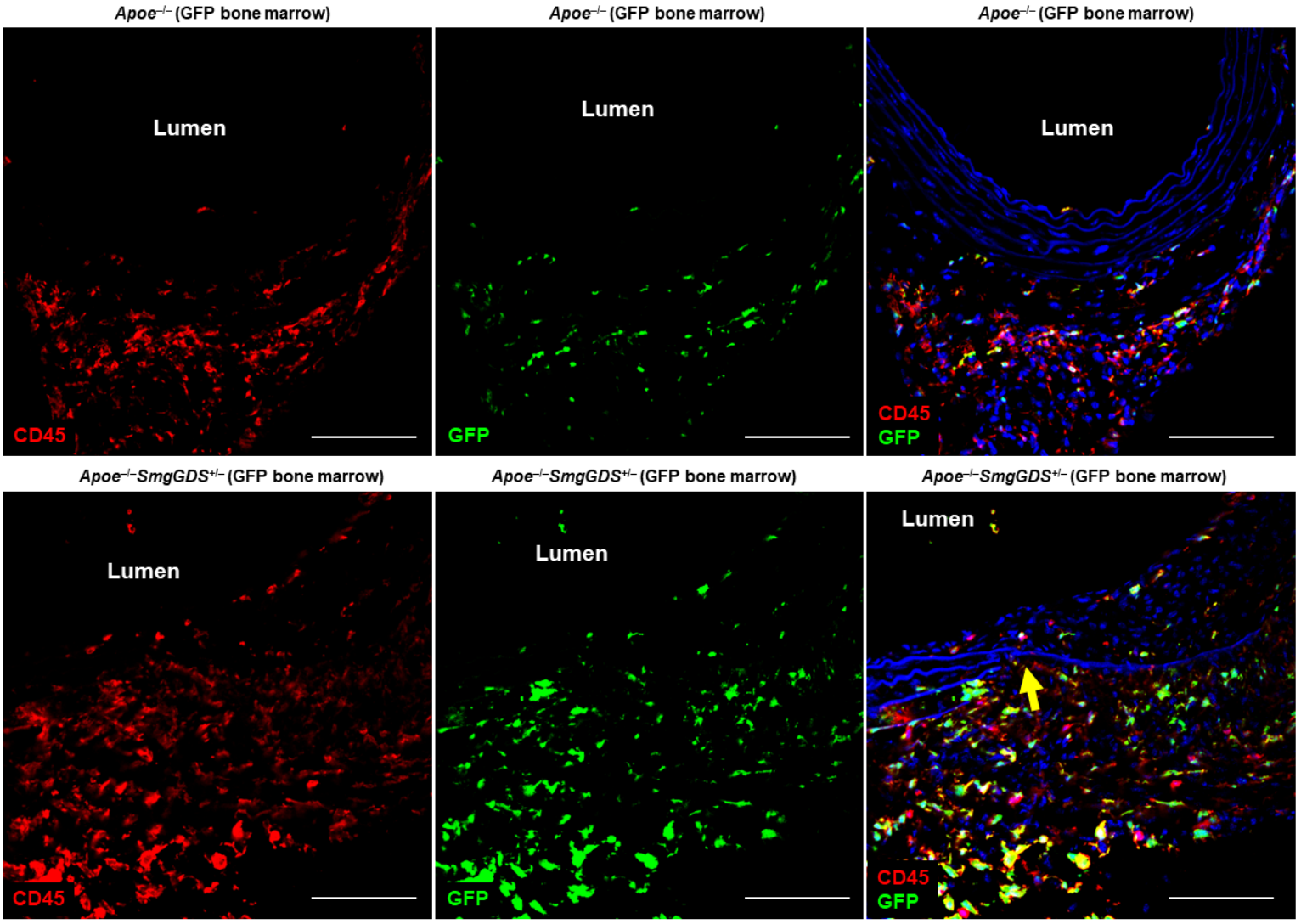


**Supplementary Figure 11. SmgGDS deficiency promotes migration of CD45$^+$ cells**
Representative immunostaining for GFP (green), CD45 (red), and DAPI (blue) in ascending aortas from *Apoe*$^{-/-}$ and *Apoe*$^{-/-}$*SmgGDS*$^{+/-}$ chimeric mice after treatment with angiotensin II (AngII, 1000 ng/kg/min) for 4 weeks. Scale bars, 100 μm.

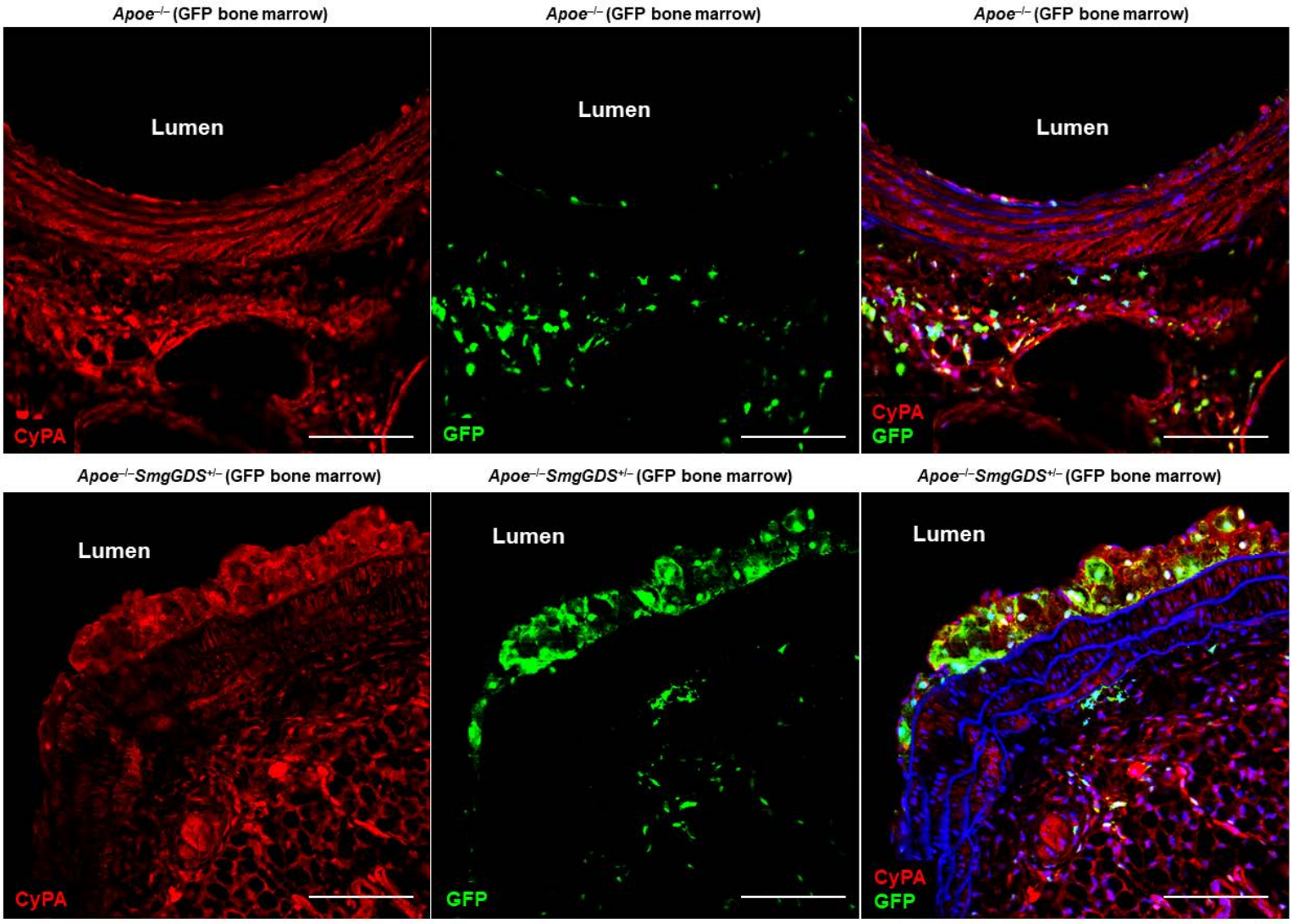


**Supplementary Figure 12. Expression of cyclophilin A (CyPA) in migrating GFP$^+$ bone marrow (BM)-derived cells**

Representative immunostaining for GFP (green), CyPA (red), and DAPI (blue) in ascending aortas from *Apoe*$^{-/-}$ and *Apoe*$^{-/-}$*SmgGDS*$^{+/-}$ chimeric mice after treatment with angiotensin II (AngII, 1000 ng/kg/min) for 4 weeks. Scale bars, 100 μm.

**Supplementary Figure 13**

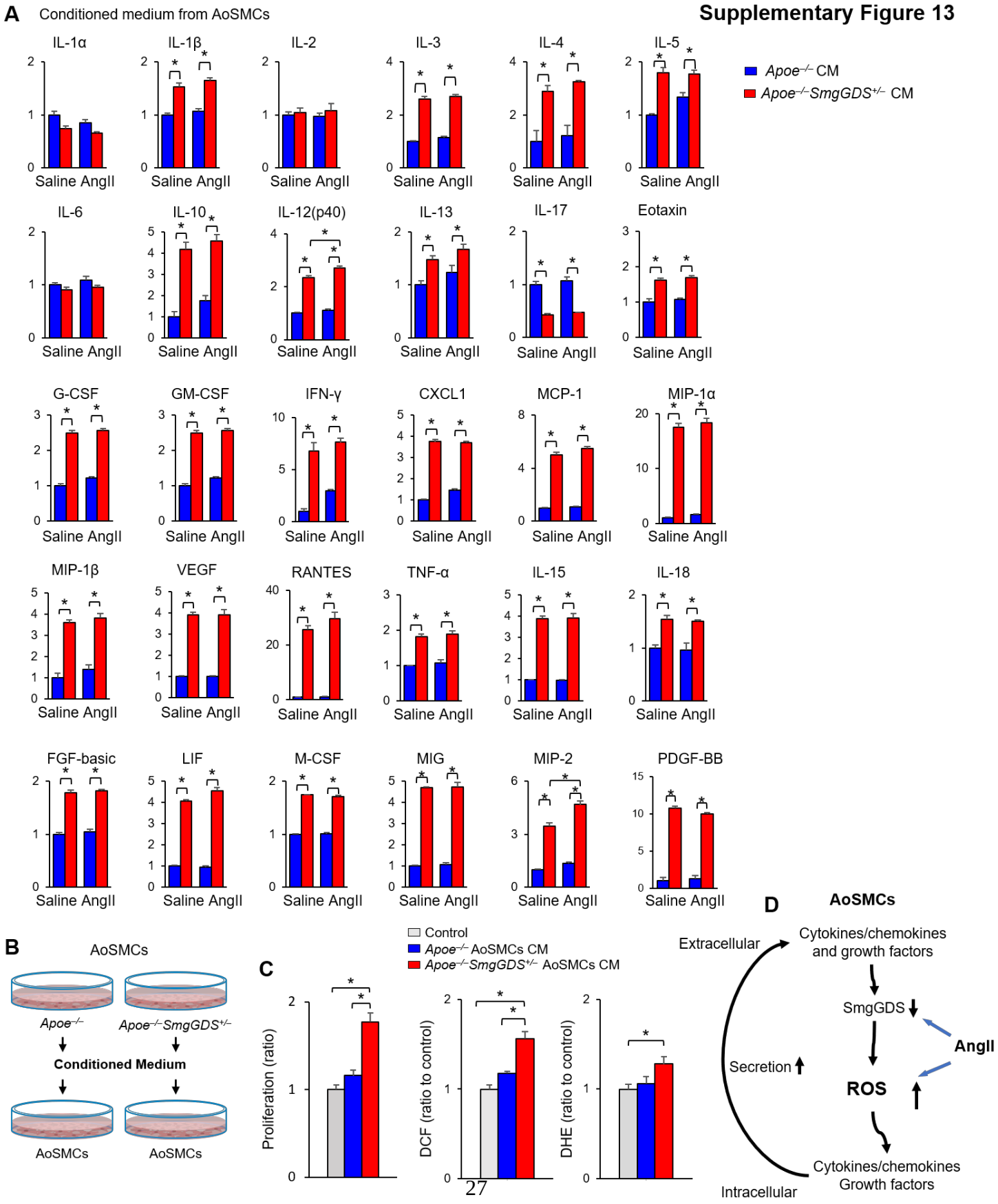

**Supplementary Figure 13. Deletion of SmgGDS in AoSMCs promotes secretion of cytokines/chemokines and growth factors**

(**A**) Levels of cytokines/chemokines and growth factors in conditioned medium (CM) prepared from *Apoe*$^{-/-}$ and *Apoe*$^{-/-}$*SmgGDS*$^{+/-}$ AoSMCs after treatment with saline or AngII (100 nM) for 24 hours. (**B**) The protocol for preparation of CM from *Apoe*$^{-/-}$ and *Apoe*$^{-/-}$*SmgGDS*$^{+/-}$ AoSMCs to stimulate AoSMCs. (**C**) Left, AoSMC proliferation by treatment with *Apoe*$^{-/-}$ and *Apoe*$^{-/-}$ *SmgGDS*$^{+/-}$ CM (10% CM/volume, $n$=8 each). Right, quantification of 2,7-dichlorodihydrofluorescein (DCF) and dihydroethidium (DHE) fluorescence intensity in AoSMCs after treatment with CM for 4 hours (10% CM/volume, $n$=5 each). (**D**) Schematic representation of the increased secretion of cytokines/chemokines and growth factors, production of reactive oxygen species (ROS), and proliferation/migration of AoSMCs by deletion of SmgGDS. Data represent the mean ± s.e.m. *$P$<0.05. Comparisons of parameters were performed with Tukey's honest significant difference test for multiple comparisons.

**Supplementary Figure 14**

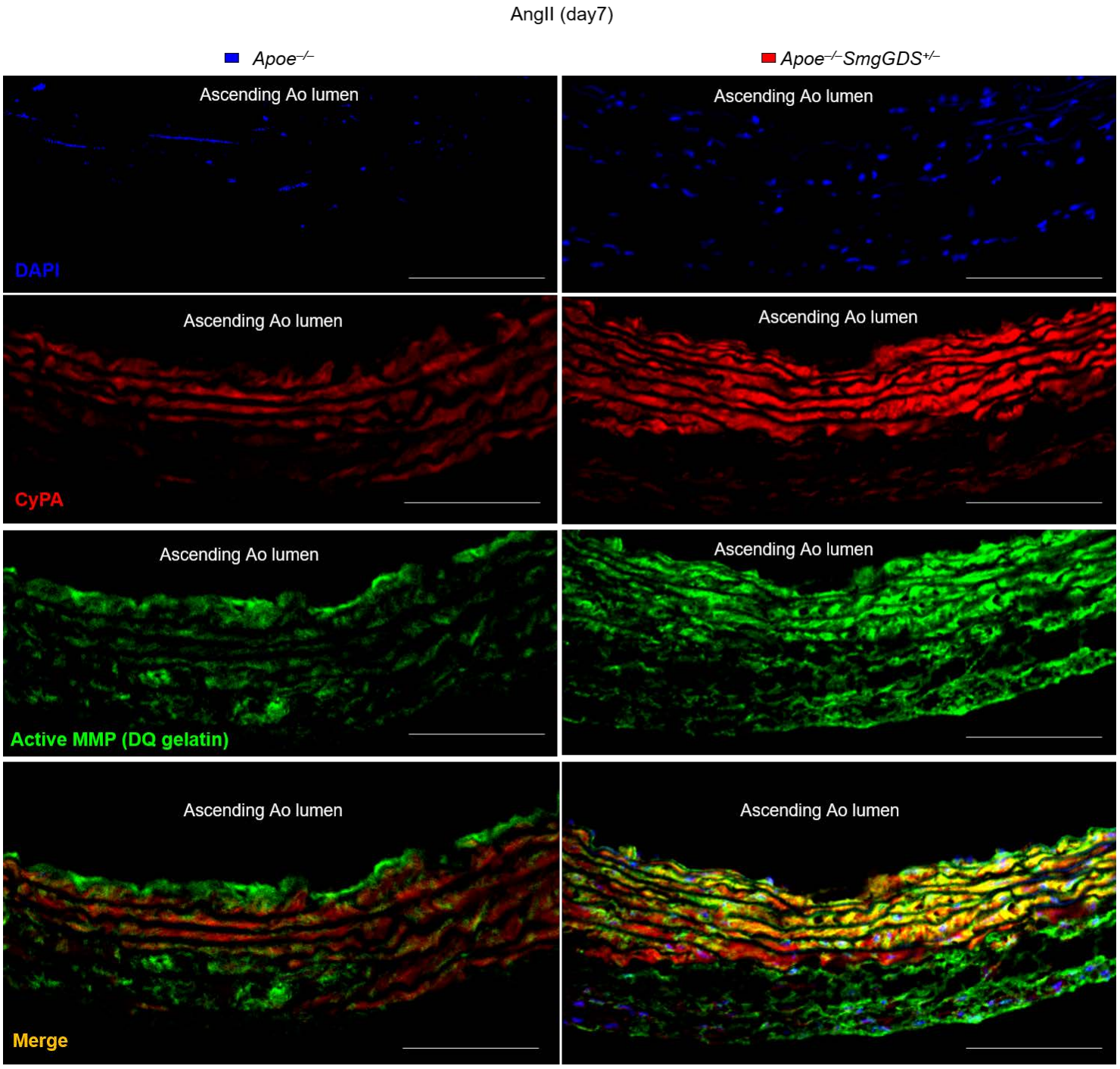


**Supplementary Figure 14. Co-localization of cyclophilin A (CyPA) and active MMPs**
Representative immunofluorescence images of *in situ* zymography (DQ gelatin, green), immunostaining for CyPA (red), and DAPI (blue) in *Apoe*$^{-/-}$ and *Apoe*$^{-/-}$*SmgGDS*$^{+/-}$ aortas after treatment with angiotensin II (AngII, 1000 ng/kg/min) for 7 days. Scale bars, 100 μm.

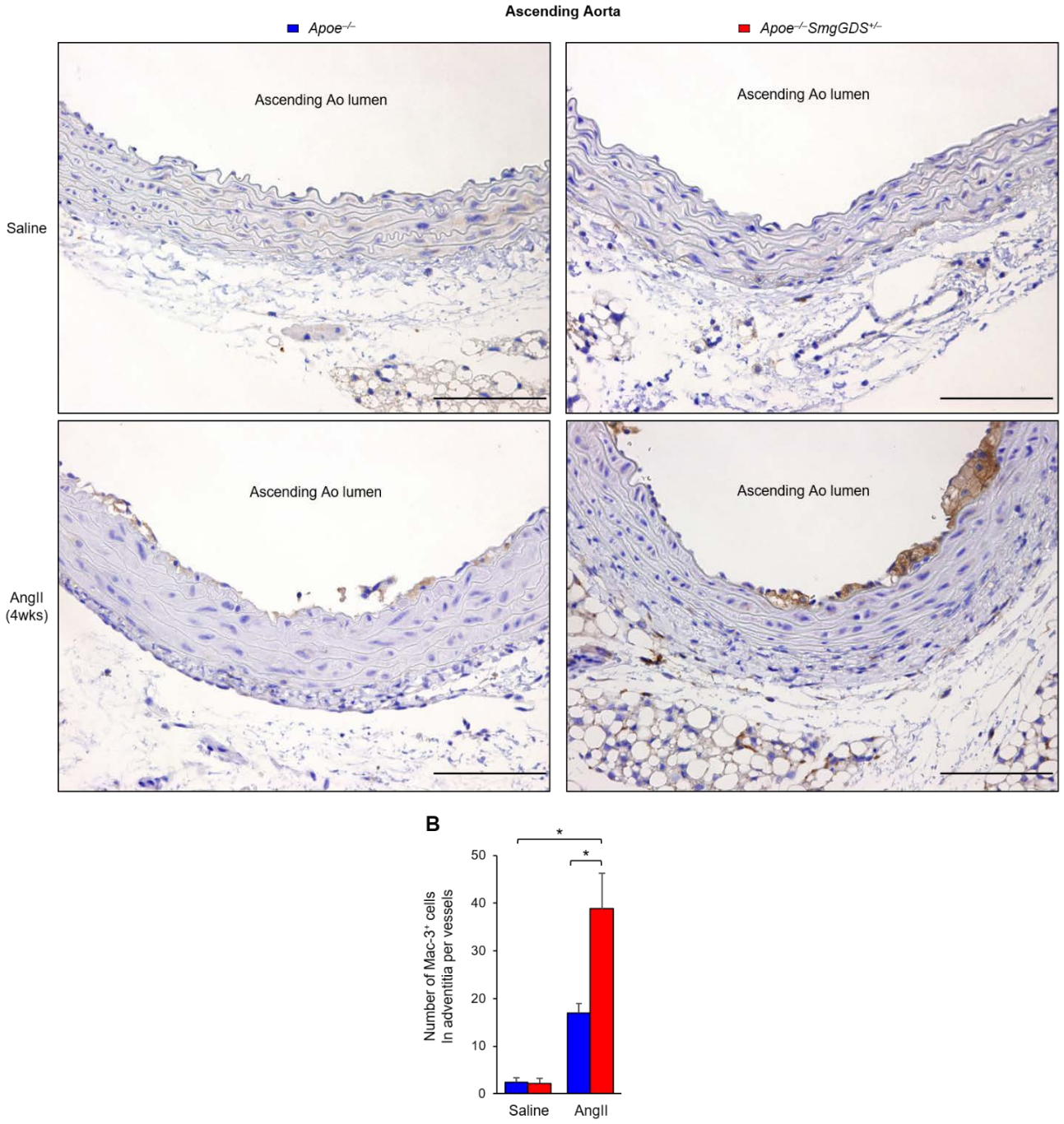


**Supplementary Figure 15. Deletion of SmgGDS increase inflammatory cell migration**

(**A**) Representative immunostaining for Mac-3 (CD107b) in *Apoe*$^{-/-}$ and *Apoe*$^{-/-}$*SmgGDS*$^{+/-}$ ascending aortas after treatment with angiotensin II (AngII, 1000 ng/kg/min) for 4 weeks. (**B**) Quantification of Mac3-positive cells in the adventitia per vessel in *Apoe*$^{-/-}$ and *Apoe*$^{-/-}$ *SmgGDS*$^{+/-}$ ascending aortas. Data represent the mean ± SEM. *$P$<0.05.

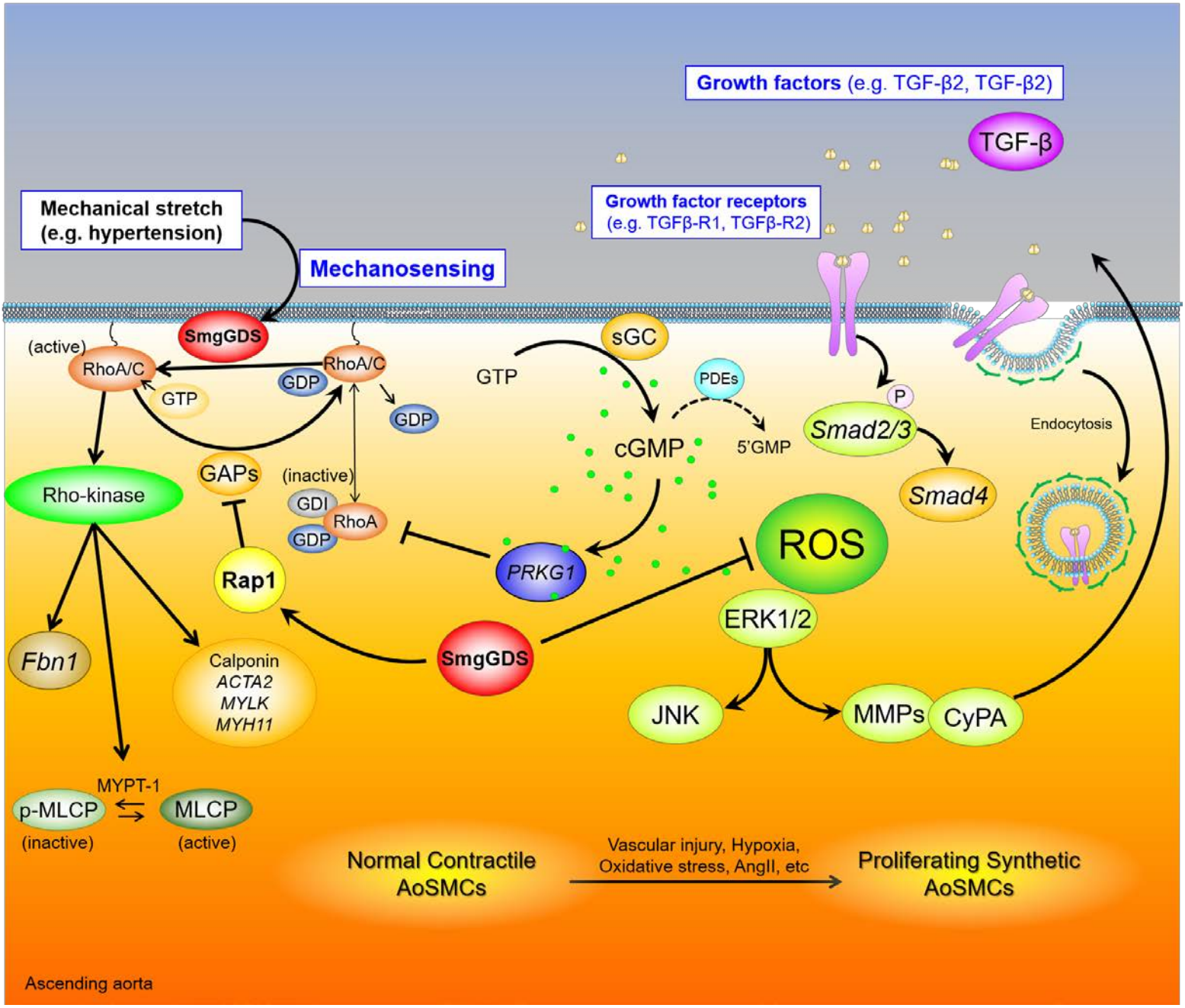


**Supplementary Figure 16. Mechanical stretch-induced SmgGDS prevents phenotypic switching of AoSMCs**

Schematic representation of the molecular mechanisms that SmgGDS plays a protective role against AoSMC phenotypic switching. Mechanical stretch-mediated upregulation of SmgGDS activates RhoA and RhoC and downstream Rho-kinase signaling. SmgGDS prevents reactive oxygen species (ROS) production and downregulates activities of matrix metalloproteinases (MMPs).

## Supplemental References


1. Satoh K, Nigro P, Matoba T, O'Dell MR, Cui Z, Shi X, Mohan A, Yan C, Abe J, Illig KA and Berk BC. Cyclophilin A enhances vascular oxidative stress and the development of angiotensin II-induced aortic aneurysms. *Nat Med*. 2009;15:649-56. doi:10.1038/nm.1958
2. Oller J, Mendez-Barbero N, Ruiz EJ, Villahoz S, Renard M, Canelas LI, Briones AM, Alberca R, Lozano-Vidal N, Hurle MA, Milewicz D, Evangelista A, Salaices M, Nistal JF, Jimenez-Borreguero LJ, De Backer J, Campanero MR and Redondo JM. Nitric oxide mediates aortic disease in mice deficient in the metalloprotease Adamts1 and in a mouse model of Marfan syndrome. *Nat Med*. 2017;23:200-212. doi:10.1038/nm.4266
3. Ayumi T, Jun M, Hiroyoshi I, Miki T, Atsushi T, Yasuko N, Hisahiro Y, Shin-ichi N and Yoshimi T. Involvement of a small GTP-binding protein (G protein) regulator, small G protein GDP dissociation stimulator, in antiapoptotic cell survival signaling. *Mol Biol Cell*. 2000;11:1875-1886. doi:10.1091/mbc.11.5.1875
4. Omura J, Satoh K, Kikuchi N, Satoh T, Kurosawa R, Nogi M, Otsuki T, Kozu K, Numano K, Suzuki K, Sunamura S, Tatebe S, Aoki T, Sugimura K, Miyata S, Hoshikawa Y, Okada Y and Shimokawa H. Protective roles of endothelial AMP-activated protein kinase against hypoxia-induced pulmonary hypertension in mice. *Circ Res*. 2016;119:197-209. doi:10.1161/CIRCRESAHA.115.308178
5. Satoh T, Satoh K, Yaoita N, Kikuchi N, Omura J, Kurosawa R, Numano K, Al-Mamun E, Siddique MA, Sunamura S, Nogi M, Suzuki K, Miyata S, Morser J and Shimokawa H. Activated TAFI promotes the development of chronic thromboembolic pulmonary hypertension: A possible novel therapeutic target. *Circ Res*. 2017;120:1246-1262. doi:10.1161/CIRCRESAHA.117.310640
6. Satoh K, Matoba T, Suzuki J, O'Dell MR, Nigro P, Cui Z, Mohan A, Pan S, Li L, Jin ZG, Yan C, Abe J and Berk BC. Cyclophilin A mediates vascular remodeling by promoting inflammation and vascular smooth muscle cell proliferation. *Circulation*. 2008;117:3088-98. doi:10.1161/CIRCULATIONAHA.107.756106
7. Suzuki J, Jin ZG, Meoli DF, Matoba T and Berk BC. Cyclophilin A is secreted by a vesicular pathway in vascular smooth muscle cells. *Circ Res*. 2006;98:811-7. doi:10.1161/01.RES.0000216405.85080.a6
8. Suzuki K, Satoh K, Ikeda S, Sunamura S, Otsuki T, Satoh T, Kikuchi N, Omura J, Kurosawa R, Nogi M, Numano K, Sugimura K, Aoki T, Tatebe S, Miyata S, Mukherjee R, Spinale FG, Kadomatsu K and Shimokawa H. Basigin promotes cardiac fibrosis and

failure in response to chronic pressure overload in mice. *Arterioscler Thromb Vasc Biol*. 2016;36:636-46. doi:10.1161/ATVBAHA.115.306686

9. A. Maziar Z, Masuko U-F, Marjorie A, Qiqin Y, Aalok S, David GH, W. Robert T and Kathy KG. Role of NADH/NADPH oxidase–derived $H_2O_2$ in angiotensin II–induced vascular hypertrophy. *Hypertension*. 1998;32:488-495. doi:10.1161/01.HYP.32.3.488
10. Kathy KG, Candace AM, Jeremy DO and R. Wayne A. Angiotensin II stimulates NADH and NADPH oxidase activity in cultured vascular smooth muscle cells. *Circ Res*. 1994;74:1141-1148.
11. Nakano M, Satoh K, Fukumoto Y, Ito Y, Kagaya Y, Ishii N, Sugamura K and Shimokawa H. Important role of erythropoietin receptor to promote VEGF expression and angiogenesis in peripheral ischemia in mice. *Circ Res*. 2007;100:662-9. doi:10.1161/01.RES.0000260179.43672.fe
12. Satoh K, Satoh T, Kikuchi N, Omura J, Kurosawa R, Suzuki K, Sugimura K, Aoki T, Nochioka K, Tatebe S, Miyamichi-Yamamoto S, Miura M, Shimizu T, Ikeda S, Yaoita N, Fukumoto Y, Minami T, Miyata S, Nakamura K, Ito H, Kadomatsu K and Shimokawa H. Basigin mediates pulmonary hypertension by promoting inflammation and vascular smooth muscle cell proliferation. *Circ Res*. 2014;115:738-50. doi:10.1161/CIRCRESAHA.115.304563
13. Ikeda S, Satoh K, Kikuchi N, Miyata S, Suzuki K, Omura J, Shimizu T, Kobayashi K, Kobayashi K, Fukumoto Y, Sakata Y and Shimokawa H. Crucial role of Rho-kinase in pressure overload-induced right ventricular hypertrophy and dysfunction in mice. *Arterioscler Thromb Vasc Biol*. 2014;34:1260-71. doi:10.1161/ATVBAHA.114.303320
14. Berg TJ, Gastonguay AJ, Lorimer EL, Kuhnmuench JR, Li R, Fields AP and Williams CL. Splice variants of SmgGDS control small GTPase prenylation and membrane localization. *J Biol Chem*. 2010;285:35255-66. doi:10.1074/jbc.M110.129916
15. Shimizu T, Fukumoto Y, Tanaka S, Satoh K, Ikeda S and Shimokawa H. Crucial role of ROCK2 in vascular smooth muscle cells for hypoxia-induced pulmonary hypertension in mice. *Arterioscler Thromb Vasc Biol*. 2013;33:2780-91. doi:10.1161/ATVBAHA.113.301357